

DYNAMIC ANALYSIS AND MODELLING OF A ROCKET LAUNCHER  
SYSTEM

A THESIS SUBMITTED TO  
THE GRADUATE SCHOOL OF NATURAL AND APPLIED SCIENCES  
OF  
MIDDLE EAST TECHNICAL UNIVERSITY

BY

BURAK CAN ÇİÇEK

IN PARTIAL FULFILLMENT OF THE REQUIREMENTS  
FOR  
THE DEGREE OF MASTER OF SCIENCE  
IN  
MECHANICAL ENGINEERING

FEBRUARY 2014



Approval of the Thesis:

**DYNAMIC ANALYSIS AND DESIGN MODELLING OF A ROCKET  
LAUNCHER SYSTEM**

submitted by **BURAK CAN ÇİÇEK** in partial fulfillment of the requirements for  
the degree of **Master of Science in Mechanical Engineering Department, Middle  
East Technical University** by,

Prof. Dr. Canan Özgen  
Dean, Graduate School of **Natural and Applied Sciences**

Prof. Dr. Süha Oral  
Head of Department, **Mechanical Engineering**

Prof. Dr. Haluk Darendeliler  
Supervisor, **Mechanical Engineering Department, METU**

Prof. Dr. Kemal İder  
Co-Supervisor, **Mechanical Engineering Department, METU**

**Examining Committee Members:**

Prof. Dr. Metin Akkök  
Mechanical Engineering Dept., METU

Prof. Dr. Haluk Darendeliler  
Mechanical Engineering Dept., METU

Prof. Dr. Kemal İder  
Mechanical Engineering Dept., METU

Assist. Prof. Dr. Gökhan Özgen  
Mechanical Engineering Dept., METU

Mr. Bülent Acar, MSc  
Lead Engineer, ROKETSAN

**Date: February 06<sup>th</sup>, 2014**

**I hereby declare that all information in this document has been obtained and presented in accordance with academic rules and ethical conduct. I also declare that, as required by these rules and conduct, I have fully cited and referenced all material and results that are not original to this work.**

Name, Last name: Burak C. Çiçek

Signature :

## **ABSTRACT**

### **DYNAMIC ANALYSIS AND MODELLING OF A ROCKET LAUNCHER SYSTEM**

Çiçek, Burak Can

M.S., Department of Mechanical Engineering

Supervisor: Prof. Dr. Haluk Darendeliler

Co-Supervisor: Prof. Dr. Kemal İder

February 2014, 128 pages

The main objective of this thesis is to evaluate the behavior of a rocket launcher system under dynamic load condition by using finite element method. For a free flight rocket accuracy and dispersion values are significant when determining its success. Although, the design of a free flight rocket is important, interaction behavior of the launching system is crucial for accuracy and dispersion. Tipoff fault which is induced at the launching (before the free flight) phase can only be reduced by detailed dynamic analyses of the launching system.

The purpose of this thesis is to figure out dynamic behavior of a rocket launcher system in order to decrease time, effort and cost consumed on prototype production and expensive tests. For this aim, two different models are created. The first model is a detailed finite element model that includes necessary kinematic and elastic connections. By composing this model, the aim is to get closer results to test results. A commercial software is utilized as a finite element program. The second model is a simple parametric finite element model which is created with a finite

element software's code. This model has less degree of freedom (DOF) when compared with the first model. Thus, shell and beam elements are utilized to compose this model. The aim is to get faster results by changing the parameters when compared with the first model. After that, tests are implemented with a prototype for verification of the models. Finally, the individual effects of the parameters on a rocket launcher systems dynamic behavior are observed on the second model. These parameters are the positions of the clamp attachments on the chassis, the cross section of stabilizer case, the cross section of outrigger case and outrigger deployment.

Keywords: Rocket Launcher System, Finite Element Method, Dynamic Analysis

## ÖZ

### BİR ROKET FIRLATMA SİSTEMİNİN MODELLENMESİ VE DİNAMİK ANALİZİ

Çiçek, Burak Can

Yüksek Lisans, Makina Mühendisliği Bölümü

Tez Yöneticisi: Prof. Dr. Haluk Darendeliler

Ortak Tez Yöneticisi: Prof. Dr. Kemal İder

Şubat 2014, 128 sayfa

Bu tezin ana hedefi sonlu elemanlar yöntemini kullanarak dinamik yükleme koşulu altında roket fırlatma sisteminin davranışını ölçmektir. Serbest uçan bir roketin başarısını saptamak için dağılım ve doğruluk değerleri önemlidir. Dağılım ve doğruluk için serbest uçan roket tasarımının önemli olmasına rağmen fırlatma sistemi ile etkileşim davranışı da çok önemlidir. Fırlatma fazında (serbest uçuştan önce) tesir eden burun eğme hatası ancak fırlatma sisteminin detaylı dinamik analizi ile azaltılabilir.

Bu tezin amacı, ilk örnek üretimi için harcanan zaman, çaba ve maliyet ile pahalı testleri azaltmak için roket fırlatma sisteminin dinamik davranışını anlamaktır. Bu amaçla, iki farklı model oluşturulmuştur. İlk model içerisinde gerekli kinematik ve esnek bağlantıları barındıran detaylı sonlu elemanlar modelidir. Bu modeli oluşturarak test sonuçlarına daha yakın sonuçlar elde etmek hedeflenmiştir. Sonlu elemanlar yazılımı olarak ticari bir yazılım kullanılmıştır. İkinci model ise bir sonlu elemanlar yazılımı kodu ile oluşturulmuş sade parametrik sonlu elemanlar

modelidir. Bu model ilk modelle karşılaştırıldığında daha az serbestlik derecesi içermektedir. Bu nedenle, modeli oluştururken kabuk ve kiriş elemanlar kullanılmıştır. Amaç, ilk modele göre parametreleri değiştirerek daha hızlı sonuçlar elde etmektir. Daha sonra modelleri doğrulamak için ilk örneğe testler uygulanmıştır. Son olarak, ikinci model üzerinde roket fırlatma sistemi dinamik davranışı üzerindeki parametrelerin birbirinde ayrı etkileri gözlenmiştir. Bu parametreler; şase üzerindeki kulakçık bağlantı yerleri, dengeleyici kılıfı kesit alanı, dirsekli iskele kılıfı kesit alanı ve dirsekli iskele açılma miktarıdır.

Anahtar Kelimeler: Fırlatma Sistemi, Sonlu Elemanlar Yöntemi, Dinamik Analiz



To My Family

## **ACKNOWLEDGEMENTS**

I would like to express my deepest thanks and gratitude to Prof. Dr. Kemal İDER and Prof. Dr. Haluk DARENDELİLER for their supervision, professional support and constant guidance throughout the completion of this thesis work.

I am indebted to Bülent ACAR, lead engineer at ROKETSAN, for his crucial advises, invaluable efforts for this thesis and encouragement throughout the completion of this thesis work.

I also thank my colleagues, Tarık OLGAR and Ali YETGİN for their technical supports during this study.

I would like to thank to ROKETSAN for partially supporting this study.

Finally, my gratitude is endless for my family to whom this thesis is devoted. Without them nothing would have been possible.

## TABLE OF CONTENTS

ABSTRACT.....	v
ÖZ.....	vii
ACKNOWLEDGEMENTS.....	x
TABLE OF CONTENTS.....	xi
LIST OF TABLES.....	xiii
LIST OF FIGURES.....	xiv
NOMENCLATURE.....	xix
LIST OF ABBREVIATIONS.....	xx
CHAPTERS	
1. INTRODUCTION.....	1
1.1 Background.....	1
1.2 Scope of the Thesis.....	6
1.3 Purpose of the Thesis.....	8
1.4 Outline of the Thesis.....	9
2. LITERATURE SURVEY.....	11
3. DETAILED FINITE ELEMENT MODEL.....	23
3.1 Detailed Finite Element Model of the Rocket Launcher System.....	24
3.2 Modeling Method And Meshing of the Detailed Finite Element Model.....	25
3.3 Material Properties and Boundary Conditions for the Detailed Finite Element Model.....	36

3.4 Modal Analysis of the Detailed Finite Element Model .....	37
3.5 Dynamic Analysis of the Detailed Finite Element Model .....	44
4. SIMPLIFIED FINITE ELEMENT MODEL .....	49
4.1 Simplified Rocket Launcher Model .....	49
4.2 Modeling Method and Meshing of the Simplified Finite Element Model.....	50
4.3 Material Properties and Boundary Conditions for the Simplified Finite Element Model.....	54
4.4 Modal Analysis of the Simplified Finite Element Model .....	55
4.4 Dynamic Analysis of the Simplified Finite Element Model.....	62
5. TEST STUDY AND VERIFICATION OF FINITE ELEMENT MODELS .....	73
5.1 Static Firing Tests .....	74
5.2 Firing Tests .....	75
5.2 Verification of the Finite Element Models .....	80
6. INDIVIDUAL EFFECTS OF THE PARAMETERS .....	86
6.1 Clamp Attachment Positions.....	86
6.2 Outrigger's Deployment .....	93
6.3 Stabilizer's Cross Section Modification .....	101
6.4 Outrigger's Cross Section Modification .....	108
7. SUMMARY AND CONCLUSIONS .....	116
7.1 Summary .....	116
7.2 General Conclusions and Discussion .....	120
REFERENCES .....	124

## LIST OF TABLES

### TABLES

Table 1. Material properties of St-37 .....	36
Table 2. Modal analysis results of the detailed model .....	38
Table 4. Modal analysis results of the simplified model .....	56
Table 5. The distance values of the third clamp attachment (Normalized to baseline) .....	88
Table 6. Deployment ratio values of the outriggers (Normalized to baseline) .....	94
Table 7. Thickness values of the stabilizers (Normalized to baseline) .....	102
Table 8. Thickness values of the outriggers (Normalized to baseline) .....	108
Table 9. Comparison of detailed FE model and simplified FE model.....	123

## LIST OF FIGURES

### FIGURES

Figure 1. Photograph of a multiple launch rocket launcher system.....	2
Figure 2. Four successive phases of the rocket and firing tube interaction [2] .....	4
Figure 3. Flowchart of the detailed modeling approach .....	7
Figure 4. Flowchart of the simplified modeling approach.....	7
Figure 5. Finite element model by Işık [1] .....	12
Figure 6. Rocket launcher system model by Cochran [3].....	13
Figure 7. Rocket launcher system model by Dziopa [4].....	14
Figure 8. The model proposed by Lee and Wilms [5] .....	15
Figure 9. The model introduced by Zhang and Xiao [6] .....	16
Figure 10. The model provided by Selmic [7].....	17
Figure 11. The model utilized by Raducanu [9] .....	18
Figure 12. Finite element model created by Hadipour [17].....	20
Figure 13. Chassis development flow chart created by Roslan [18].....	21
Figure 14. Detailed FE model, simplified FE model and a representative prototype .....	24
Figure 15. Meshed detailed rocket launcher finite element model .....	26
Figure 16. Positioning of the stabilizers and the outriggers.....	27
Figure 17. Hydraulic system in the stabilizers and the outriggers .....	27
Figure 18. Telescopic structure of the stabilizers and outriggers .....	28
Figure 19. Glue contacts in the stabilizers and outriggers .....	28
Figure 20. Contact between auxiliary chassis and stabilizers.....	29
Figure 21. Clamp attachments between the chassis and the auxiliary chassis.....	30
Figure 22. Details of the clamp attachments.....	31
Figure 23. The connection between cross members and chassis .....	32

Figure 24. Cradle's welding connections .....	33
Figure 25. Slewing ring's finite element model .....	34
Figure 26. Spring elements for representing slewing ring's ball parts .....	35
Figure 27. Lumped masses of the rocket launcher system.....	36
Figure 28. The First mode shape of the detailed model .....	39
Figure 29. The second mode shape of the detailed model .....	39
Figure 30. The 7th mode shape of the detailed model .....	40
Figure 31. The 9th mode shape of the detailed model .....	40
Figure 32. The 10th mode shape of the detailed model .....	41
Figure 33. The 11th mode shape of the detailed model .....	42
Figure 34. The 13th mode shape of the detailed model .....	42
Figure 35. The 19th mode shape of the detailed model .....	43
Figure 36. The 20th mode shape of the detailed model .....	44
Figure 37. Plume force applied area .....	45
Figure 38. Dynamic plume load.....	45
Figure 39. Numbering system for the stabilizers and outriggers .....	46
Figure 40. Reaction forces of the stabilizers and outriggers in the Y axis.....	47
Figure 41. The displacement in the Y axis of the center of the firing tube (Tip-off) .....	47
Figure 42. Clamp attachments of the simplified rocket launcher system .....	50
Figure 43. Rigid connections of the cross members .....	51
Figure 44. Simplified rocket launcher system.....	52
Figure 45. Simplified rocket launcher system without lumped masses .....	53
Figure 46. Simplified rocket launcher system with beam elements' shapes .....	54
Figure 47. Boundary condition of the rocket launcher system FE model.....	55
Figure 48. Comparison of the first mode shape of detailed FE model and the first mode shape of simplified FE model .....	57
Figure 49. Comparison of the second mode shape of detailed FE model and the second mode shape of simplified FE model .....	57
Figure 50. Comparison of the seventh mode shape of detailed FE model and the forth mode shape of simplified FE model.....	58

Figure 51. Comparison of the ninth mode shape of detailed FE model and the fifth mode shape of simplified FE model .....	59
Figure 52. Comparison of the tenth mode shape of detailed FE model and the seventh mode shape of simplified FE model .....	59
Figure 53. Comparison of the eleventh mode shape of detailed FE model and the ninth mode shape of simplified FE model .....	60
Figure 54. Comparison of the thirteenth mode shape of detailed FE model and the twelfth mode shape of simplified FE model .....	61
Figure 55. Comparison of the nineteenth mode shape of detailed FE model and the fifteenth mode shape of simplified FE model .....	61
Figure 56. Comparison of the twentieth mode shape of detailed FE model and the sixteenth mode shape of simplified FE model .....	62
Figure 57. Fixed platform areas where dynamic load applied .....	63
Figure 58. Numbering system for the stabilizers and outriggers .....	64
Figure 59. Total reaction force comparison in the Y axis .....	65
Figure 60. Reaction force comparison of L1 in the Y axis .....	66
Figure 61. Reaction force comparison of L2 in the Y axis .....	67
Figure 62. Reaction force comparison of L3 in the Y axis .....	68
Figure 63. The reaction force comparison of L4 in the Y axis .....	69
Figure 64. The reaction forces of the stabilizers and outriggers of the baseline model .....	70
Figure 65. The simplified model's cradle mass center .....	71
Figure 66. The displacement in the Y axis of the mass center of the cradle (Tip-off) .....	72
Figure 67. Horizontal thrust measurement system [1] .....	74
Figure 68. Positions of the cradle legs [1] .....	76
Figure 69. Potentiometer locations on the cradle .....	76
Figure 70. A representative rocket launcher system .....	77
Figure 71. Laser distance sensor set up on a representative system .....	78
Figure 72. Reaction forces of the stabilizers and outriggers in the Y axis .....	79
Figure 73. Displacement in the Y axis of the tip point of the elevation platform ...	80



Figure 74. Total reaction force comparison .....	81
Figure 75. Reaction force of L1 .....	82
Figure 76. Reaction force of L2 .....	82
Figure 77. Reaction force of L3 .....	83
Figure 78. Reaction force of L4 .....	83
Figure 79. Displacement in Y axis (Tip-off).....	84
Figure 80. Clamp attachments' positions on the chassis .....	87
Figure 81. Clamp attachment couples on the chassis.....	87
Figure 82. Third clamp attachment's position measurement method.....	88
Figure 83. Third clamp attachment's position of CAP1 model.....	89
Figure 84. Third clamp attachment's position of CAP2 model.....	89
Figure 85. Comparison of the total reaction forces.....	90
Figure 86. Comparison of the reaction forces of L1 .....	91
Figure 87. Comparison of the reaction forces of L2 .....	91
Figure 88. Comparison of the reaction forces of L3 .....	92
Figure 89. Comparison of the reaction forces of L4 .....	92
Figure 90. Comparison of the mass center of the cradle in Y axis .....	93
Figure 91. Stabilizers and outriggers of the rocket launcher system .....	94
Figure 92. Outrigger's deployment ratio measurement method.....	95
Figure 93. Outrigger's deployment of DR1 model.....	95
Figure 94. Outrigger's deployment of DR2 model.....	96
Figure 95. Comparison of the total reaction forces.....	97
Figure 96. Comparison of the reaction forces of L1 .....	98
Figure 97. Comparison of the reaction forces of L2 .....	98
Figure 98. Comparison of the reaction forces of L3 .....	99
Figure 99. Comparison of the reaction forces of L4 .....	100
Figure 100. Comparison of the mass center of the cradle in Y axis .....	100
Figure 101. Stabilizers of the rocket launcher system .....	101
Figure 102. Stabilizer's thickness changing method .....	102
Figure 103. Mid points of the stabilizers and outriggers .....	103
Figure 104. Comparison of the displacement of L1 in Z axis.....	104

Figure 105. Comparison of the displacement of L2 in Z axis .....	104
Figure 106. Comparison of the displacement of L3 in Z axis .....	105
Figure 107. Comparison of the displacement of L4 in Z axis .....	106
Figure 108. Comparison of the mass center of the cradle in Y axis .....	107
Figure 109. Outriggers of the rocket launcher system .....	108
Figure 110. Outrigger's thickness changing method.....	109
Figure 111. Mid points of the stabilizers and outriggers .....	110
Figure 112. Comparison of the displacement of L1 in Z axis .....	110
Figure 113. Comparison of the displacement of L2 in Z axis .....	111
Figure 114. Comparison of the displacement of L3 in Z axis .....	112
Figure 115. Comparison of the displacement of L4 in Z axis .....	113
Figure 116. Comparison of the mass center of the cradle in Y axis .....	113
Figure 117. Flowchart for the future projects .....	117
Figure 118. Comparison of the preparation, solution and post-processing of the detailed FE model and simplified FE model with respect to time .....	122

## NOMENCLATURE

$\alpha$	Constant mass matrix multiplier
$\beta$	Constant stiffness matrix multiplier
C	Damping matrix
K	Stiffness matrix
$\mu$	Friction co-efficient
M	Mass matrix

## LIST OF ABBREVIATIONS

APDL	ANSYS Parametric Design Language
CAD	Computer Aided Drawing
CAP1	90% of the Third Clamp Attachment Distance
CAP2	80% of the Third Clamp Attachment Distance
DOF	Degree of Freedom
DR1	80 % Deployment Ratio
DR2	60% Deployment Ratio
FE	Finite Element
FEA	Finite Element Analysis
FEM	Finite Element Method
MEFMASS	Modal Effective Mass
L1	Left Front Leg of the Rocket Launcher System
L2	Right Front Leg of the Rocket Launcher System
L3	Left Backward Leg of the Rocket Launcher System
L4	Right Backward Leg of the Rocket Launcher System
OT1	75% of the Outrigger Thickness
OT2	50% of the Outrigger Thickness
ST1	75% of the Stabilizer Thickness
ST2	50% of the Stabilizer Thickness

# CHAPTER 1

## INTRODUCTION

### 1.1 Background

A rocket is an air vehicle that acquires thrust from its motor. Rocket term is expressed to state the unguided air vehicles. Range of the rocket alters by its motor design. In this thesis artillery rocket systems are examined which are used for ground to ground tactical usage. Rocket launcher systems are utilized to cover a specific area by heavy artillery fire instead of single accurate fire. Depends on the need, some of the rocket launcher systems are little some of the rocket launcher systems are enormous. Independent of its size, a rocket launcher system is composed of subsystems in order to position, orient and increase the accuracy and dispersion of the rocket. A typical rocket launcher system is shown in Figure 1 which is called as RAYO Multiple Launch Rocket Launcher System. Multiple launch refers to more than one rocket storage capacity.

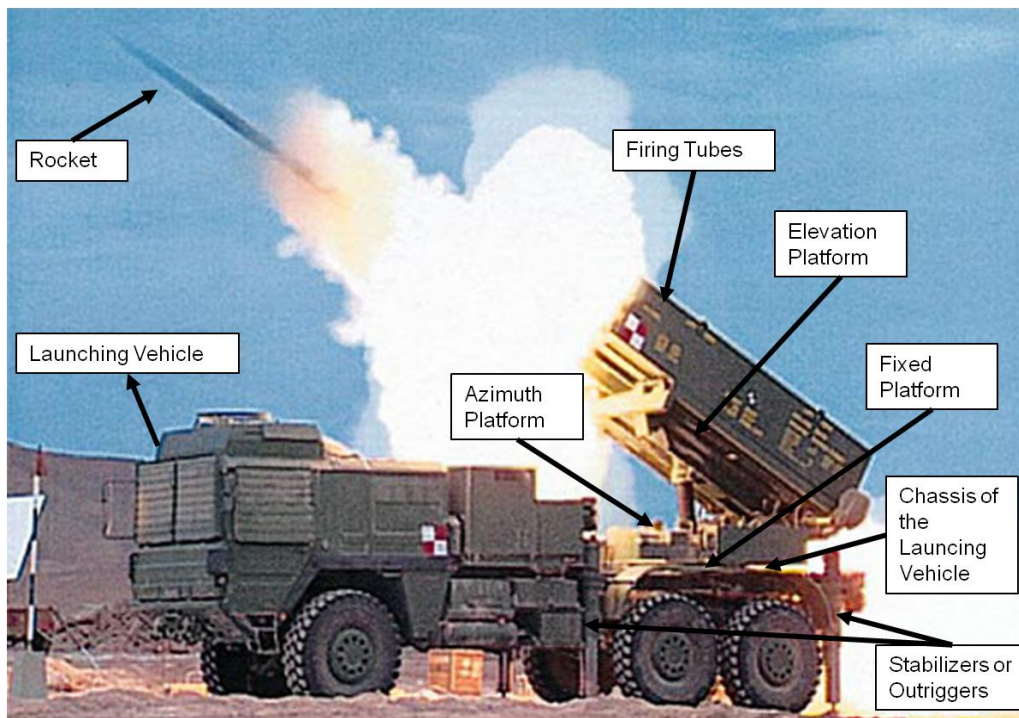


**Figure 1. Photograph of a multiple launch rocket launcher system**

Launcher system consists of a launching vehicle, cradle, firing tubes and munitions.

Launching vehicle is a vehicle that position on the ground with stabilizers and outriggers.

Stabilizers and outriggers are used for increasing the stability of the rocket launcher system.

Outriggers are stabilizers that have deployment property in the horizontal direction, additionally. Some of the launching vehicle has outriggers in order to adjust the stability of the system by using this horizontal deployment property.

Auxiliary chassis is used in order to increase the stability of the rocket launcher system which is mounted on the chassis by clamp attachments. Stabilizers, outriggers and additional chassis are used for heavy firing load munitions.

Cradle is mounted on the launching vehicle and composed of fixed platform, azimuth platform and elevation platform.

Cradle mounted on the launching vehicle by fixed platform.

Azimuth platform is mounted on the fixed platform in order to rotate the cradle about its vertical axis to orient in the azimuth plane.

Elevation platform is mounted on the azimuth platform in order to provide the required elevation angle of the firing tubes.

Firing tubes are mounted on the elevation platform and contains the munitions. Due to the fact that rockets do not have guidance, initial position and orientation is very important for accuracy of the rocket.

Before the rocket leaves the firing tube, rocket and firing tube are in an interaction. This interaction can be separated into four successive phases. As stated by Wicks [2] these phases can be named as "Detent Phase", "Guidance Phase", "Tipoff Phase", and "Free Flight Phase". Detent phase starts after ignition and last with the rocket motion. Guidance phase starts with rockets first motion in the firing tube and last just before the first interaction point of the rocket leaves the firing tube. Tipoff phase starts with the first interaction point of the rocket leaves the firing tube and last with the whole rocket leaves the firing tube. Free flight phase starts with the whole rocket leaves the firing tube and last when the rocket arrives its target. These phases are shown in Figure 2 schematically.

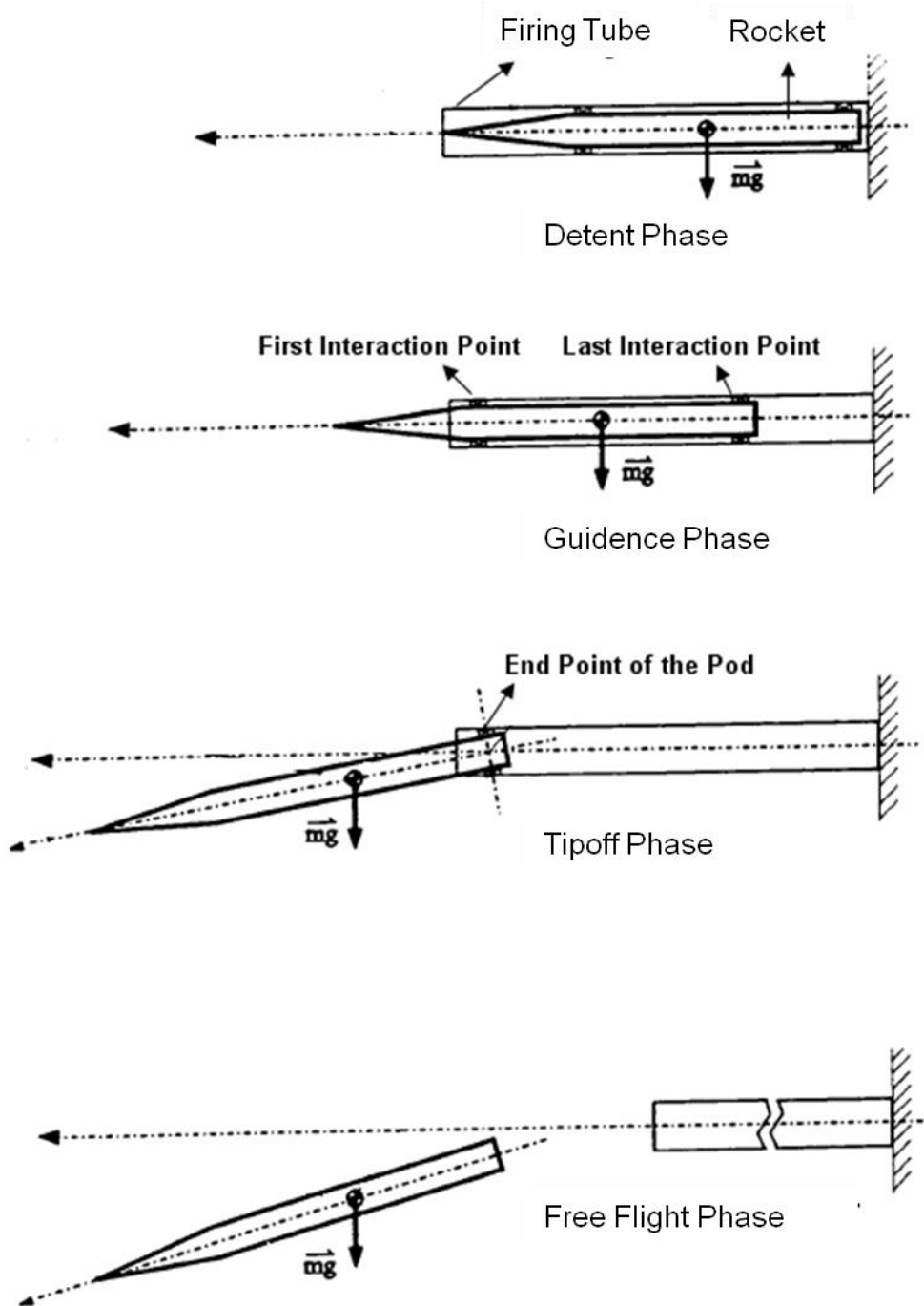


**Figure 2. Four successive phases of the rocket and firing tube interaction [2]**

The primary mission of a rocket launcher system is to support the rocket in the aimed initial direction and maintain the aiming during rocket reaches the sufficient velocity [24]. After that free flight rocket will be stabilized by moments which are



gyroscopic for spin stabilized projectiles [8]. In order to improve dispersion of the rockets stiffness of the rocket launcher system should be increased as practical. Errors which are affecting the launching process are called as "mal-launch". Mal-launch errors are required to be minimized in the engineering point of view [1].

By researching the references [1], [2], [3], [4], [5], [6], [7], [8], [9], [17], [19] and [22] most effective parameters on the rocket launcher system are discovered. These parameters are chassis, auxiliary chassis, clamp attachment of the auxiliary chassis to chassis, stabilizers, outriggers, cradle, joint between cradle and auxiliary chassis, flexibility characteristics of the rocket, motor thrust, mass unbalance and thrust misalignment. Motor thrust, cradle and joint between cradle and auxiliary chassis parameters are examined. In our model, chassis, auxiliary chassis, clamp attachment of the auxiliary chassis to chassis, stabilizers, outriggers will be examined. Flexibility characteristics of the rocket, mass unbalance and thrust misalignment effects are not included in our model. Involved parameters can be explained briefly such that:

**Chassis:** The bottom construction of a rocket launcher system and it is composed of the truck frames [20].

**Auxiliary chassis:** It is an alternative way of changing the dynamic behavior and rigidity of the chassis positively [17]. It is also used for giving extra strength to the system against heavy concentrated loads [19].

**Clamp attachment:** It is used for mounting auxiliary chassis on the chassis with brackets. Welding is not preferred due to fatigue problem [19].

**Stabilizers:** They are used as couples and utilized for increasing the stability of a rocket launcher system.

**Outriggers:** They are deployable stabilizers and used for adjusting the deployment positions in the horizontal direction.

## 1.2 Scope of the Thesis

Main subject of this thesis is dynamics of the rocket launcher systems during the launch of the rocket due to fact that decrease the required time of the development phase in order to produce and market a new rocket launcher system as fast as possible. Therefore, reduced degree of freedom finite element model is composed to implement the modifications and get the results quickly.

In the scope of this thesis, a FORTRAN based ANSYS Parametric Design Language (APDL) code is composed in order to build the parametric simplified FE MODEL, define the boundary conditions and material properties, perform analysis and get the results. This scripting language code allows automating the aforementioned tasks and performs these tasks just by running the code in the finite element software.

The rocket launcher system dynamic is included during so-called detent and tipoff phases. The motion of the rocket after the tipoff phase is not taken into account since it is already well described and documented [8].

Chassis, auxiliary chassis, cross members of both chassis and auxiliary chassis, clamp attachments of chassis and auxiliary chassis, stabilizers, outriggers, cradle and firing tubes are included in order to figure out the dynamics of the rocket launcher system. Rocket and cradle interactions are not taken into account. Rocket thrust is taken into account as plume force. Flexibility characteristics of the rocket, mass unbalance and thrust misalignment effects are not included in our model.

Regarding the methods used in this thesis, numerical methods via commercial software and experimental ones are utilized. Two different finite element models are composed in the scope of the thesis. In the first model, detailed finite element mode is created. In the second model, code language of commercial software is used in order to parameterize the clamp attachment positions on the chassis, stabilizer case cross section, outrigger case cross section and outrigger deployment. Experimental studies are performed in order to verify the aforementioned two

models. Optimization is not convenient and not included in the scope of this thesis since rocket launcher system models have contact nonlinearities and complexity.

The flowcharts of the detailed and simple models of this thesis work are given in Figure 3 and Figure 4 respectively.

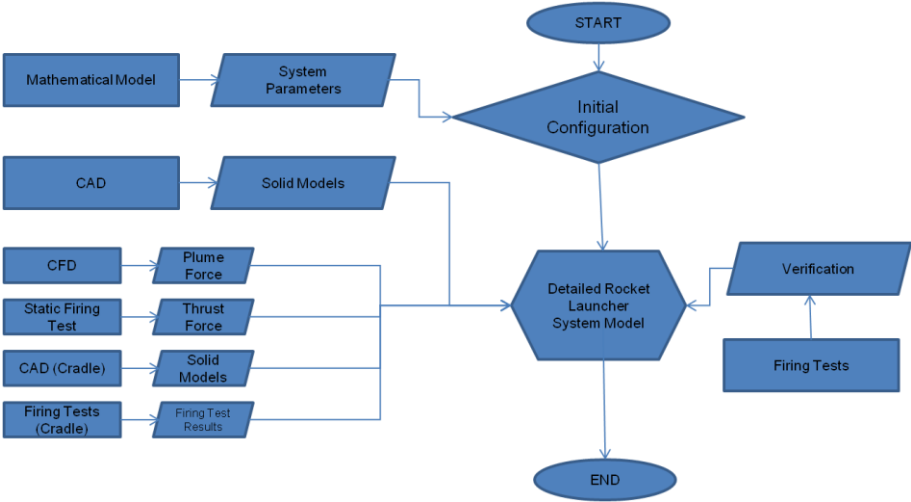


**Figure 3. Flowchart of the detailed modeling approach**

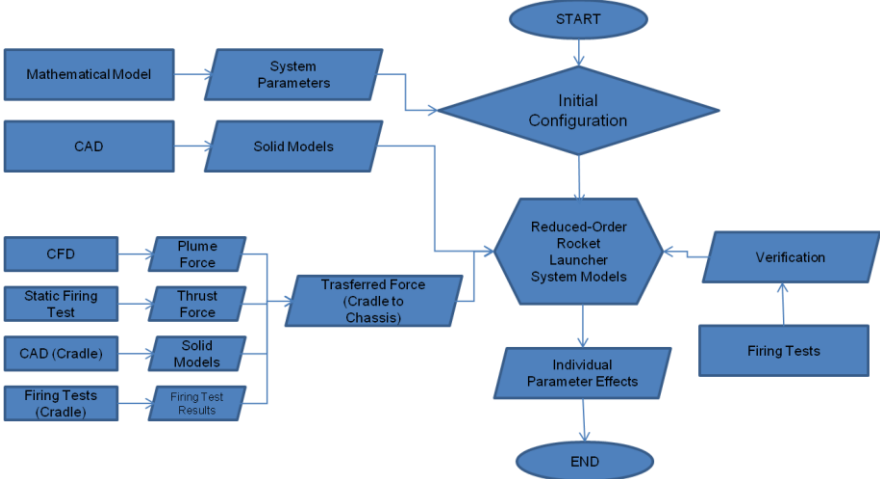


**Figure 4. Flowchart of the simplified modeling approach**

### **1.3 Purpose of the Thesis**

Defense industry is one of the significant industries in a country since it provides power to compete other countries in defense systems. Our country Turkey has an important position both politically and geographically. Thus, our national target is to develop our own defense systems. Defense industry is a challenging industry. Therefore, spent time for the development phase should be minimized. Moreover, spent money for development should also be reduced. To achieve the aforementioned goals, the dynamic deviations of the rocket launcher systems during launch phase must be kept at the lowest level as possible due to the fact that accuracy and dispersion values are significant for artillery rocket systems. Furthermore, artillery rocket systems are crucial in the defense industry.

The main objective of this thesis is to create a simplified model in order to decrease the required time for the development phase of the rocket launcher system since preparing the simplified model is 10 times faster than the detailed model and solution time of the simplified model is 100 times faster than the detailed model. A FORTRAN based ANSYS Parametric Design Language (APDL) code is create in order to compose the parametric simplified FE MODEL, define the boundary conditions and material properties, perform analysis and get the results. This code automates the aforementioned tasks and performs these tasks just by running the code in the finite element software.

Simplified model and detailed model is aimed to be verified by comparing with the experimental studies. Moreover, modifications are done on the simplified model to figure out the change in the behavior of a rocket launcher system under the dynamic load condition.

In other words, spent time, effort and cost aimed to be decreased by creating the simplified finite element model since creating this model, performing dynamic analysis and making modifications on the model and performing dynamic analysis

after modifications can be done faster. For this purpose, a simplified finite element model, detailed finite element models are composed and experimental studies are performed.

It is considered that this study will increase the analysis capabilities of the System Design Department of ROKETSAN Rocket Industries Inc.

#### **1.4 Outline of the Thesis**

The chapters are organized as follows. In Chapter 2, literature survey on rocket launcher models for dynamic analysis and reduction methods used for modeling a rocket launcher system are introduced. In Chapter 3, modeling method, meshing, material properties, boundary conditions and analyses of the detailed FE MODEL are given. In Chapter 4, modeling method, meshing, material properties, boundary conditions and analyses of the simplified FE MODEL are given. In Chapter 5, test study and verifications of the FE MODEL's are given. In Chapter 6, dynamic analyses that are performed on the simplified FE MODEL in order to figure out the individual effects of the parameters and results of the analyses are provided. In Chapter 7, summary and conclusions of this thesis study are given.



## CHAPTER 2

### LITERATURE SURVEY

The main objectives of this thesis are to figure out the dynamic behavior of a rocket launcher system and individual effects of the most significant parameters on it.

The rocket launcher dynamics problem is a very complicated issue. Thus, detailed investigation in the available literature is required in order to comprehend the every detail. On the other hand, there are limited open source about the rocket launcher systems due to the fact that studies on this subject are specific concepts and mostly not published or published as secret. Even though, most of the companies in defense industry have their own techniques and held as confidential, there are limited numbers of articles in this subject. Models used in these articles are mostly mathematical models with a few degrees of freedom. In addition to this, several software programs are utilized on chassis design. Hence, abilities of the software's on this subject iare also investigated.

Işık [1] is one of the engineers who worked on dynamic behavior of the rocket launcher systems in ROKETSAN. In his work, he investigated upper part of the launcher systems such that only cradle and firing tubes are included. He created, simple mathematical model, finite element model and flexible multi-body model. After that, he evaluated the results under same dynamic load conditions. Furthermore, he compared his approaches with the experimental results. Finite element model of Işık [1] is shown in Figure 5.

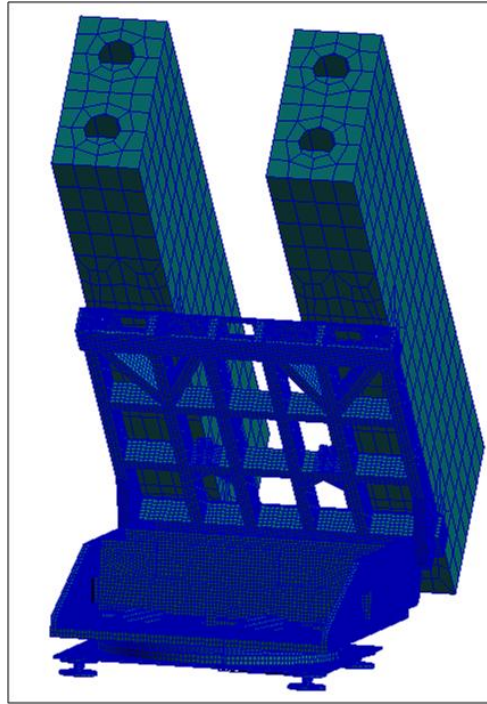


**Figure 5. Finite element model by Işık [1]**

Cochran [3] created a model composed of rigid bodies which are connected with flexible elements such as springs and dampers in order to insight into mal-launch parameters of the rocket. In his study, both interaction between rocket with the launcher system and launcher system with ground is taken into account. The rocket launcher system has three rotational degrees of freedom in yaw, pitch and roll axes. Rocket is free to move in the firing direction. The model of the launcher system of Cochran [3] is shown in Figure 6.



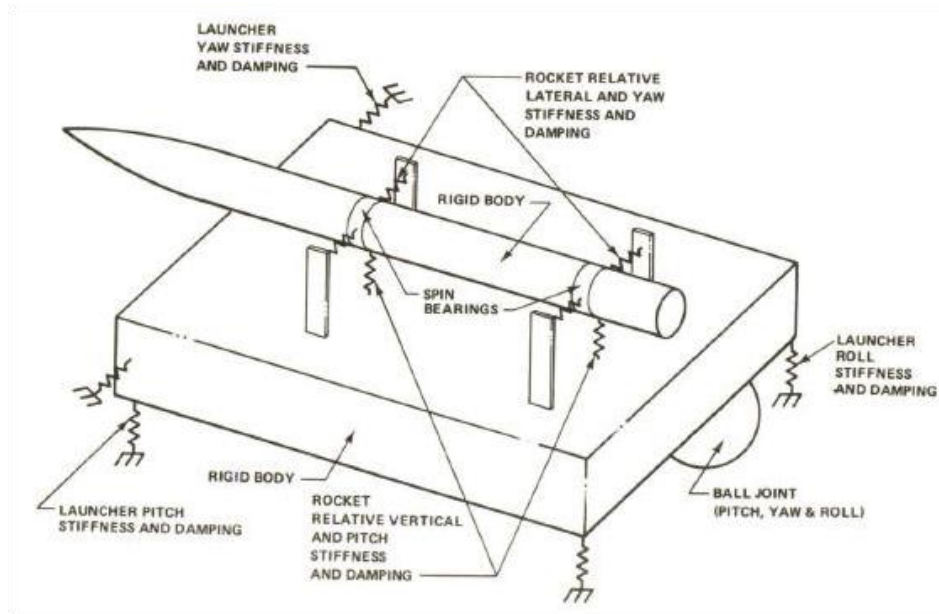


**Figure 6. Rocket launcher system model by Cochran [3]**

Dziopa et al [4] developed a four degrees of freedom mathematical model of the rocket launcher system. The launcher system has rotational degrees of freedom in the yaw and pitch axes. Moreover, the launcher has a degree of freedom in the vertical axis. Rocket has only degree of freedom in the firing direction. Bodies are considered as rigid, connections are modeled as flexible such that springs and dampers are utilized. In order to estimate the dynamic response of the system, Lagrange's energy method is used. The model of the launcher system of Dziopa [4] is shown in Figure 7.

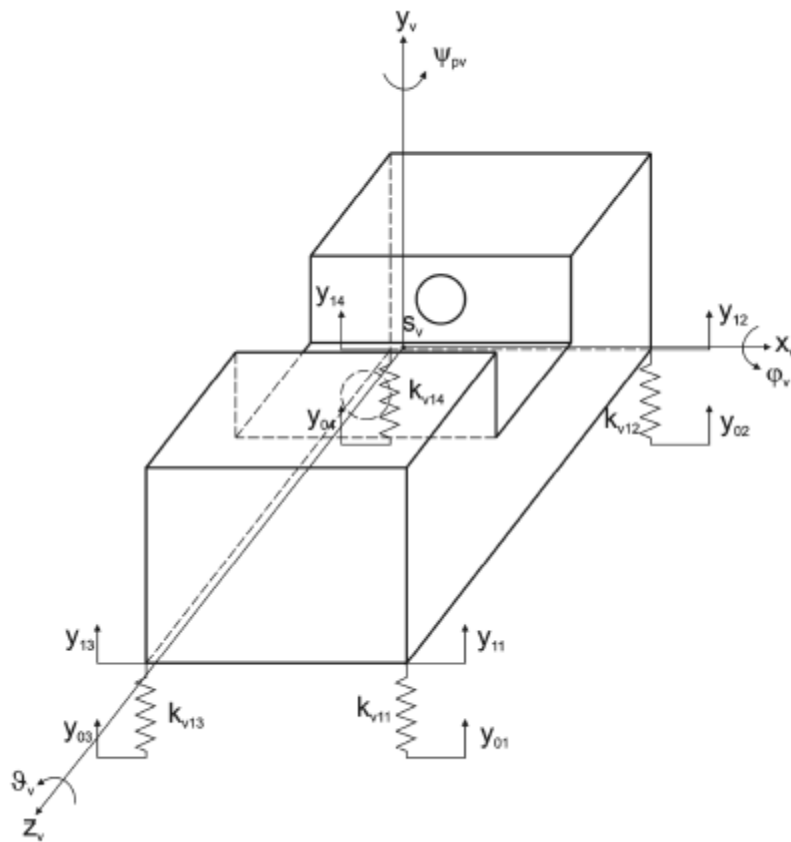


**Figure 7. Rocket launcher system model by Dziopa [4]**

Lee and Wilms [5] proposed four degrees of freedom rocket launcher model. Rocket launcher system is modeled as rigid body and its elastic behavior is provided by using torsion springs and dampers. Plume effects on the firing tubes are also included in the model. The model proposed by Lee and Wilms [5] is shown in Figure 8.

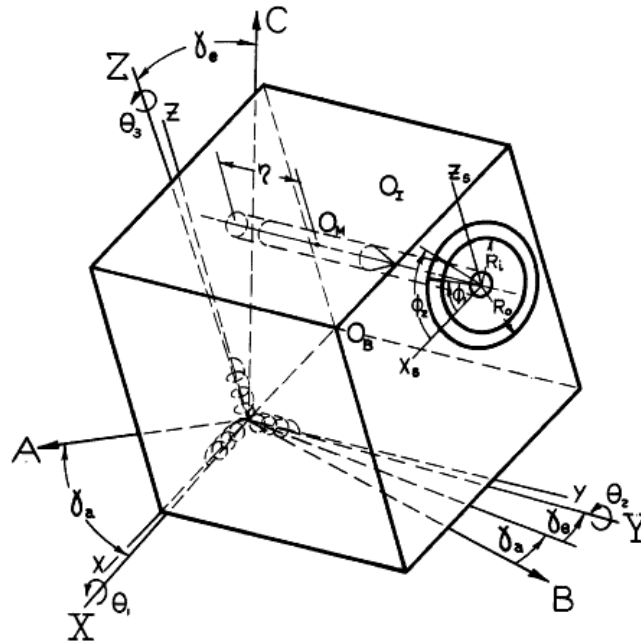


**Figure 8. The model proposed by Lee and Wilms [5]**

Zhang and Xiao [6] introduced a rocket launcher model which includes the vehicle part also. Their model is composed of launching vehicle, yaw body, pitch body and rocket. Vehicle is connected to the ground with elastic parts such as springs and dampers. Yaw body is also connected to the vehicle by torsion spring and dampers. Pitch body is connected with the yaw body with rigid and flexible connections. Interactions between the bodies are evaluated. The model introduced by Zhang and Xiao [6] is shown in Figure 9.

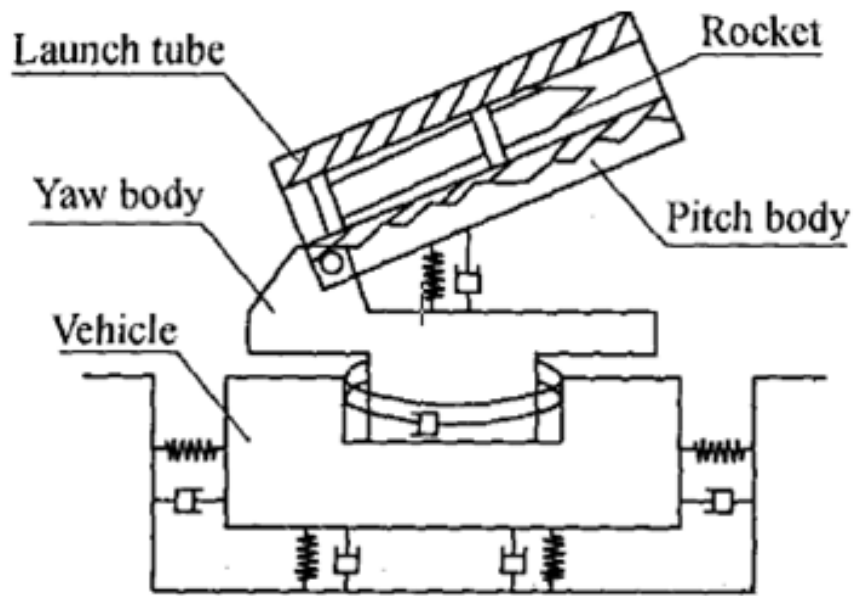
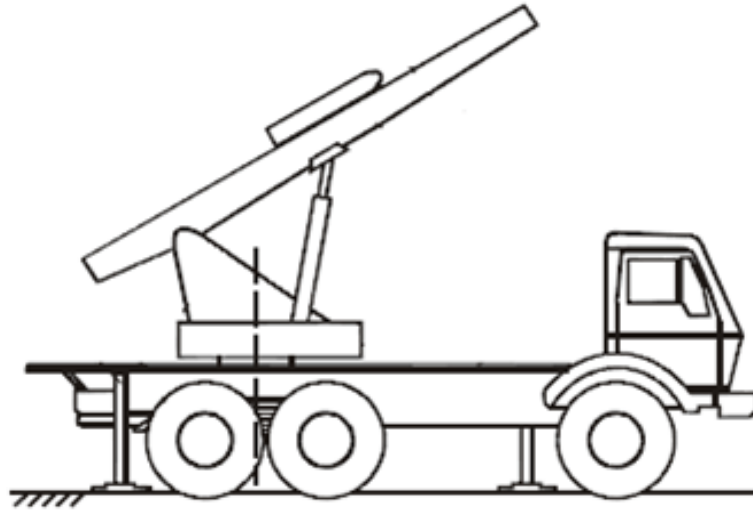


Figure 9. The model introduced by Zhang and Xiao [6]

Selmic et al. [7] provided a rocket launcher model including launcher system chassis, supports such as stabilizers and pneumatics. Chassis is modeled as rigid body which has degrees of freedom in the vertical axis and rotational axis in the yaw axis. Stabilizers and pneumatics are modeled as rigid. On the other hand, ground is modeled as elastic by using spring and damper. Firing tube is modeled as flexible body. Cradle and launching vehicle connection is modeled as rigid. Lagrange's equation is used in order to obtain the dynamic response of the rocket launcher system. The model provided by Selmic [7] is shown in Figure 10.



**Figure 10. The model provided by Selmic [7]**

Cömert. [8] studied the dynamics of interaction between rocket and its launcher. He investigated the dominant flexibility effects in a rocket launcher system. Then modeled the launcher system as rigid parts on flexible supports. Rotational equation of motion is used for evaluating the yaw, pitch and roll angles, angular velocities and angular accelerations with respect to time.

Raducanu et al. [9] studied the dynamics of the rocket launcher systems and evaluated rocket trajectories by changing the launcher parameters and initial conditions. They modeled the rocket launcher system as rigid bodies such as vehicle chassis, tilting platform and rockets. Moreover, these rigid body connections are modeled with elastic elements. They studied the launching oscillations in order to evaluate the accuracy of the firing precisely. The model provided by Raducanu [9] is shown in Figure 11.

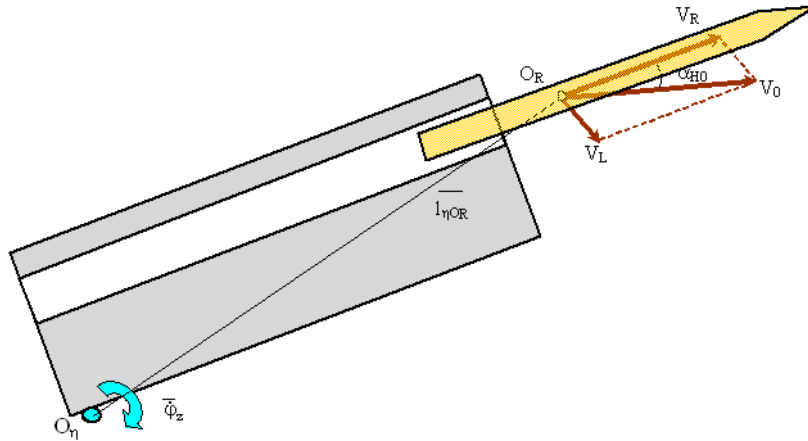


**Figure 11. The model utilized by Raducanu [9]**

Rixen [10] illustrated the dual Craig-Bampton approach efficiency for decreasing the solution time of the dynamic analysis. He used aforementioned method for very large linear systems such as in the order of millions of degrees of freedom due to the fact that inverse iteration of a dynamic analysis such large finite element models requires too much power, storage and time. Furthermore, he composed reduced subparts such as super elements in order to get fast and effective results. In his paper, a numerical solutions of the reduced models and non-reduced models of a beam frame are compared in order to show the efficiency of the reduction method applied.

Fransen [11] studied sub-structuring techniques and overview of these methodologies usage in launcher dynamic analysis. In his paper, fixed interface Craig-Bampton method is outlined between component mode synthesis methods in order to reduce the costs of transient analysis computation. The total motion of the structure is modeled with rigid body motion of the structure and elastic motion of the system relative to the rigid body motion. In his model, pre-stress and fluid effects are also taken into account.

Zhao et al. [12] in their work proposed the theory of ADAMS flexible body fundamentals and stated some methods of building flexible bodies in ADAMS software. They stated the importance of the modeling the elastic deformations as well as the rigid body motions of the macro model for understanding the dynamic behavior of the systems. Moreover, they mentioned the usage of the modal neutral file which includes the small and linear elastic deformation information of the system generated by a finite element program. Complexity of the geometry of the model is not effective when the deformations are small and model is linear. Systems dynamic behavior is transferred to ADAMS by converting the finite element models system matrices in modal domain. At the end of the paper, a tower crane's dynamic analysis is performed in order to show the validity of the approach.

Zhang et al. [13] created chassis/suspension models with beam elements in order to evaluate the vehicle chassis/suspension dynamic analysis. They used both rigid and flexible beam models. These two models results are compared in this paper. They also stated that rigid body approach is commonly used technique; small deformations are required to be taken into account for further analyses such as durability of the vehicle body.

Tiso et al [14] introduced a reduction method for the geometrical nonlinear finite element analysis of the shell structures. Linear modal superposition and perturbation approaches are utilized in order to decrease the computation cost for complex and detailed finite element analyses. In their studies, the systems have geometrical nonlinearities under dynamic loads are handled by using second order modes and displacement fields.

Liu [15] studied frequency response function based substructure synthesis method in order to evaluate the reaction force and velocities of the vehicle body. In his study, vehicle body is derived from frequency response function by coupling with finite element analysis model in order to predict the total system dynamic behavior.

Hadipour et al. [17] developed a finite element model in order to investigate the increase in rigidity of the chassis by adding auxiliary chassis. Modal analysis is

performed by using ANSYS software in order to show how the auxiliary chassis changes the vibration characteristics of the chassis. They also stated that adding auxiliary chassis on the main chassis is an alternative and popular way of permitting overload and increasing rigidity of the system and applied by truck producers. Finite element model created by Hadipour [17] is shown in Figure 12.

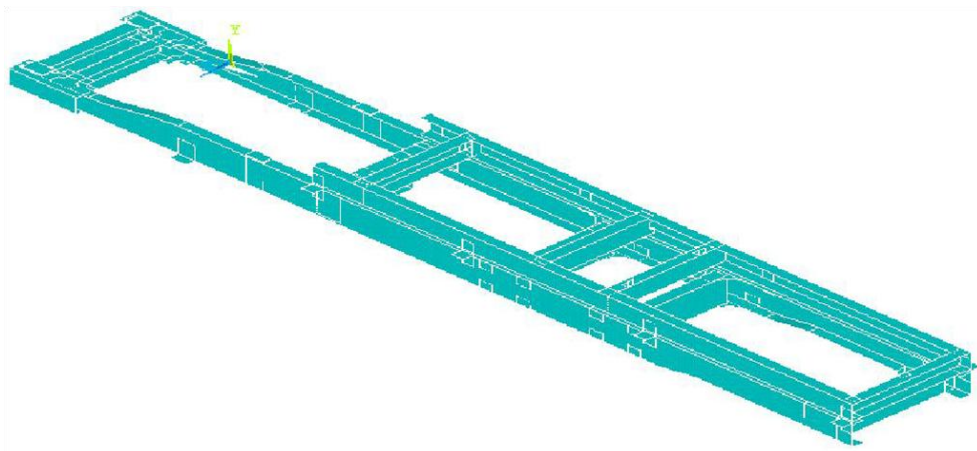


**Figure 12. Finite element model created by Hadipour [17]**

Roslan et al [18] studied the key characteristics of a truck chassis. They stated that modal analysis is performed via finite element method then modal updating of the truck chassis model is done by performing experimental modal analysis in order to predict the dynamic behavior of the vehicle system. Cross members, connection brackets and other major parts are taken into account in their finite element model. Chassis development flow chart created by Roslan [18] is shown in Figure 13.



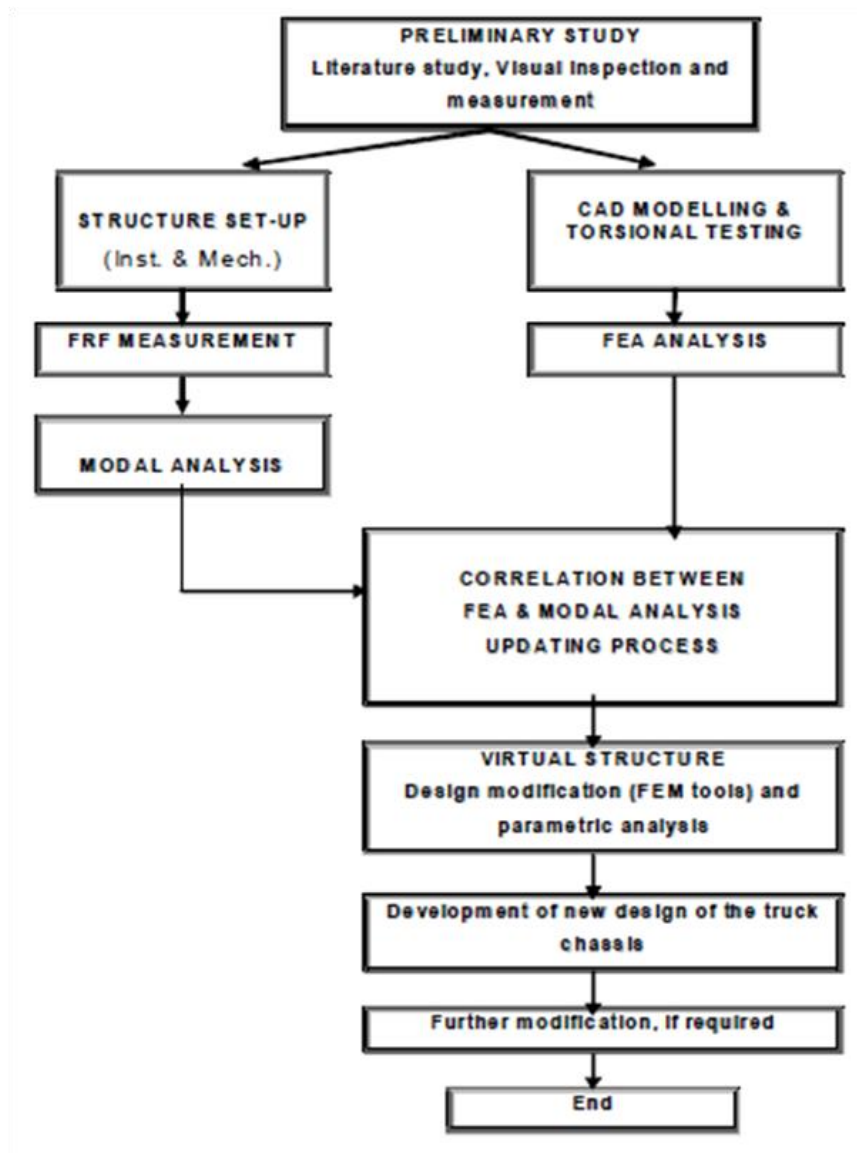


**Figure 13. Chassis development flow chart created by Roslan [18]**

Sane et al [22] studied on robustness of the chassis under different load cases by using finite element model. Chassis components are meshed with thin shell elements. They also used finite element method for shortening the design and development process.

After reviewing literature, it can be concluded that there are different kind of approaches for decreasing the degree of freedom of a rocket launcher system in order to prepare the model and get the results as fast as possible. Some approaches can be grouped that rigid bodies and elastic elements are utilized in order to reduce the degree of freedom and evaluate the dynamic behavior of the system. Other approaches can be grouped that modal reduction techniques are utilized in order to reduce the degree of freedom of the system.

In this thesis, lumped mass, shell and beam elements are utilized in order to reduce the degree of freedom of the system. Modal reduction techniques are not used due to the fact that system has contact non-linearity.

Some of the studies included the chassis, auxiliary chassis, connections of them and chassis cross members by creating their finite element models in order to investigate the further dynamic analysis although most of the studies try to comprehend the major parameters of the dynamics of the system and focus on improving their design by performing quick modifications.

In this thesis, some parts of the simplified model are modeled as parametric in order to make modifications of the rocket launcher system's major parameters just by changing a value in the finite element code since the main objective is to get the dynamic behavior of the system.

## **CHAPTER 3**

### **DETAILED FINITE ELEMENT MODEL**

Finite element method (FEM) is a computational method and finite element analysis (FEA) consists of a computer model of a design which is analyzed for specific outputs. This method is utilized for both new product design and refinement of an existing product. FEA utilize a complicated system of points called nodes which produce a grid called mesh. This grid composed of structural and material properties of the system in order to figure out how the system behaves under certain loading conditions.

In our study, two different finite element models are composed and FEA are performed on these models. The first finite element model is detailed model which contains most of the details in the real rocket launcher model. The second model is simplified FE MODEL which is parametric model and includes necessary kinematic and elastic connections. Modal, static and dynamic analyses are performed with these two models. Moreover, they are verified by a prototype in the experimental studies. Detailed FE MODEL, simplified FE MODEL and a representative prototype are shown in the Figure 14.

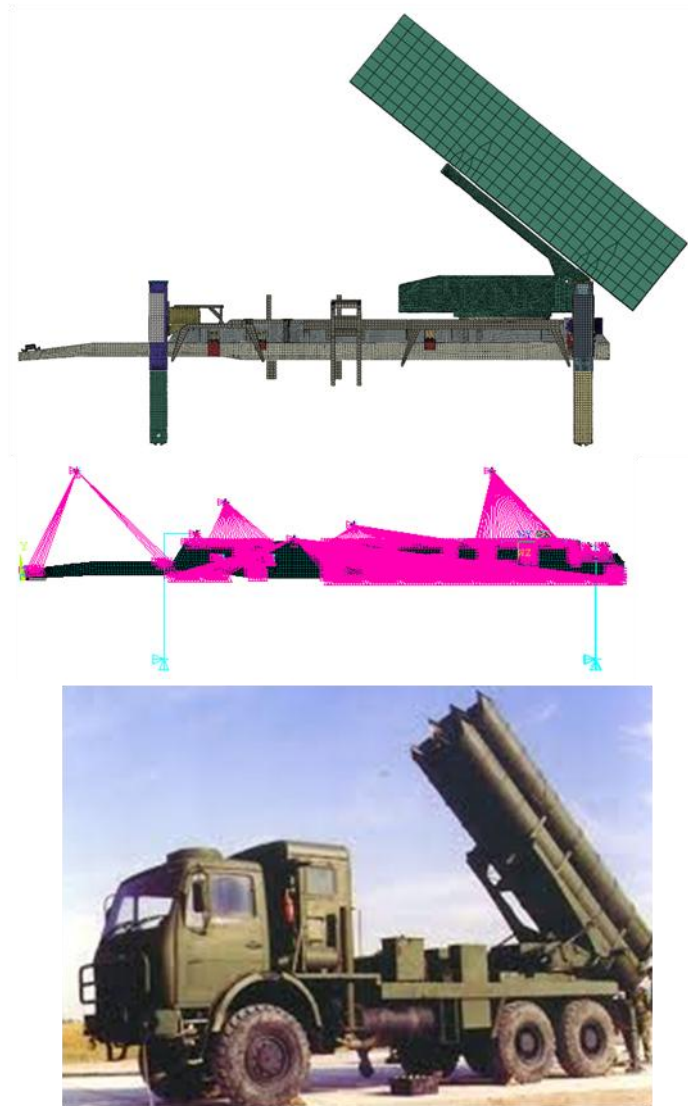


**Figure 14. Detailed FE model, simplified FE model and a representative prototype**

### **3.1 Detailed Finite Element Model of the Rocket Launcher System**

Detailed FE model of the rocket launcher system is composed of firing tubes, cradle (elevation platform, azimuth platform and fixed platform), auxiliary chassis,

chassis, clamp attachments, stabilizers and outriggers. Truck and other less important parts are modeled as lumped mass with inertia. Rocket is not included in the model. On the other hand, effects of the rocket on the launcher system is included by applying the plume force.

### **3.2 Modeling Method And Meshing of the Detailed Finite Element Model**

Detailed FE model is composed of approximately 3.5 million DOF and includes solid, shell and beam elements. A group of people worked in order to create the detailed FE model since it is a huge model.

When determining the type of the elements, the ratios of the length over thickness of the parts are examined. If the ratio is greater than 20 then 2D shell elements can be utilized as a rule of thumb. Otherwise, solid elements should be used for a better approach. Moreover, in the non-critical zones some simplifications are performed such as filling little holes and deleting chamfers. Meshed detailed rocket launcher finite element model can be seen in Figure 15.

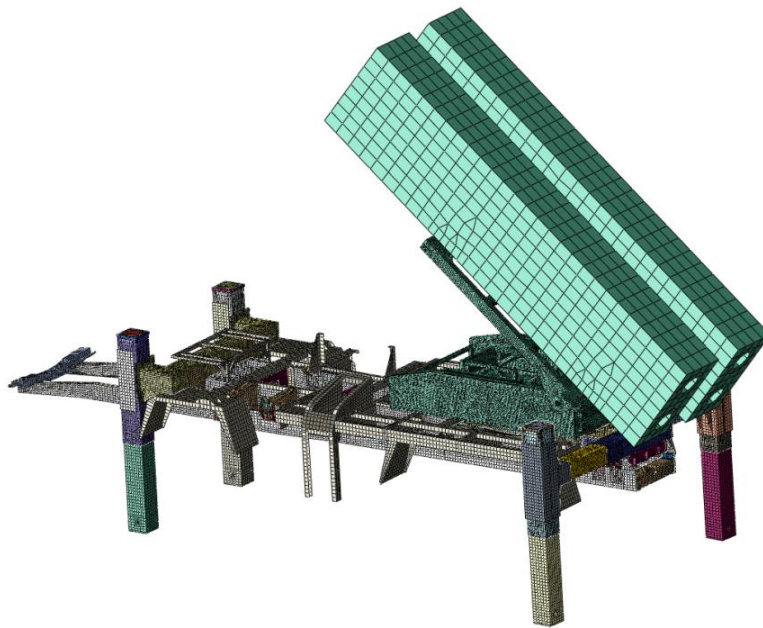


**Figure 15. Meshed detailed rocket launcher finite element model**

Stabilizers and outriggers are modeled as deployed when the firing is performed. Hydraulic system in the stabilizers and the outriggers are modeled as truss elements by giving stiffness in the axial direction. In Figure 16, positioning of the stabilizers and the outriggers is given. In Figure 17, hydraulic system in the stabilizers and the outriggers is given.

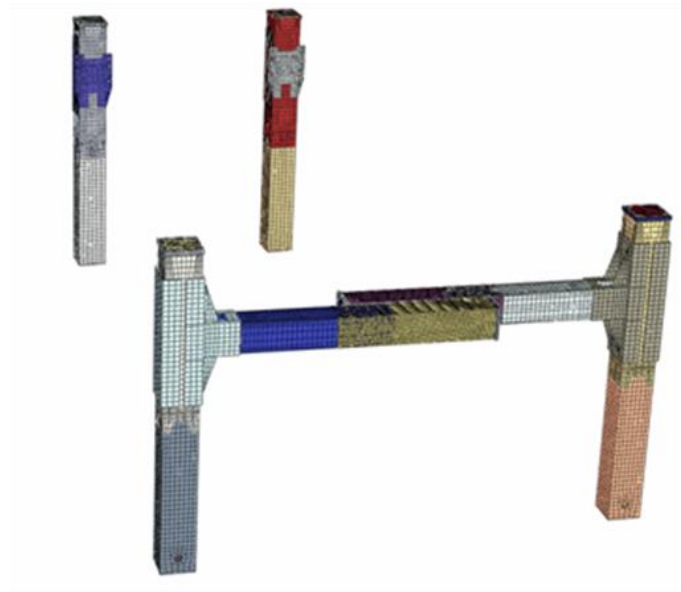


**Figure 16. Positioning of the stabilizers and the outriggers**

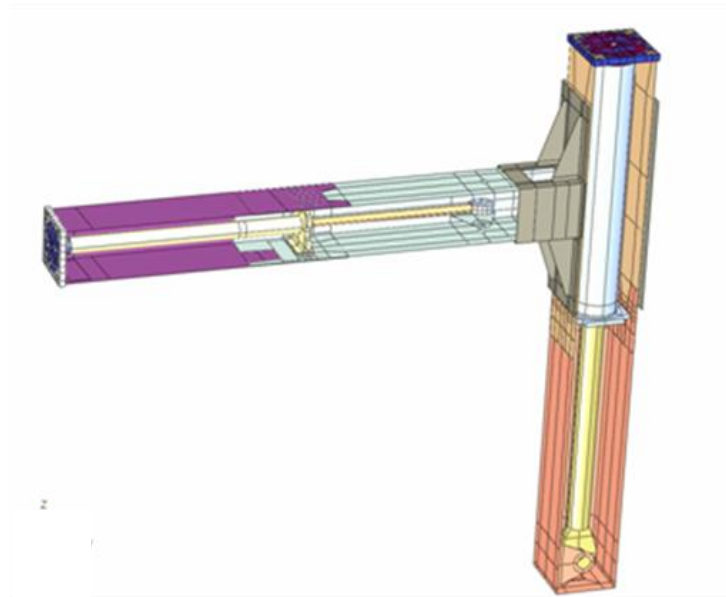


**Figure 17. Hydraulic system in the stabilizers and the outriggers**

Telescopic structure of the stabilizers and outriggers is given in Figure 18.

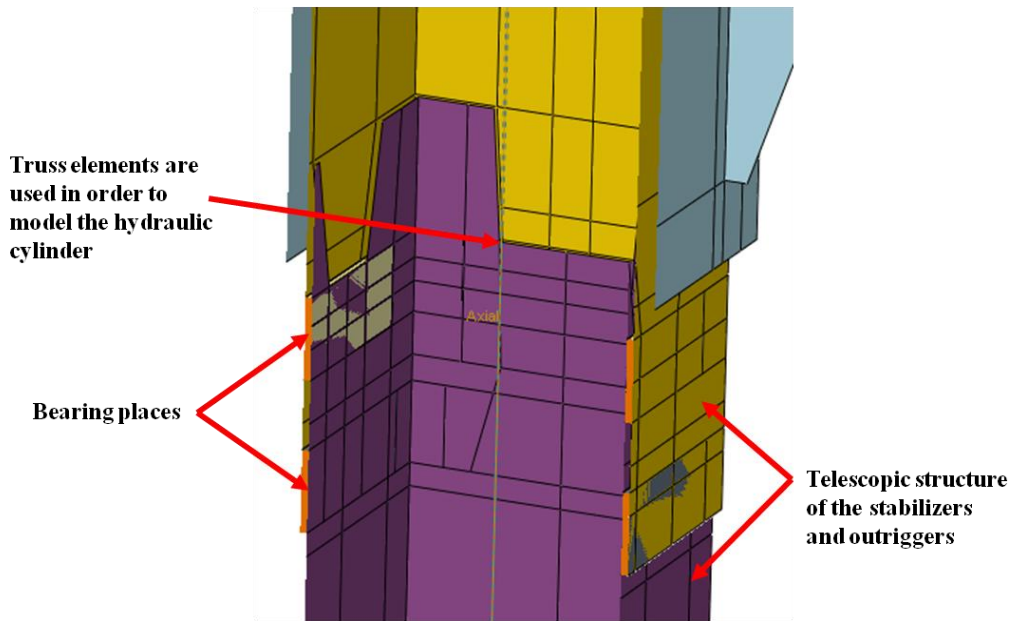


**Figure 18. Telescopic structure of the stabilizers and outriggers**

Glue contacts in the stabilizers and outriggers are given in Figure 19.

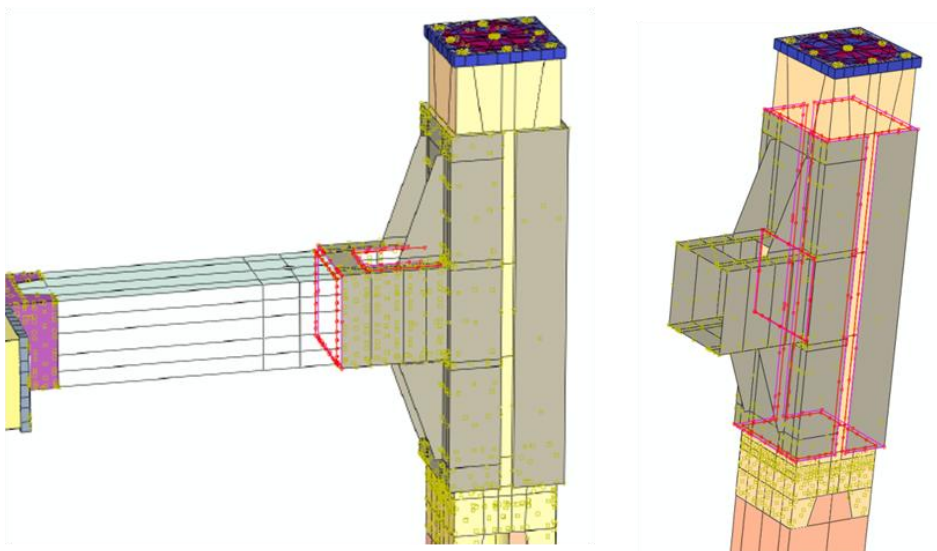


**Figure 19. Glue contacts in the stabilizers and outriggers**



The connection between auxiliary chassis and stabilizers is shown in Figure 20.

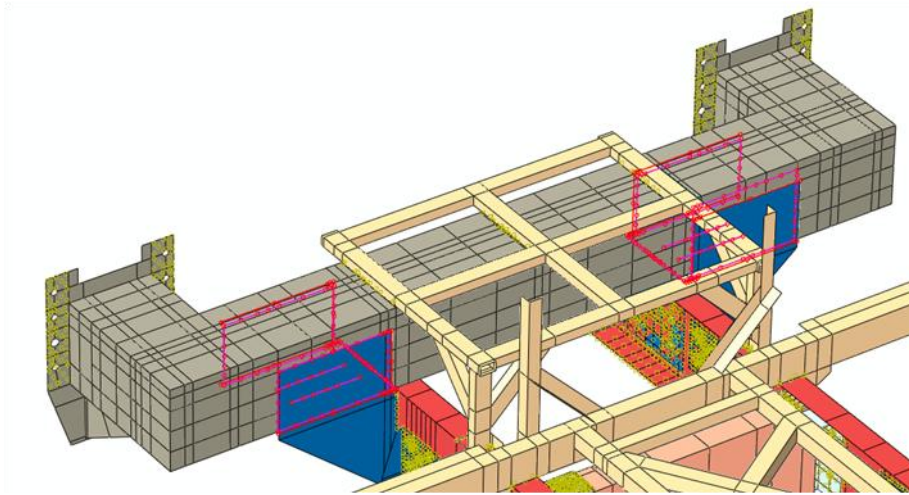


**Figure 20. Contact between auxiliary chassis and stabilizers**

Clamp attachments between the chassis and the auxiliary chassis are modeled. Beam elements are used in order to represent the bolts between upper and the lower parts of the clamp attachments. Contact is defined between auxiliary chassis and the lower part of the clamp attachment. This type of connection provides flexibility to the launcher vehicle for road trip. There are 6 clamp attachments in the rocket launcher system. The number of the clamp attachments is determined by considering the launcher vehicles road trips. If the number of the clamp attachments is increased, rigidity of the connection between the chassis and the auxiliary chassis will be increased. As a result, damage will be occurred during road trips. If the number of the clamp attachments is decreased, rigidity of the connection between the chassis and the auxiliary chassis will be decreased. As a result, stiffness of the rocket launcher system will be decreased and advantage of using auxiliary chassis will be lost. Clamp attachments between the chassis and the auxiliary chassis are shown in Figure 21.

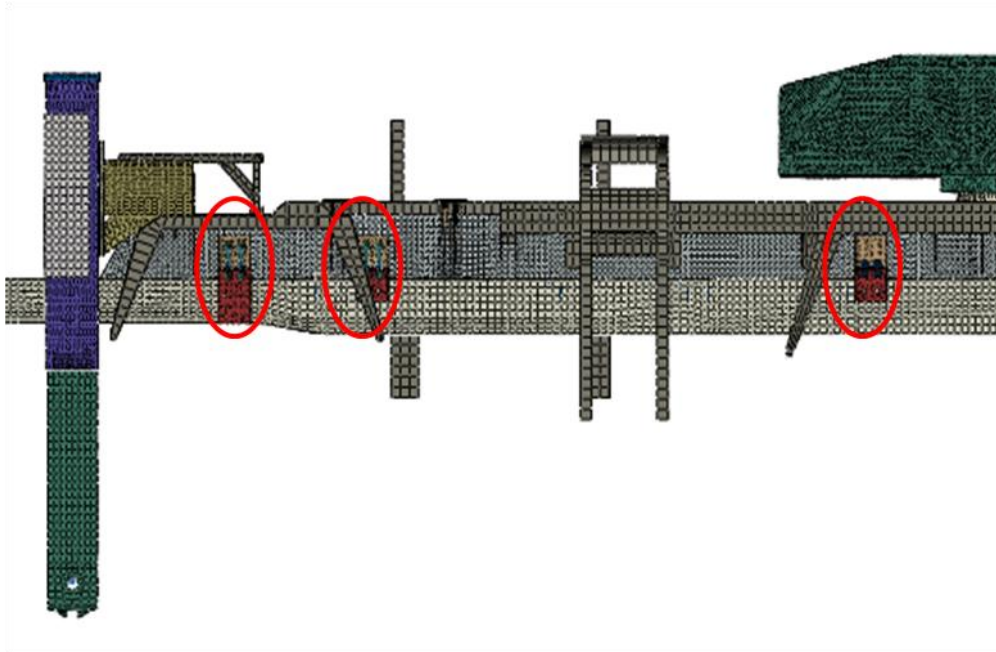


**Figure 21. Clamp attachments between the chassis and the auxiliary chassis**

Details of the clamp attachments are shown in Figure 22.

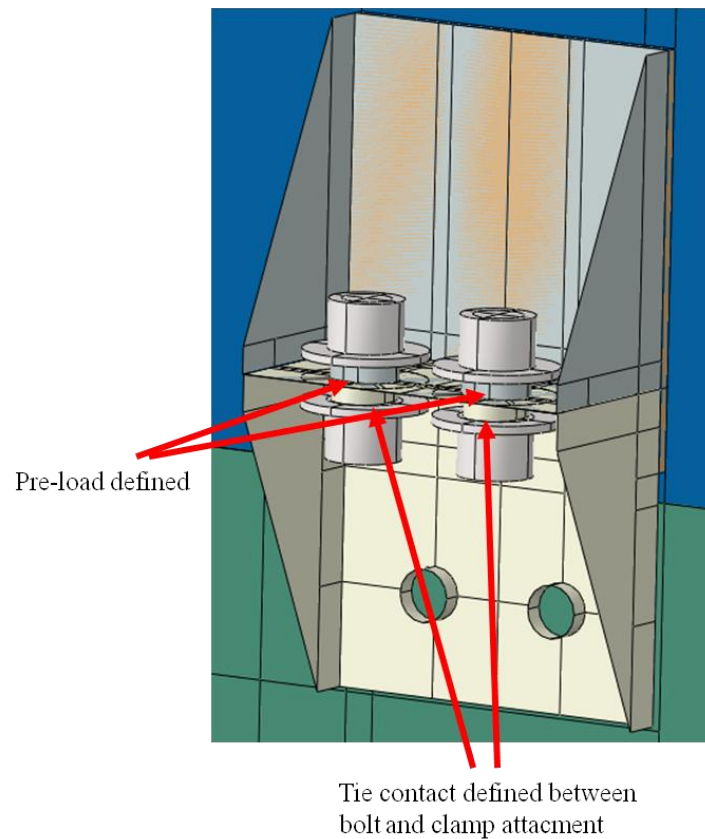


**Figure 22. Details of the clamp attachments**

Furthermore, contact is defined between the chassis and the auxiliary chassis in order to take the stiffness of the both chassis and the auxiliary chassis into account. Friction coefficient is set as 0.1 for both static and dynamic solutions. Cross members of the chassis are modeled with shell elements and glue contact are defined between chassis and the cross members in order to represent the connection. The connection between cross members and chassis is given in Figure 23.

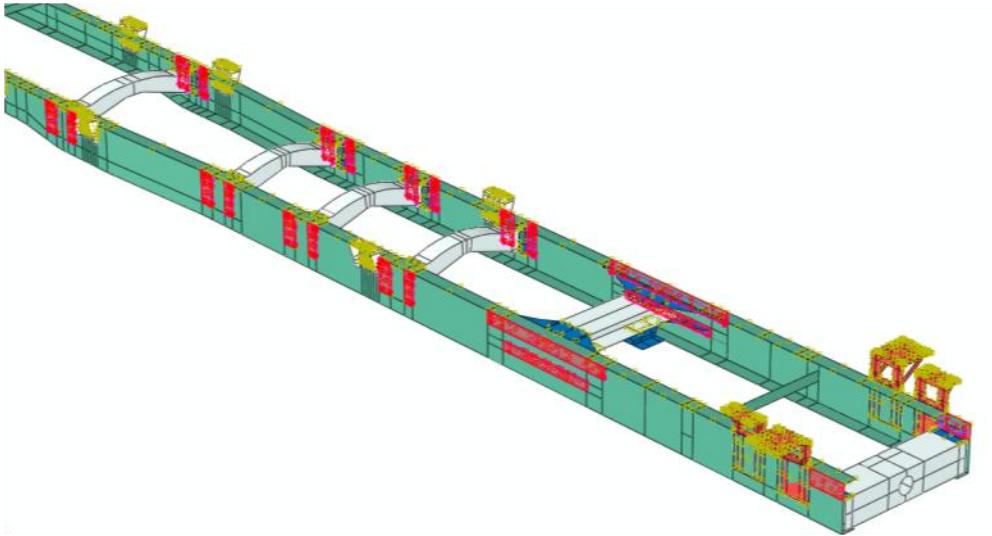


**Figure 23. The connection between cross members and chassis**

Full cradle model is created. Cradle is mounted on the auxiliary chassis with fixed platform. Cradle's spot welding are modeled with fasteners, and other welding connections are modeled with glue contact. Cradle's welding connections are shown in Figure 24.

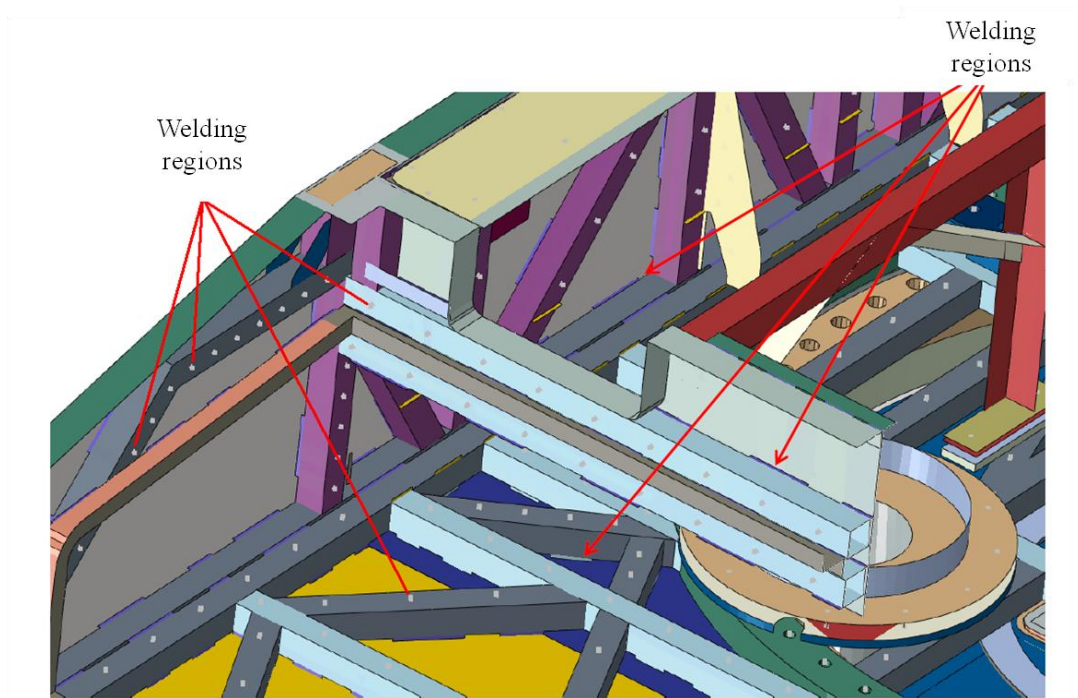


**Figure 24. Cradle's welding connections**

Azimuth platform is located on the fixed platform with slewing ring mechanism. Slewing ring finite element model is shown in Figure 25.

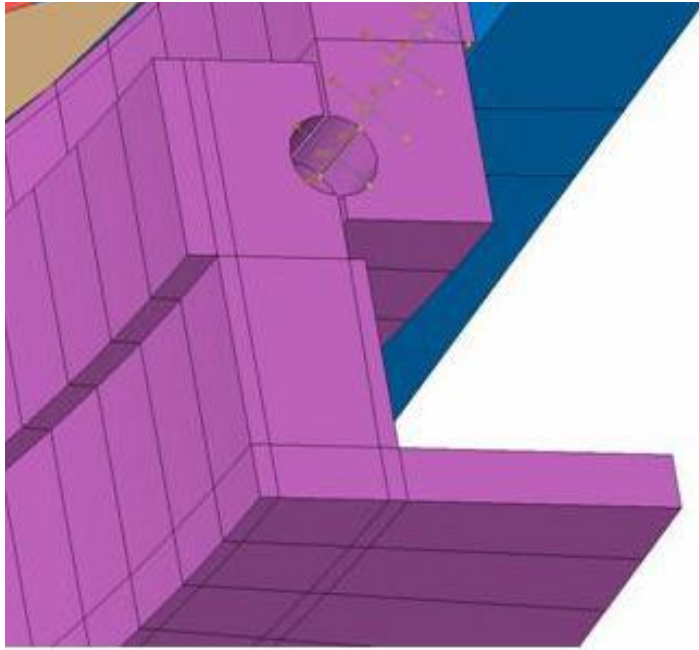


**Figure 25. Slewing ring's finite element model**

Spring elements are utilized in order to represent the slewing ring's ball parts. Spring elements are shown in Figure 26. Slewing ring modeling is verified in Isik's studies [1].

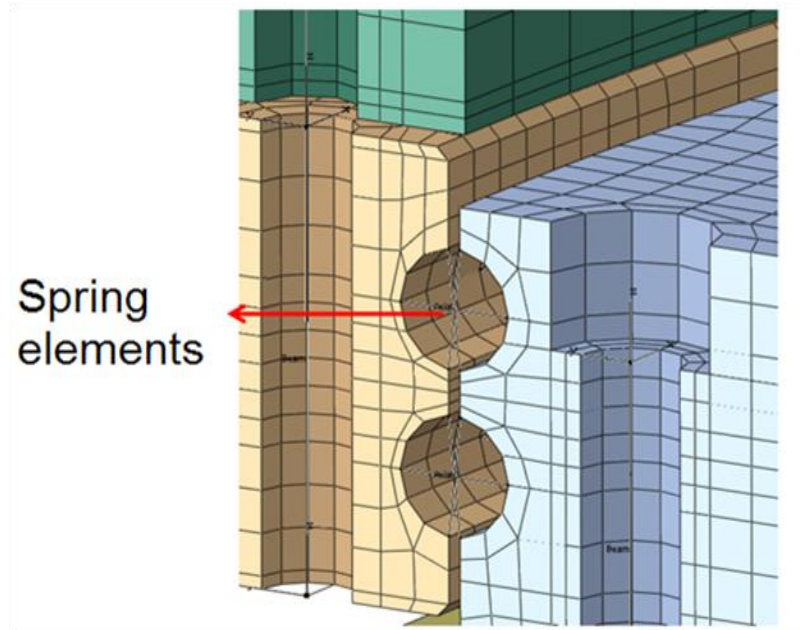


**Figure 26. Spring elements for representing slewing ring's ball parts**

Lumped masses with inertial effects are defined in order to represent the non-structural parts' mass and inertia effects. Only for truck head's lumped mass connection is modeled as rigid constraint since it provides the rigidity. The other lump mass connections are modeled with force distributed connections. Lumped masses are shown in Figure 27.



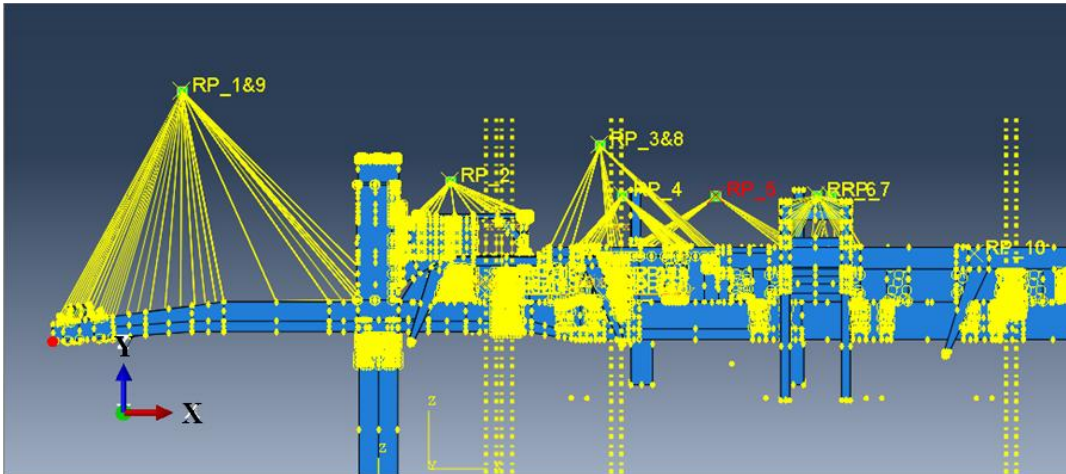


**Figure 27. Lumped masses of the rocket launcher system**

### **3.3 Material Properties and Boundary Conditions for the Detailed Finite Element Model**

In the rocket launcher model, every part is produced from St-37 steel material. Properties of St-37 steel can be seen in Table 1.

**Table 1. Material properties of St-37**

Elastic Modulus	Poisson's Ratio	Density	$\mu$
205 GPa	0.3	7800 kg/m <sup>3</sup>	0.1

Zero displacement in three axes as the boundary condition is applied to the stabilizers' and outriggers' bottom positions. Spherical joint approximation is used for modeling the connection between stabilizers, outriggers and the ground.



### **3.4 Modal Analysis of the Detailed Finite Element Model**

In order to figure out the rocket launcher system's dynamic behavior, modal analysis is performed. Moreover, modal effective masses are calculated to determine the each mode's contribution to the rigid body motion. Modes that have relatively high modal effective masses, can be easily excited by base excitation. For modal analysis, zero displacement in three axes as the boundary condition is applied to the stabilizers' and outriggers' bottom positions. Spherical joint approximation is used for modeling the connection between stabilizers, outriggers and the ground. Furthermore, glue contact is applied between chassis and the auxiliary chassis and other contact areas in order to get a linear finite element model. To get better results, modal masses should be at least 80% of the actual model. Therefore, 20 modes extracted from the modal analysis and 9 mode are examined due to the fact that minimum %80 of the modal effective mass criteria is satisfied in the X and Y directions which are defined in Figure 27. Modal analysis results are given such as natural frequencies and modal effective mass values in Table 2.

**Table 2. Modal analysis results of the detailed model**

Mode No	Natural Frequencies (Hz)	X-Comp.	Y-Comp.	Z-Comp.
1	3.0	0.0001	0.0000	3.0166
2	3.7	0.0047	0.0140	8.6458
7	6.4	6.7030	7.3392	0.0003
9	8.8	0.0203	0.0037	5.9737
10	10.5	2.7783	12.6130	0.0021
11	12.5	2.5380	0.1564	0.0346
13	16.2	12.0570	0.0438	0.0066
19	23.4	0.3204	1.6061	0.3212
20	24.5	0.0002	1.6535	0.5455
Modal Effective Mass (MEFMASS)	Mass	24.4220	23.4297	18.5463
MEFMASS/Actual Mass		0.8972	0.8608	0.6813

The second, seventh, ninth, tenth and thirteenth modes are more significant when compared with the other modes in Table 2.

The first mode is a combination of torsion mode of the cradle and bending mode of the front part of the chassis. Mode shape is given in Figure 28.

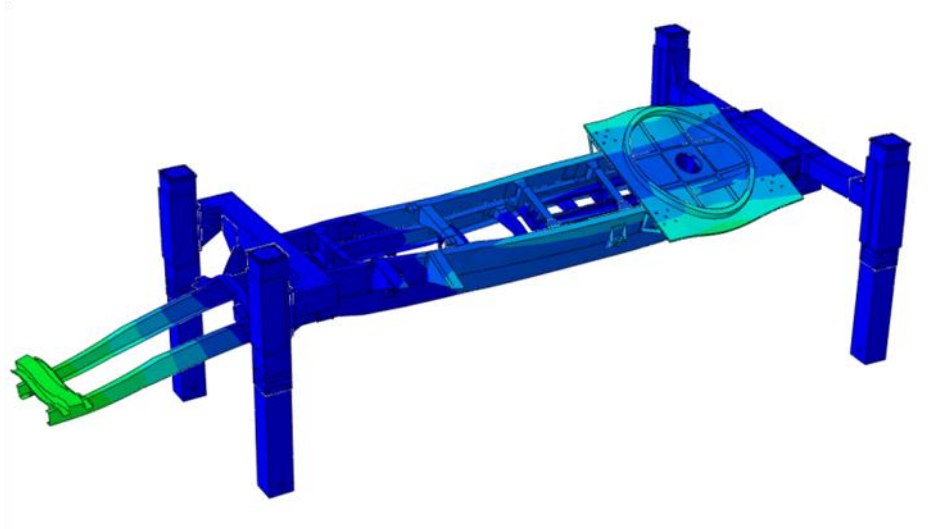


**Figure 28. The First mode shape of the detailed model**

The second mode is torsion mode of the front part of the chassis and mode shape is given in Figure 29.

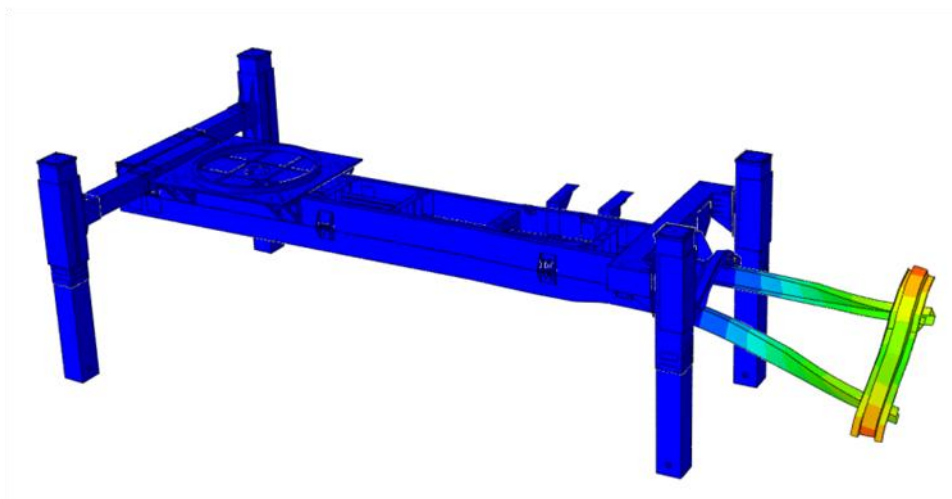


**Figure 29. The second mode shape of the detailed model**

The seventh mode is bending mode and mode shape is given in Figure 30.

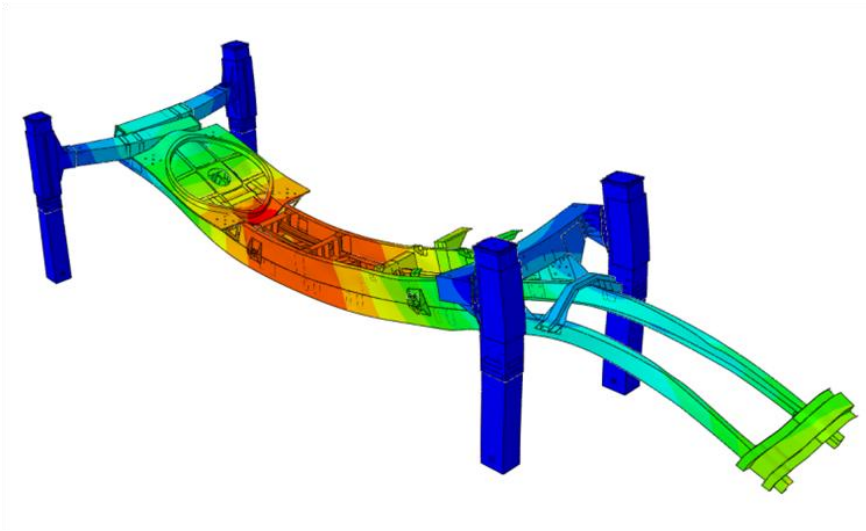


**Figure 30. The 7th mode shape of the detailed model**

The ninth mode is bending mode in the transverse direction and mode shape is given in Figure 31.

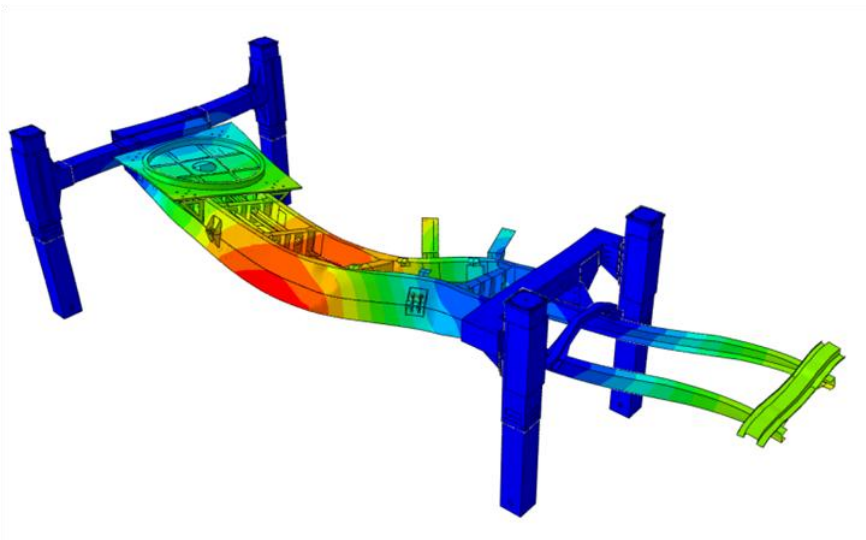


**Figure 31. The 9th mode shape of the detailed model**

The tenth mode is bending mode of the backward part of the chassis and mode shape is given in Figure 32.

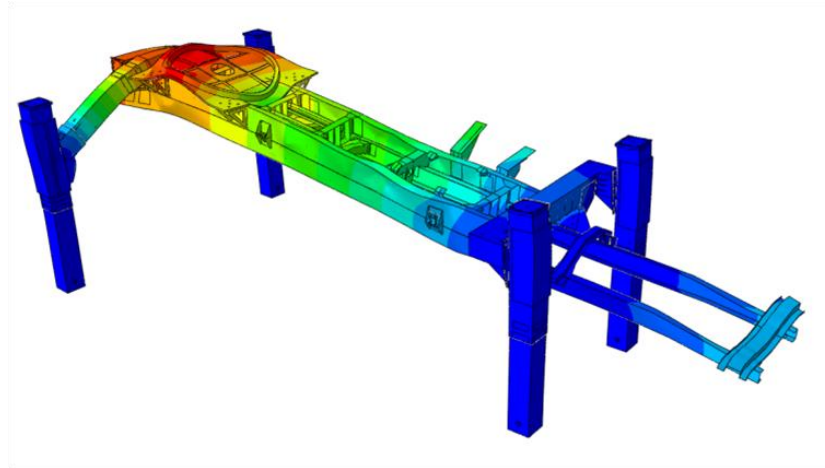


**Figure 32. The 10th mode shape of the detailed model**

The eleventh mode is combination of the longitudinal mode and a local mode. Mode shape is given in Figure 33.

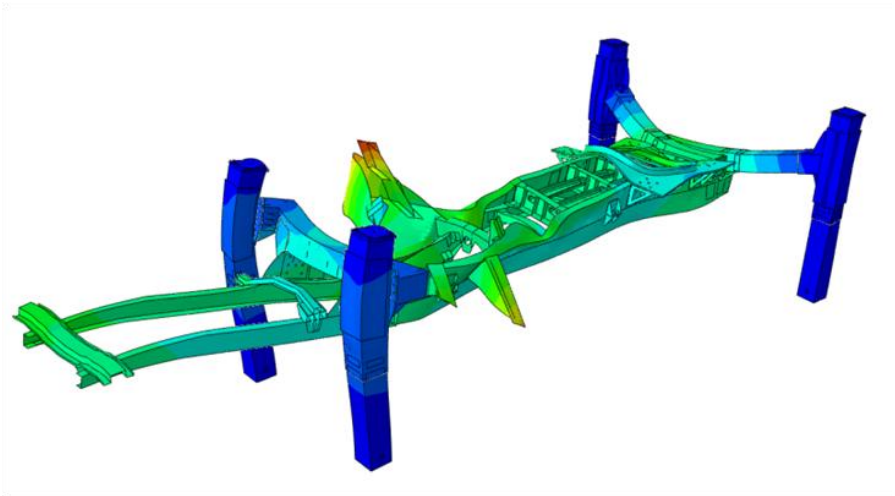


**Figure 33. The 11th mode shape of the detailed model**

The thirteenth mode is the longitudinal mode and mode shape is given in Figure 34.

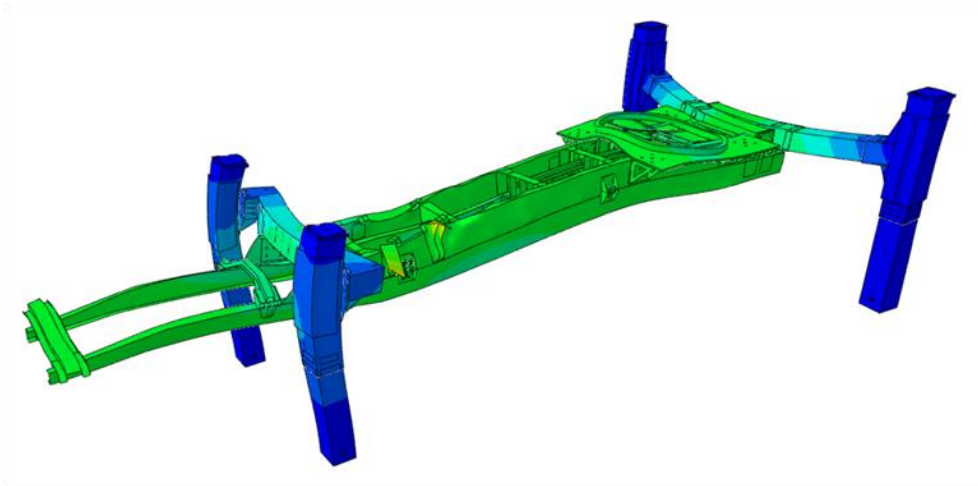


**Figure 34. The 13th mode shape of the detailed model**

The nineteenth mode is a combination of torsion mode of the cradle and bending mode of the front part of the chassis. Mode shape is given in Figure 35.

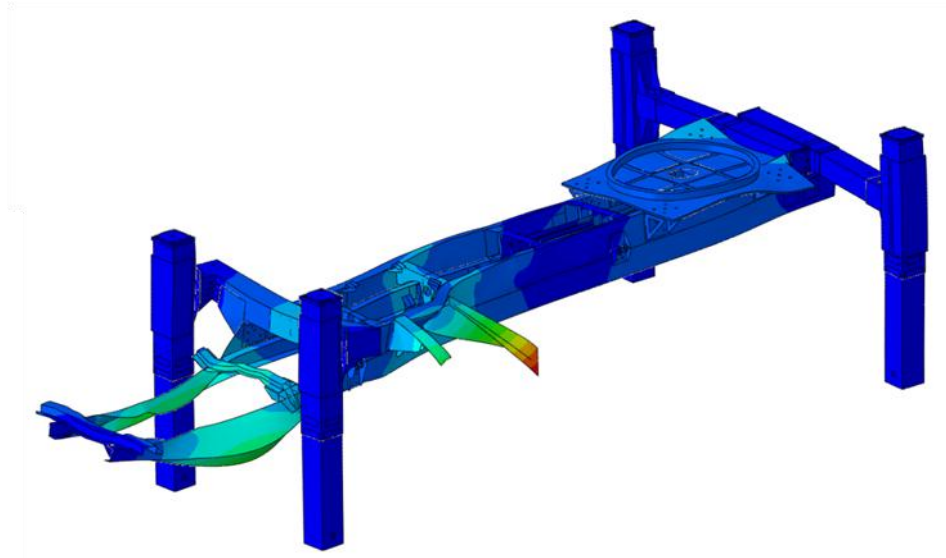


**Figure 35. The 19th mode shape of the detailed model**

The twentieth mode is a combination of bending mode of the cradle and bending mode of the front part of the chassis. Mode shape is given in Figure 36.

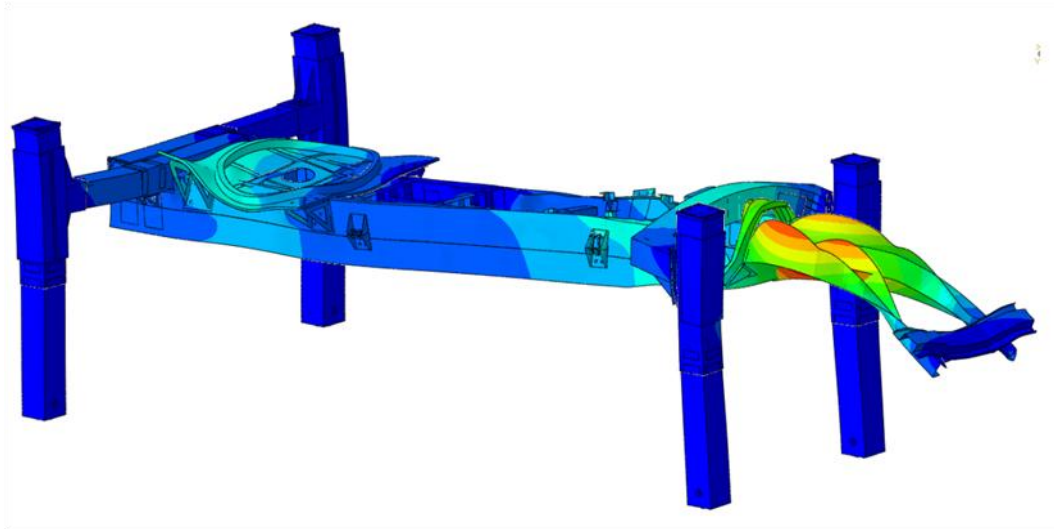


**Figure 36. The 20th mode shape of the detailed model**

### **3.5 Dynamic Analysis of the Detailed Finite Element Model**

In order to perform the dynamic analysis of the rocket launcher system, static analysis is performed under the rocket launcher system's own weight. Gravitational acceleration is applied in order to take into account the weight of the rocket launcher system. Dynamic rocket plume force is applied over the system when it is in the static equilibrium position. The area on the rocket launcher system where the plume force applied is shown in Figure 37.



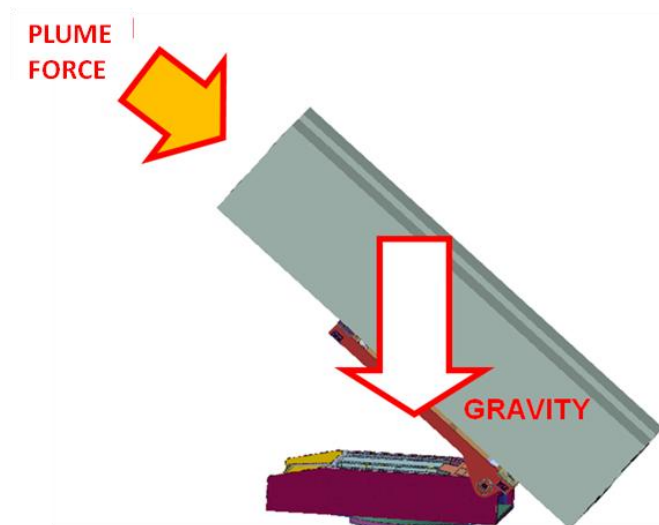


**Figure 37. Plume force applied area**

Dynamic plume load is given in Figure 38 as normalized by itself.

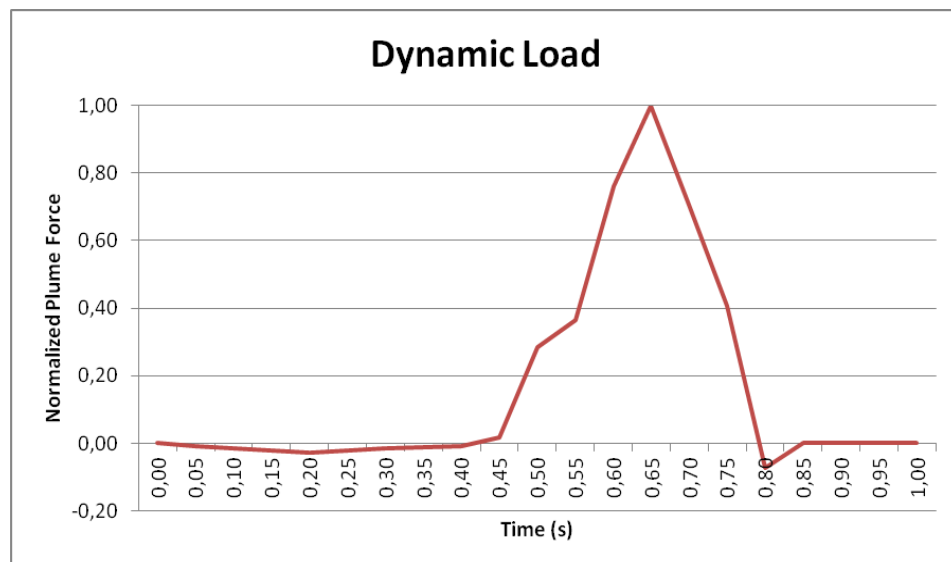


**Figure 38. Dynamic plume load**

As a result of the dynamic analysis, reaction force in the Y axis is gathered from the stabilizers and the outriggers due to the fact that tip-off is directly affected from the behavior of the rocket launcher system in Y axis. Moreover, displacement in the Y axis of the center of the firing tube which the rocket plume force applied is measured. Numbering system for the stabilizers and outriggers are given in the Figure 39.

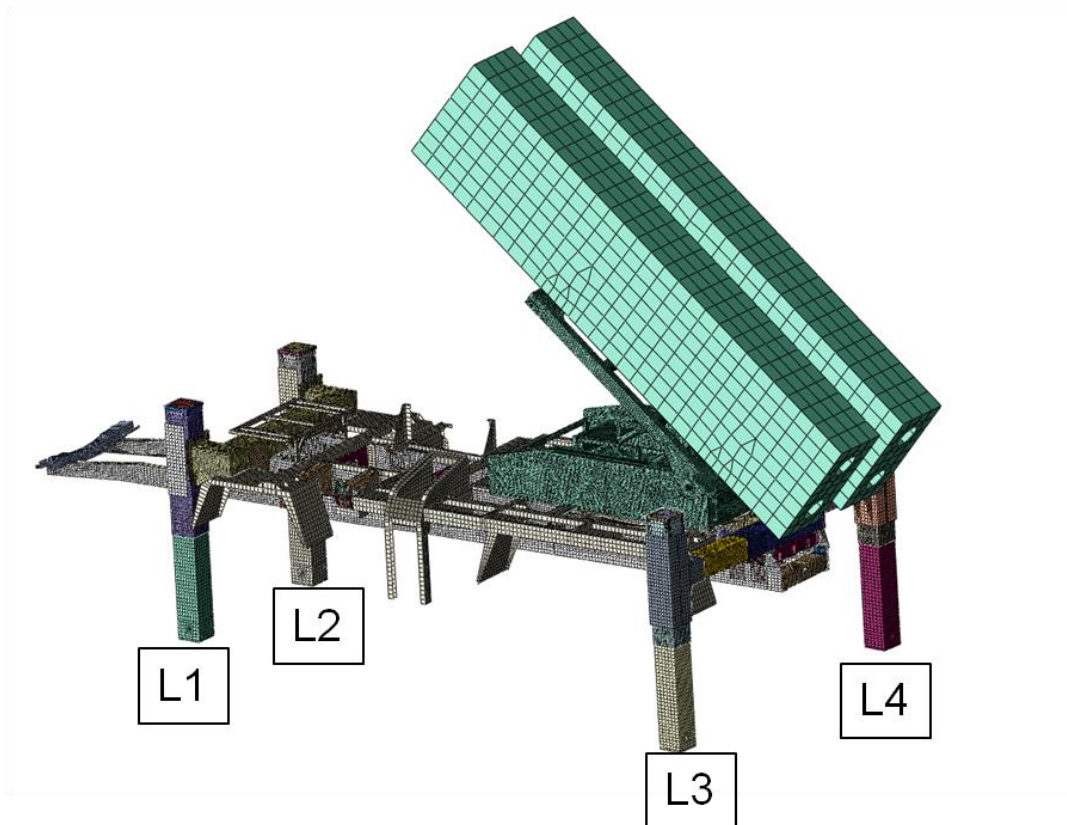


**Figure 39. Numbering system for the stabilizers and outriggers**

The reaction forces of the stabilizers and outriggers in the Y axis as normalized by itself are given in the Figure 40.

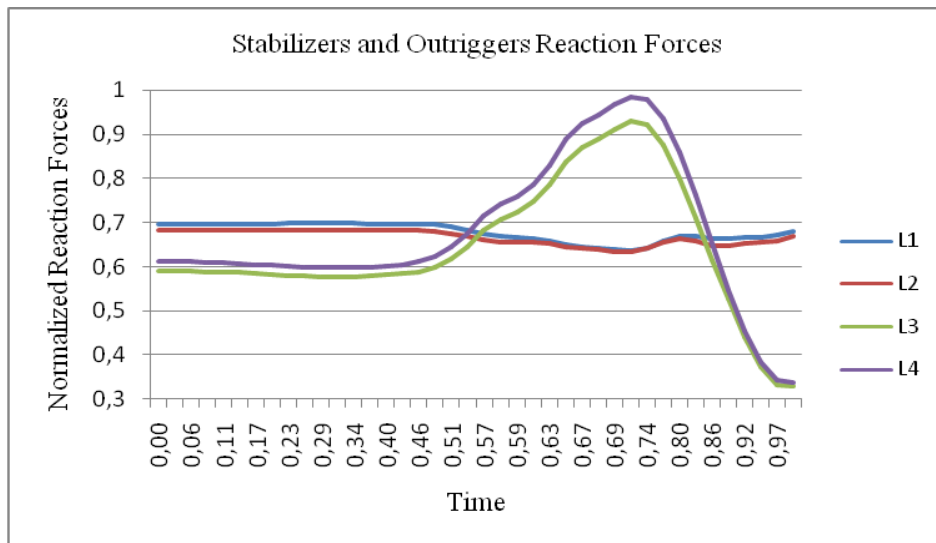


**Figure 40. Reaction forces of the stabilizers and outriggers in the Y axis**

The displacement in the Y axis of the center of the firing tube which the rocket plume force applied is given in the Figure 41.

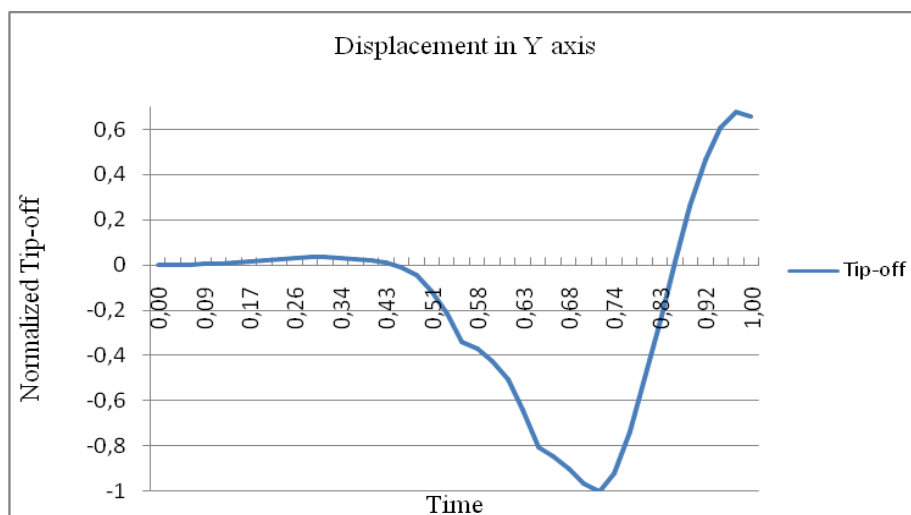


**Figure 41. The displacement in the Y axis of the center of the firing tube (Tip-off)**



## **CHAPTER 4**

### **SIMPLIFIED FINITE ELEMENT MODEL**

In this part of the study, simplified finite element model is discussed. Reduced degree of freedom, simple parametric model that includes necessary kinematic and elastic connections is generated in order to get faster results. Detailed finite element model takes too much time to generate and it is hard to modify and make the analysis again and again. Therefore, parametric model has a huge advantage on detailed model on preparation time and making modifications. There are various types of finite element software. On the other hand ANSYS APDL is preferred since the language is easy to generate a code. ANSYS code is generated in ANSYS Parametric Design Language of the rocket launcher system. Clamp attachment positions on the chassis, stabilizer case cross section, outrigger case cross section and outrigger deployment are modeled as parametric in the code so they can easily be changed.

#### **4.1 Simplified Rocket Launcher Model**

Simplified FE model of the rocket launcher system is composed of fixed platform, auxiliary chassis, chassis, clamp attachments, stabilizers and outriggers. Rocket, auxiliary chassis' unimportant parts, elevation platform and azimuth platforms are not included in the model. On the other hand, excluded parts are modeled as lumped mass and effects of the rocket on the launcher system is included by applying the

plume force on the fixed platform. Plume force is directly carried on the fixed platform by considering the elevation and azimuth platforms are rigid since measuring the rocket launcher system's behavior in a faster way is the main concern.

#### 4.2 Modeling Method and Meshing of the Simplified Finite Element Model

Simplified FE model is composed of 55,000 DOF. Shell and beam elements are utilized in order to generate this model in order to minimize the DOF. Moreover, in the non-critical zones some simplifications are performed such as filling little holes and deleting chamfers. Stabilizers and outriggers are modeled with beam elements. Hydraulic system in the stabilizers and the outriggers are modeled as truss elements by giving stiffness in the axial direction.

Clamp attachments between the chassis and the auxiliary chassis are modeled. Beam elements are used in order to represent the bolts between upper and the lower parts of the clamp attachments. Clamp attachments are shown in Figure 42.

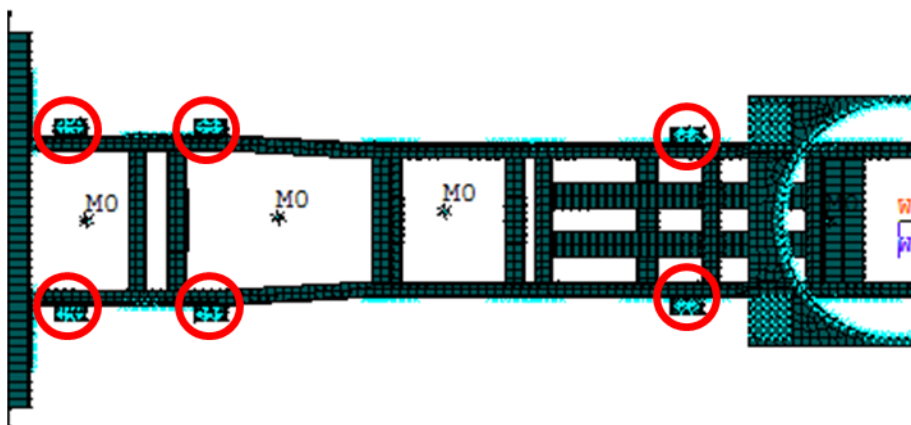
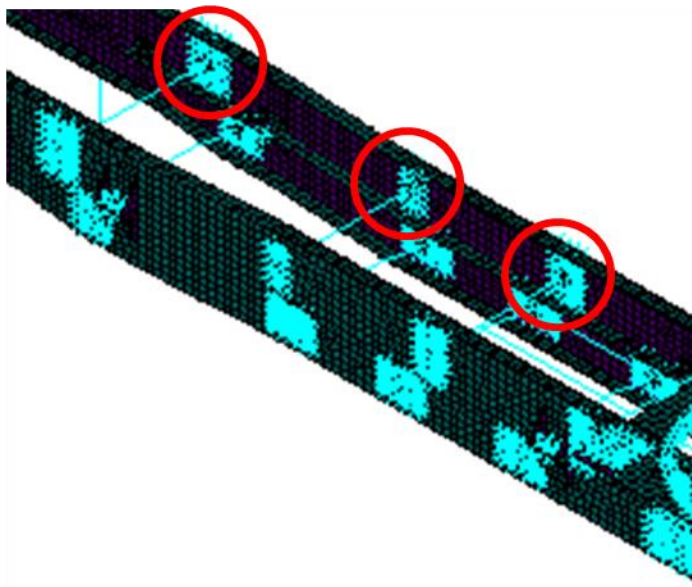


Figure 42. Clamp attachments of the simplified rocket launcher system

Both chassis' and auxiliary chassis' cross members are modeled with beam elements. Rigid constraints are utilized to represent the connection between chassis and cross members. Some of the rigid connections of the cross members are shown in the Figure 43.



**Figure 43. Rigid connections of the cross members**

For modeling both truck head and cradle, lumped mass with inertia are used and rigid constraints are used for connections. For other lumped masses, force distributed connections are utilized. Contact is defined between the chassis and the auxiliary chassis in order to take the stiffness of the both chassis and the auxiliary chassis into account. Friction coefficient is set as 0.1 for both static and dynamic solutions. Another contact is defined between auxiliary chassis and the lower part of

the clamp attachment. Meshed simplified rocket launcher finite element model can be seen in Figure 44.

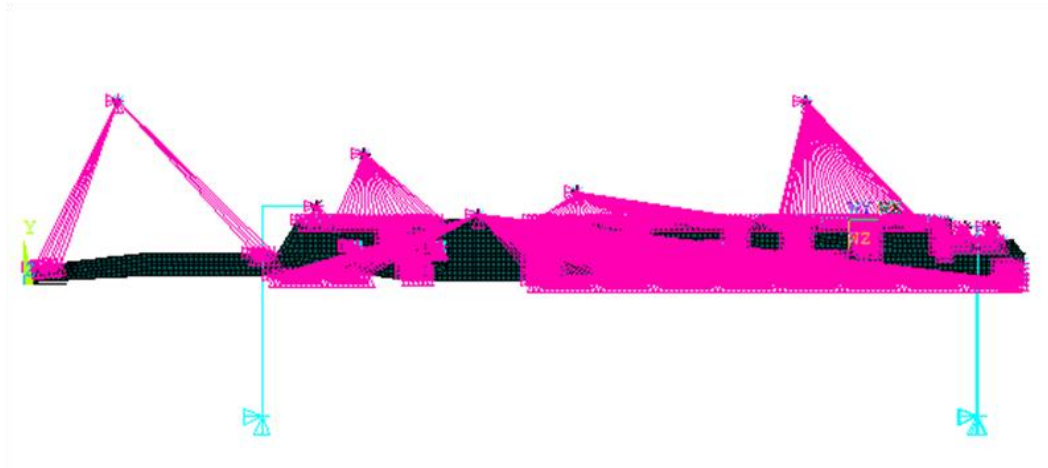


**Figure 44. Simplified rocket launcher system**

The meshed simplified rocket launcher finite element model can be seen without lumped masses and by showing the beam elements' shapes in Figure 45.



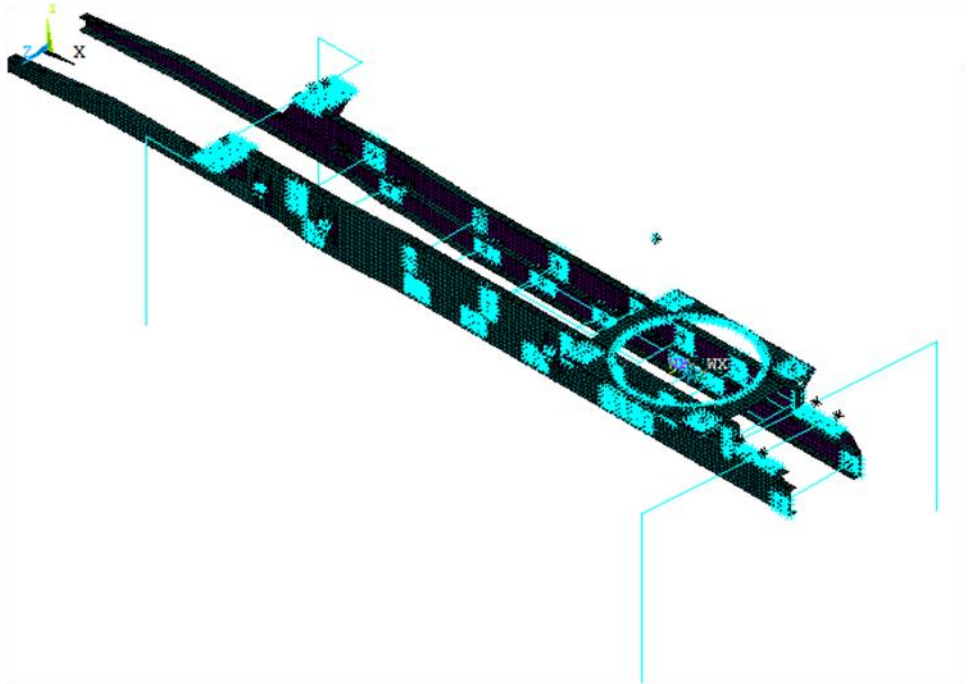


**Figure 45. Simplified rocket launcher system without lumped masses**

Meshed simplified rocket launcher finite element model can be seen without lumped masses and by showing the beam elements' shapes in Figure 46.

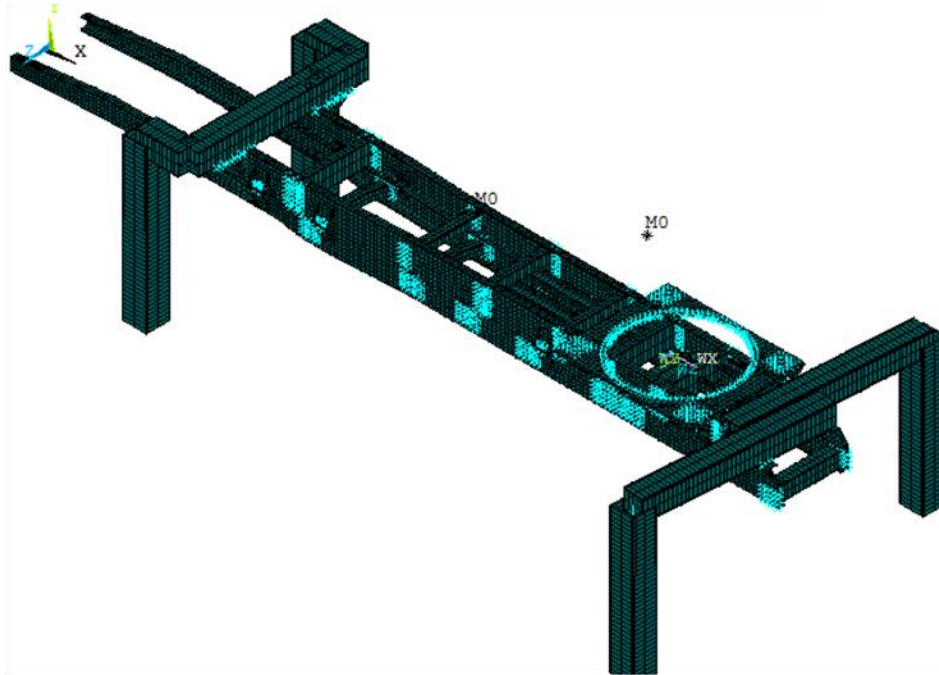


**Figure 46. Simplified rocket launcher system with beam elements' shapes**

### **4.3 Material Properties and Boundary Conditions for the Simplified Finite Element Model**

In the rocket launcher model, every part is produced from St-37 steel material. Properties of St-37 steel can be seen in Table 1.

Zero displacement in three axes as the boundary condition is applied to the stabilizers' and outriggers' bottom positions. Spherical joint approximation is used for modeling the connection between stabilizers, outriggers and the ground.

In Figure 47, boundary condition of the simplified rocket launcher FE model is shown.

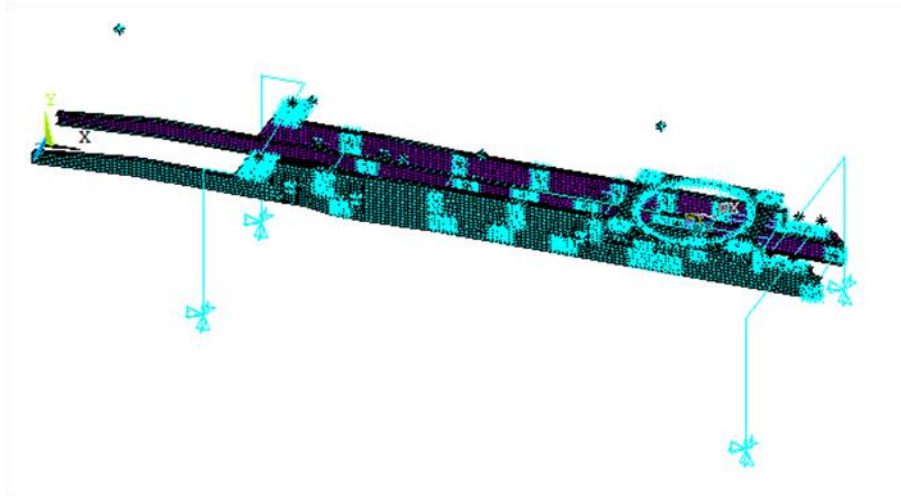


**Figure 47. Boundary condition of the rocket launcher system FE model**

#### **4.4 Modal Analysis of the Simplified Finite Element Model**

In order to understand the dynamic behavior of the rocket launcher system, modal analysis is done. For modal analysis, zero displacement in three axes as the boundary condition is applied to the stabilizers' and outriggers' bottom positions. Spherical joint approximation is used for modeling the connection between stabilizers, outriggers and the ground. Furthermore, glue contact is applied between chassis and the auxiliary chassis and other contact areas in order to get a linear finite element model.

When the most significant modes are compared with the detailed model, it is seen that Mode shapes are so similar. On the other hand, natural frequencies are higher due to the fact that simplified model includes more rigid connections. Modal analysis results are given in the Table 3.

**Table 3. Modal analysis results of the simplified model**

Detailed FE model		Simplified FE model	
Mode No	Natural Frequencies (Hz)	Mode No	Natural Frequencies (Hz)
1	3.0	1	3.6
2	3.7	2	4.2
7	6.4	4	7.1
9	8.8	5	9.4
10	10.5	7	11.0
11	12.5	9	12.9
13	16.2	12	17.8
19	23.4	15	24.8
20	24.5	16	26.5

When the natural frequencies of the detailed FE model and simplified FE model are compared, it can be seen that the difference is less than 20%.

The mode shapes of the simplified model (given in the right side) with mode shapes of the detailed model (given in the left side) are given below.

Comparison of the first mode shape of detailed FE model and the first mode shape of simplified FE model is given in Figure 48. The mode shapes are similar since the torsion mode of the cradle is significant in both modes.

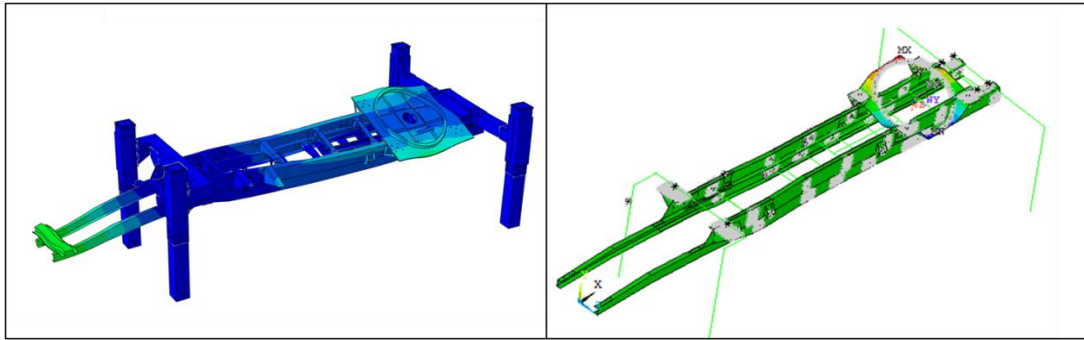


**Figure 48. Comparison of the first mode shape of detailed FE model and the first mode shape of simplified FE model**

Comparison of the second mode shape of detailed FE model and the second mode shape of simplified FE model is given in Figure 49. The mode shapes are similar since the torsion mode of the front part of the chassis is significant in both modes.

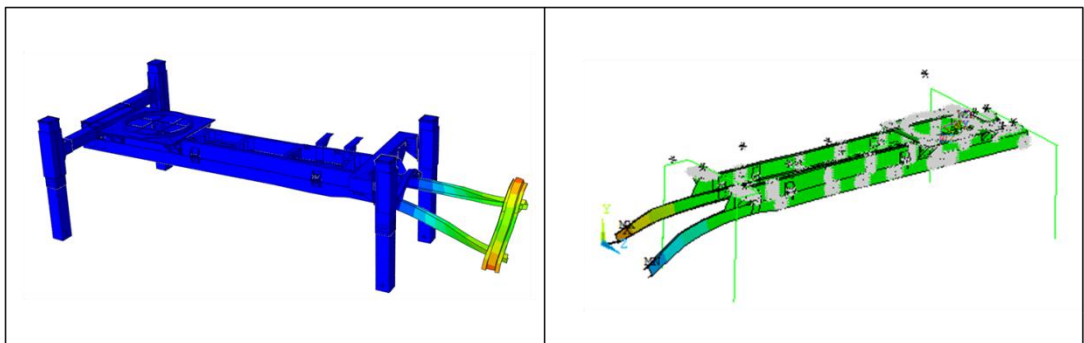


**Figure 49. Comparison of the second mode shape of detailed FE model and the second mode shape of simplified FE model**

Comparison of the seventh mode shape of detailed FE model and the fourth mode shape of simplified FE model is given in Figure 50. The mode shapes are similar since the bending mode of the chassis is significant in both modes.

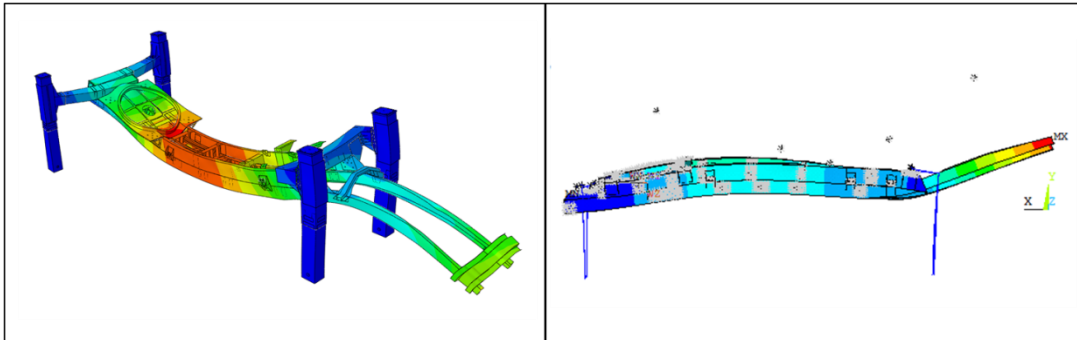


**Figure 50. Comparison of the seventh mode shape of detailed FE model and the fourth mode shape of simplified FE model**

Comparison of the ninth mode shape of detailed FE model and the fifth mode shape of simplified FE model is given in Figure 51. The mode shapes are similar since the bending mode of the chassis in the transverse direction is significant in both modes.

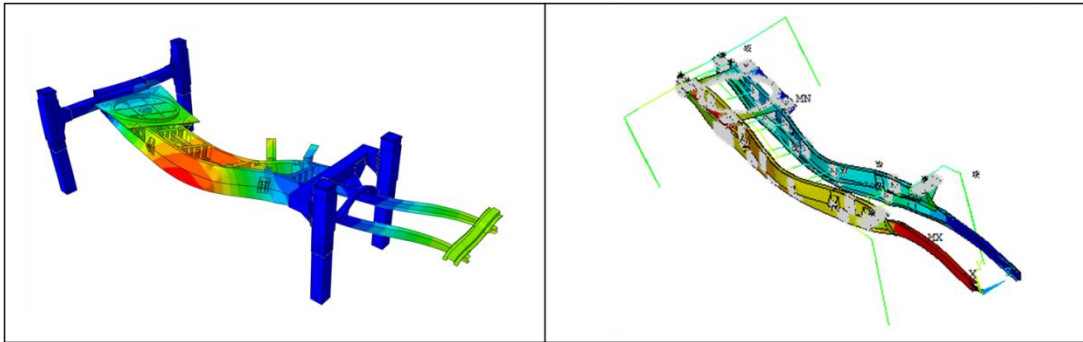


**Figure 51. Comparison of the ninth mode shape of detailed FE model and the fifth mode shape of simplified FE model**

Comparison of the tenth mode shape of detailed FE model and the seventh mode shape of simplified FE model is given in Figure 52. The mode shapes are similar since the bending mode of the backward part of the chassis is significant in both modes.

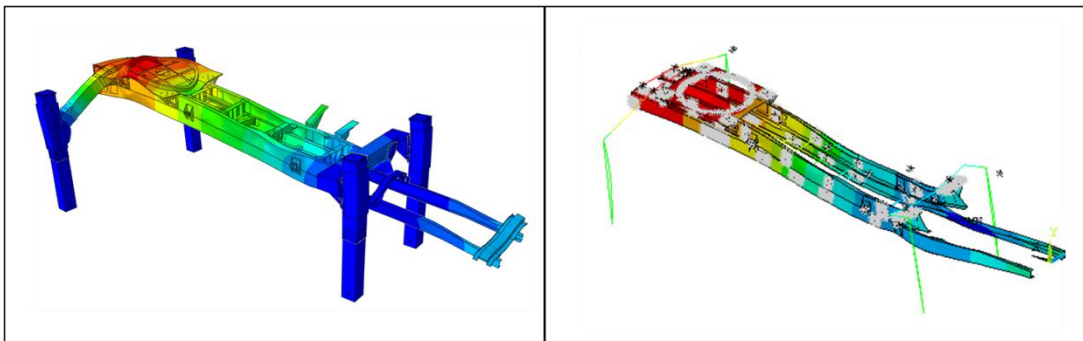


**Figure 52. Comparison of the tenth mode shape of detailed FE model and the seventh mode shape of simplified FE model**

Comparison of the eleventh mode shape of detailed FE model and the ninth mode shape of simplified FE model is given in Figure 53. The mode shapes are similar since the longitudinal mode of the chassis is significant in both modes.

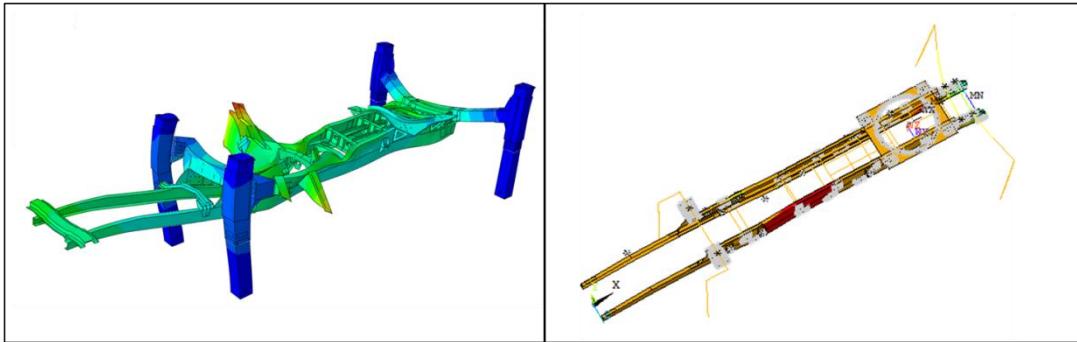


**Figure 53. Comparison of the eleventh mode shape of detailed FE model and the ninth mode shape of simplified FE model**

Comparison of the thirteenth mode shape of detailed FE model and the twelfth mode shape of simplified FE model is given in Figure 54. The mode shapes are similar since the longitudinal mode of the chassis is significant in both modes.



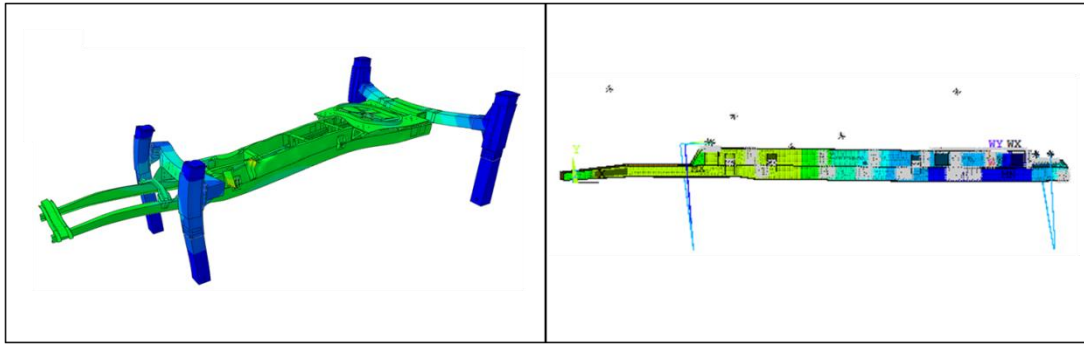


**Figure 54. Comparison of the thirteenth mode shape of detailed FE model and the twelfth mode shape of simplified FE model**

Comparison of the nineteenth mode shape of detailed FE model and the fifteenth mode shape of simplified FE model is given in Figure 55. The mode shapes are similar since the bending mode of the front part of the chassis is significant in both modes.

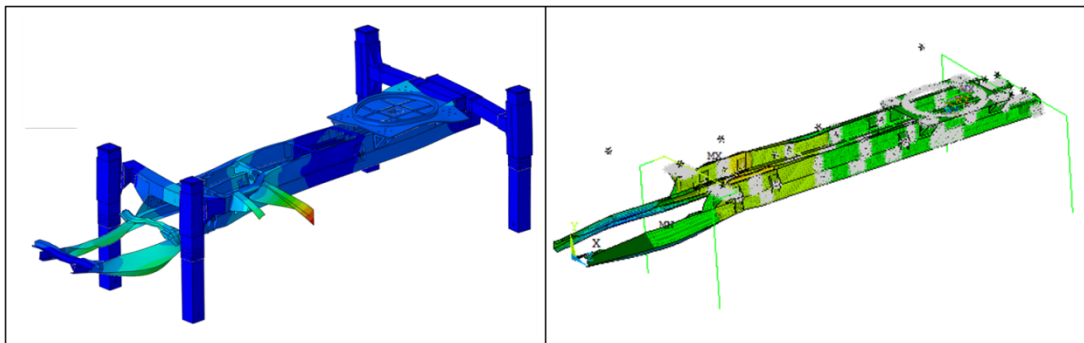


**Figure 55. Comparison of the nineteenth mode shape of detailed FE model and the fifteenth mode shape of simplified FE model**

Comparison of the twentieth mode shape of detailed FE model and the sixteenth mode shape of simplified FE model is given in Figure 56. The mode shapes are similar since the bending mode of the front part of the chassis is significant in both modes.

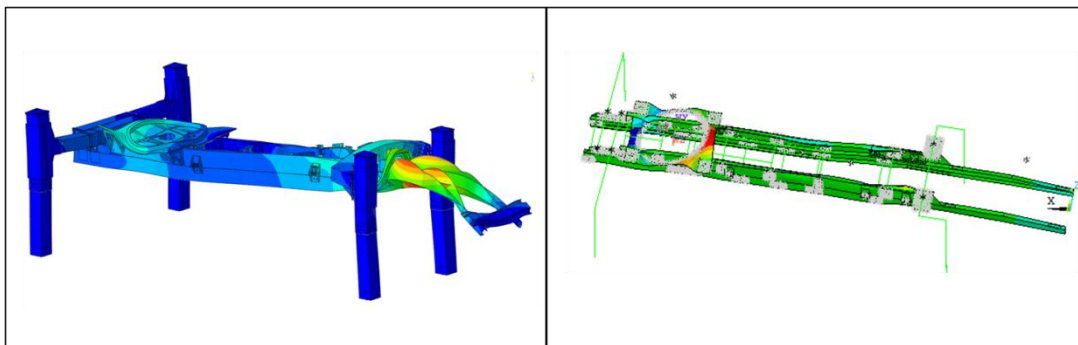


**Figure 56. Comparison of the twentieth mode shape of detailed FE model and the sixteenth mode shape of simplified FE model**

#### **4.4 Dynamic Analysis of the Simplified Finite Element Model**

In order to perform the dynamic analysis of the rocket launcher system, static analysis is performed under the rocket launcher system's own weight. Gravitational acceleration is applied in order to take into account the weight of the rocket launcher system. Dynamic rocket plume force is applied over the system when it is in the static equilibrium position. Plume force is directly carried on the fixed platform by considering the elevation and azimuth platforms are rigid since measuring the rocket launcher system's behavior in a faster way is the main concern. The area on the rocket launcher system where the dynamic load applied is shown in Figure 57.

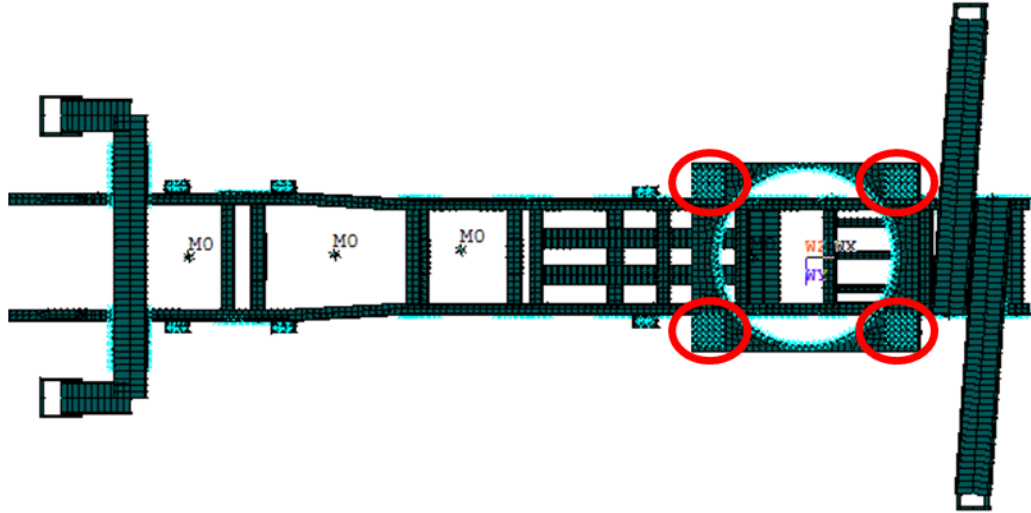


**Figure 57. Fixed platform areas where dynamic load applied**

As a result of the dynamic analysis, reaction force in the Y axis is gathered from the stabilizers and the outriggers due to the fact that tip-off is directly affected from the behavior of the rocket launcher system in Y axis. Moreover, displacement in the Y axis of the mass center of the cradle is measured since cradle is modeled as a lumped mass. In this model, the displacement of the center of the firing tube and the mass center of the cradle are almost same in the Y axes. Same numbering system for the stabilizers and outriggers is used for the simplified model. Numbering system for the stabilizers and outriggers are shown in Figure 58.

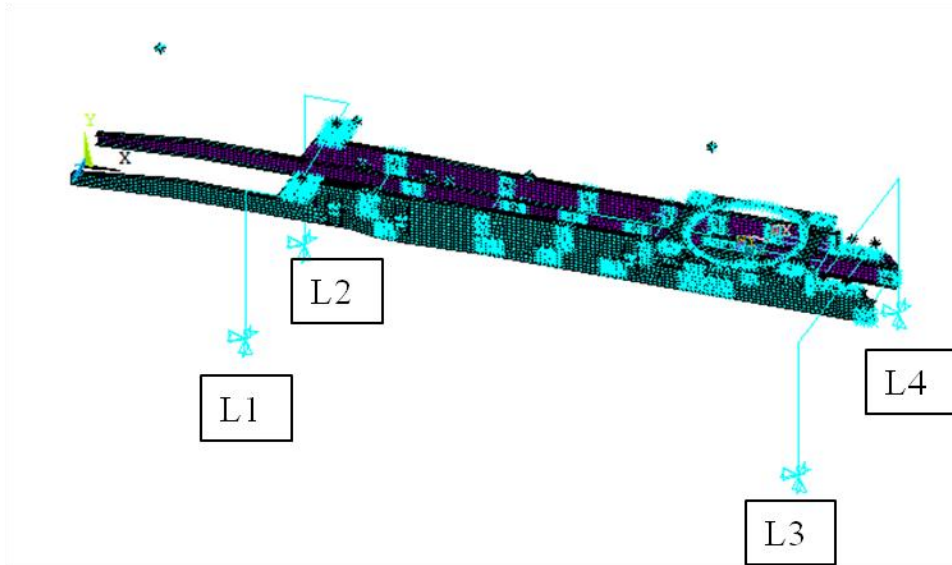


**Figure 58. Numbering system for the stabilizers and outriggers**

In order to figure out the damping characteristic of the system, different damping values are used and dynamic analyses results are collected. Proportional damping is utilized in the FEA [26].

$$[C] = \alpha[M] + \beta[K] \quad (4.1)$$

The simplified FE model is stiffer when it is compared with the detailed FE model since most of the connections are modeled with rigid elements. Therefore, damping value of this system should be assigned in order to make a better approach. Reaction force in the Y axis comparison can be seen related to constant mass matrix multiplier  $\alpha$  and constant stiffness matrix multiplier  $\beta$ .

Total reaction force in the Y axis comparison is given in Figure 59.

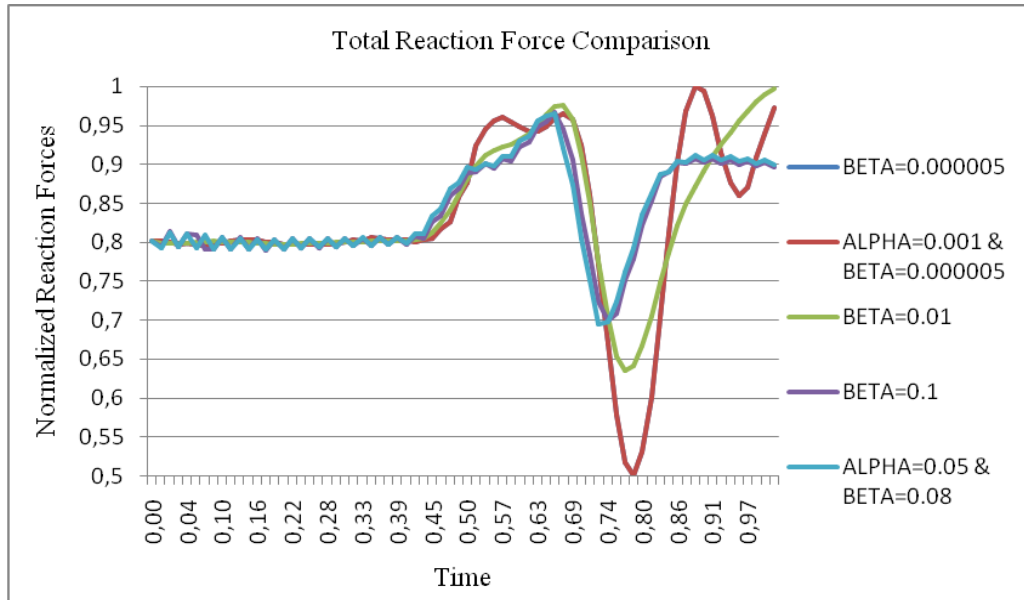


**Figure 59. Total reaction force comparison in the Y axis**

The reaction force of L1 in the Y axis comparison is given in Figure 60.

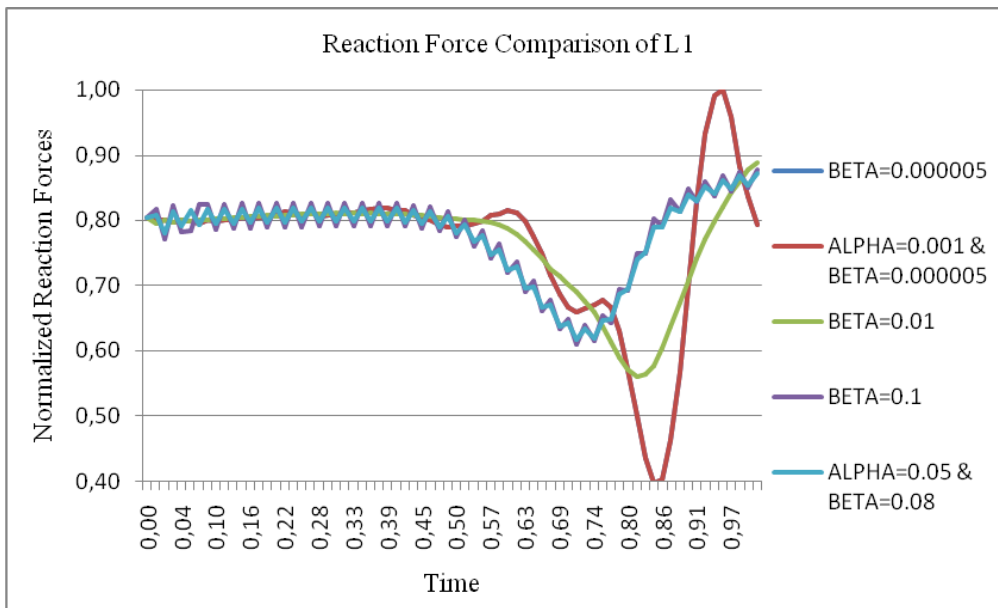


**Figure 60. Reaction force comparison of L1 in the Y axis**

The reaction force of L2 in the Y axis comparison is given in Figure 61.

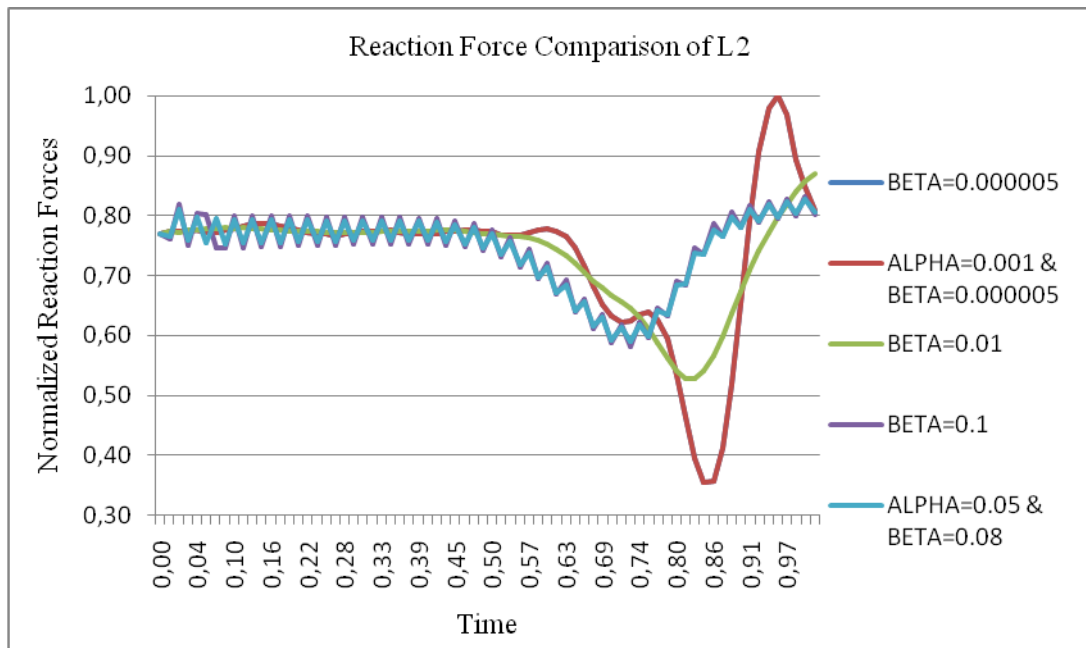


**Figure 61. Reaction force comparison of L2 in the Y axis**

The reaction force of L3 in the Y axis comparison is given in Figure 62.

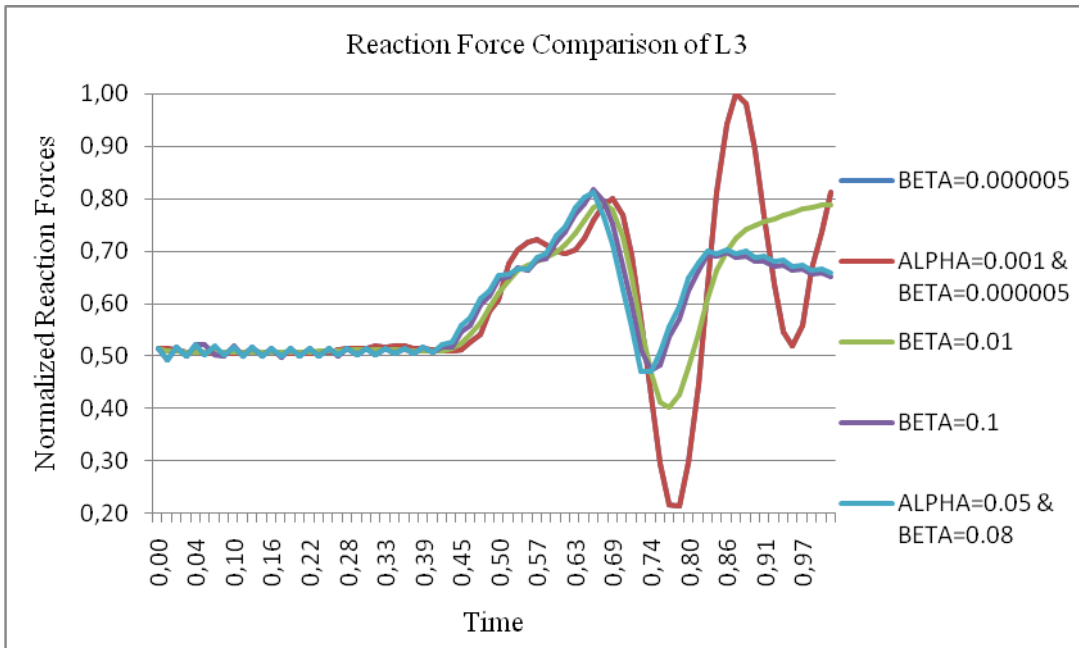


**Figure 62. Reaction force comparison of L3 in the Y axis**

The reaction force of L4 in the Y axis comparison is given in Figure 63.



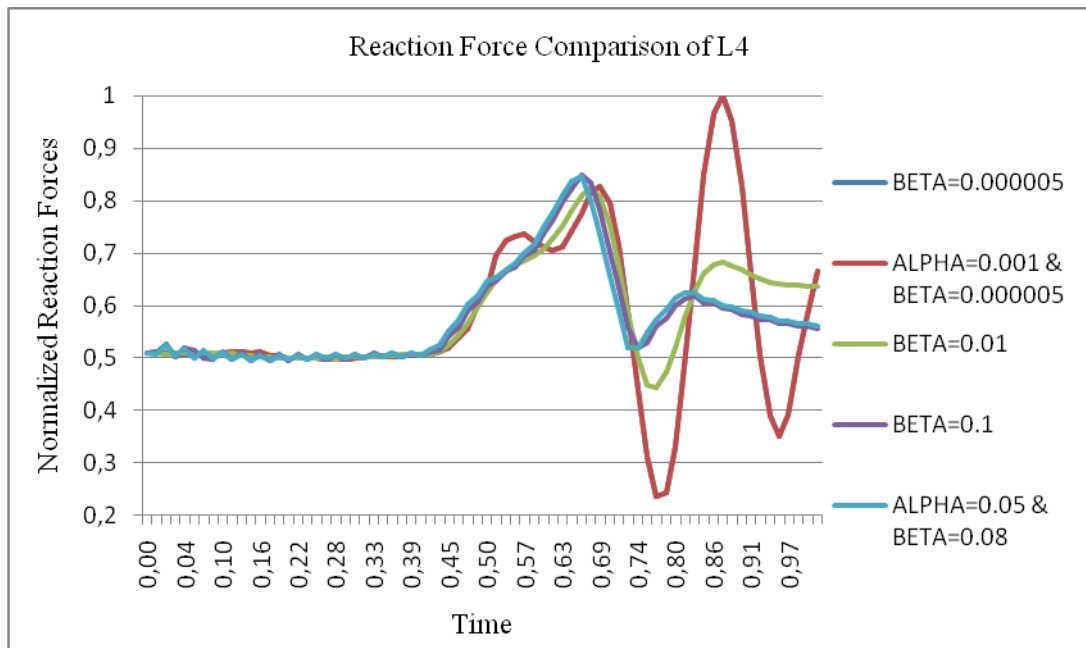


**Figure 63. The reaction force comparison of L4 in the Y axis**

When the analyses results are evaluated, it is concluded that constant mass matrix multiplier  $\alpha$  is negligible effect on the dynamic behavior of the system. On the other hand, the constant stiffness matrix multiplier  $\beta$  has a dominant effect on the damping characteristic of the system. Moreover,  $\beta$  should be defined as a reasonable value since the main material of the system is steel. Furthermore, the detailed FE model results are examined when selecting the  $\beta$  value. In addition to these, detailed FE model results are examined in order to determine the damping values. Therefore,  $\alpha$  is selected as zero and  $\beta$  is selected as 0.01 and this model will be mentioned as baseline model.

Reaction forces of the stabilizers and outriggers in the Y axis are shown in the Figure 64. The outrigger's reaction forces are higher than the stabilizer's reaction forces as expected.

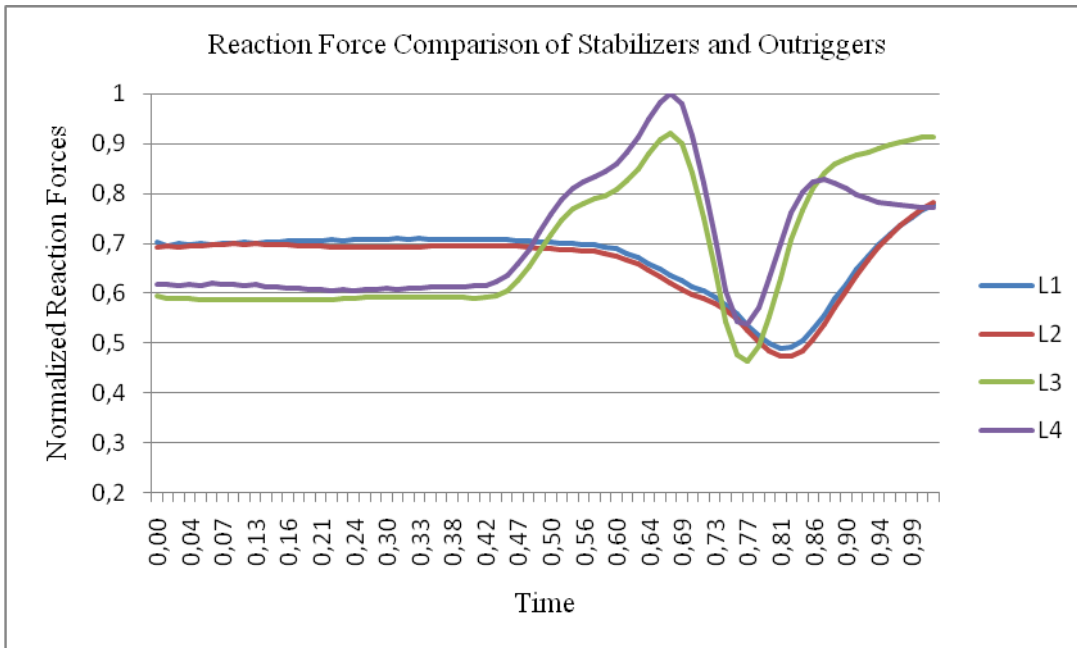


**Figure 64. The reaction forces of the stabilizers and outriggers of the baseline model**

The simplified model's cradle mass center is shown in Figure 65. Tip-off values are calculated from the cradle's mass center.

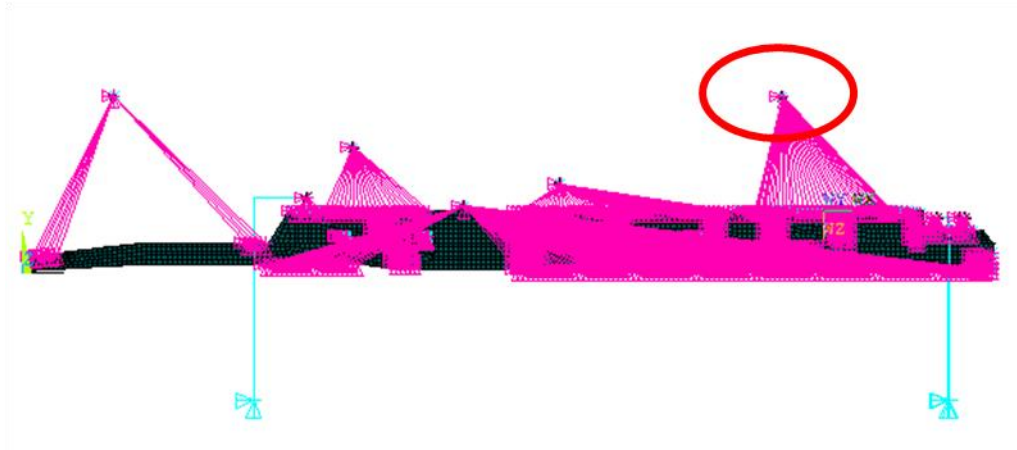


**Figure 65. The simplified model's cradle mass center**

The displacement in the Y axis of the mass center of the cradle is given in Figure 66.

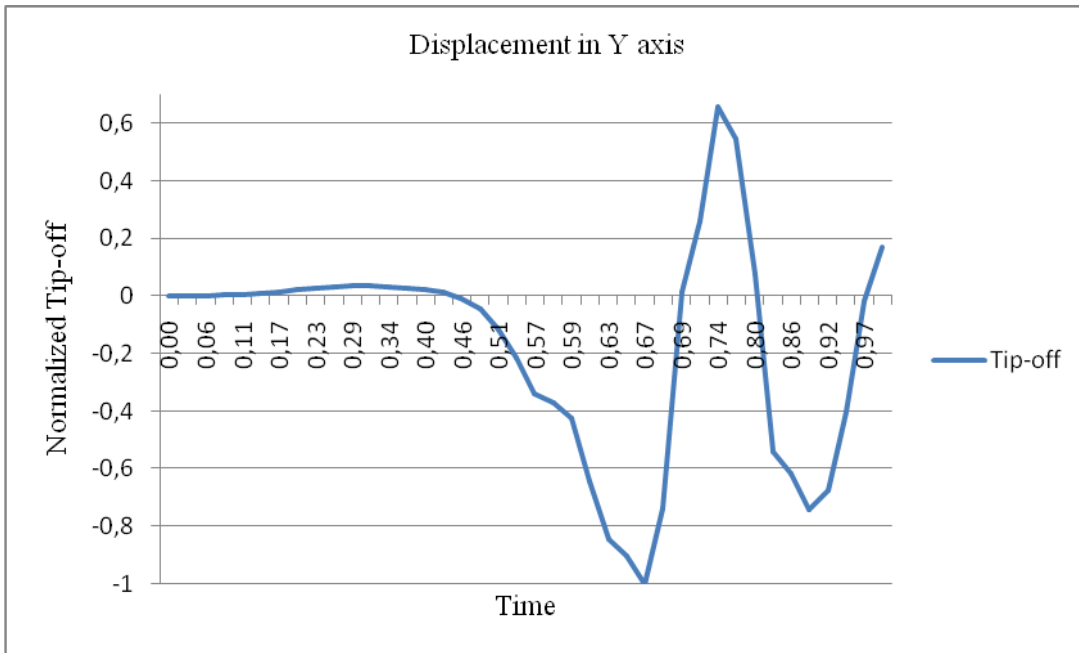


**Figure 66. The displacement in the Y axis of the mass center of the cradle (Tip-off)**

## **CHAPTER 5**

### **TEST STUDY AND VERIFICATION OF FINITE ELEMENT MODELS**

Finite element method provides designers to evaluate their design. Although calculations and analyses are done during the design period, they are not direct proof that system works as desired. In the scope of this thesis work, the detailed FE model and simplified model will be verified via experimental studies. Moreover, any kind of measurements tried to be taken during test studies in order to provide significant and valuable information about the system's real behavior. According to the test results, design can be modified or totally changed.

For a rocket launcher system static firing tests are crucial since rockets thrust force can only be obtained via this method. After that, firing tests are performed in order to verify the finite element models. At first, firing tests are performed on the cradle which includes fixed platform, azimuth platform, elevation platform and firing tubes. After firing test results gathered from cradle model, firing tests of the whole rocket launcher system are performed.

The rocket launcher system prototype is manufactured and equipped with all necessary electronic and mechanical elements. The real system is then tested under actual operational conditions. Real firing tests are conducted on the rocket launcher and certain measurements are taken during tests. Some of these measurements are reaction force measurements at stabilizers, outriggers from the hydraulic system and displacement measurements from the elevation platform. In order to perform the

firing test, over 20 people are worked as a group. Moreover, in order to gather the aforementioned data, 3 person worked as a group.

### 5.1 Static Firing Tests

A static firing test is a kind of method to measure the rocket motor thrust force. The details of the static firing tests are not in the scope of this work since brief information is provided. On the other hand, static firing test results are used in order to be an input for the finite element models.

There are different configurations for measuring the rocket motor's thrust force. An example of widely used "Horizontal Thrust Measurement System" is given in Figure 67.

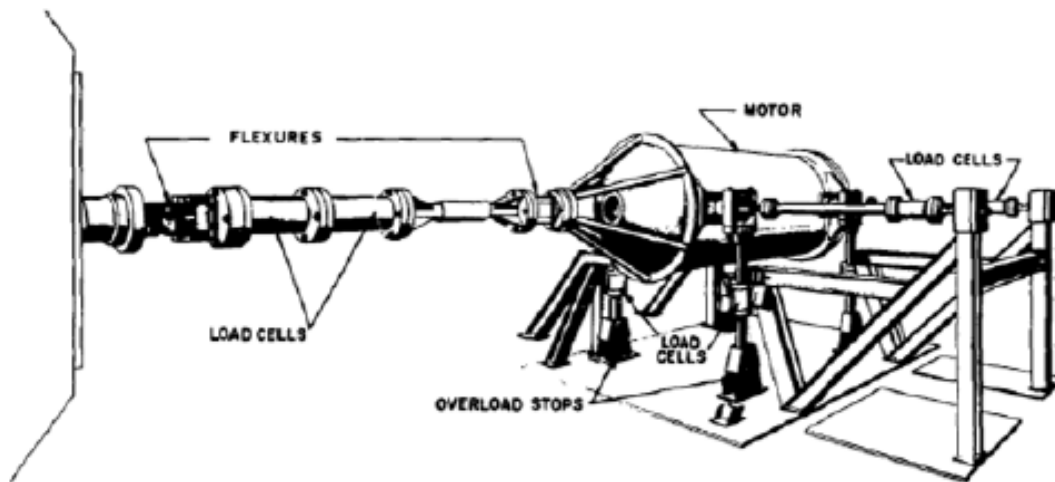


Figure 67. Horizontal thrust measurement system [1]

Main purpose of measuring the rocket motor's thrust force is to maintain the motor stable position during static firing tests. Load cells are utilized in order to measure the thrust force. Load cell position in the axial direction is crucial due to the fact that thrust force occurs in the axial direction. Force measurements are collected in all axes but forces other than axial direction are negligible small.

## **5.2 Firing Tests**

Firing tests are hard to repeat since preparation takes too much time, cost, effort and military permissions. Therefore, taking as many data as possible is crucial.

At first firing tests performed over cradle which includes fixed platform, azimuth platform, elevation platform and firing tubes. In order to verify the cradle, launching vehicle is not included in this firing test. Instead of launching vehicle concrete platform is used. On the concrete platform, a steel plate is positioned. Four leg parts are positioned on the steel plate in order to gather the strain gauge data. Positions of the legs are shown in Figure 68.

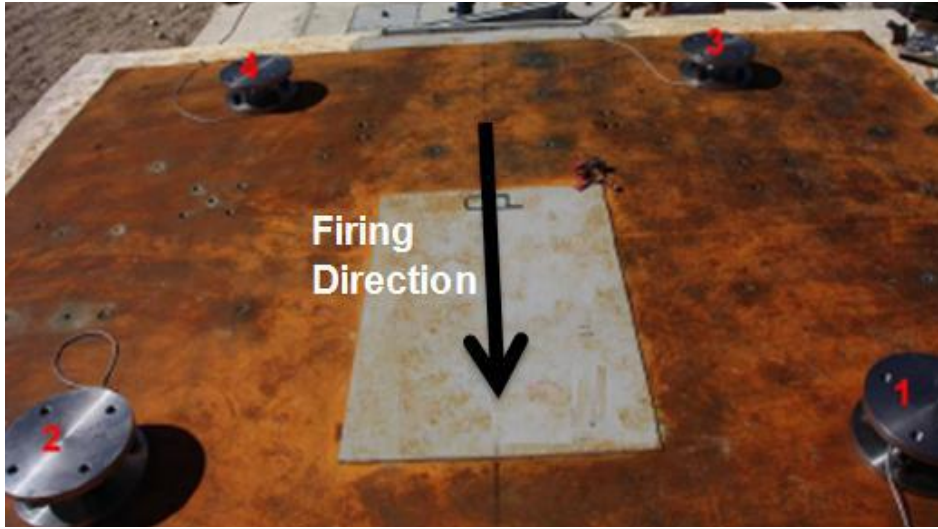


**Figure 68. Positions of the cradle legs [1]**

Moreover, potentiometer data is gathered from the specified parts of the cradle. Positions of the potentiometers on the azimuth platform are shown in Figure 69.



**Figure 69. Potentiometer locations on the cradle**



Comparison of the test results and finite element model is studied and finite element model of the cradle is verified.

Second firing test is performed over the rocket launcher system that launching vehicle is included. In order to understand the dynamic behavior of the rocket launcher system, elevation platform's displacement and reaction force measured from the stabilizers and outriggers are measured during the firing tests. Actual rocket launcher system is shown in Figure 70.



**Figure 70. A representative rocket launcher system**

Stabilizers and outriggers have driven by hydraulic system. Moreover, hydraulic pressure is measured at any time from the hydraulic control system. Reaction force data is measured from the hydraulic pressure of the stabilizers and outriggers.

Tip-off is measured from the displacement of the elevation platform's tip point due to the fact that displacement of the firing tube's center point is too hard to measure. Plume gases cover the front part of the firing tube. Therefore, taking measurement is not possible. Laser distance sensors are utilized to measure the elevation platform's tip point. Laser distance sensor set up is shown in Figure 71.



**Figure 71. Laser distance sensor set up on a representative system**

Laser distance sensor is optoelectronic sensor for non-contact distance. There is a sensor and a reflector in this system. Both sensor and reflector works according to the phase comparison principle.

Reaction forces of the stabilizers and outriggers in the Y axis (opposite direction with the gravity) as normalized by itself are given in Figure 72.

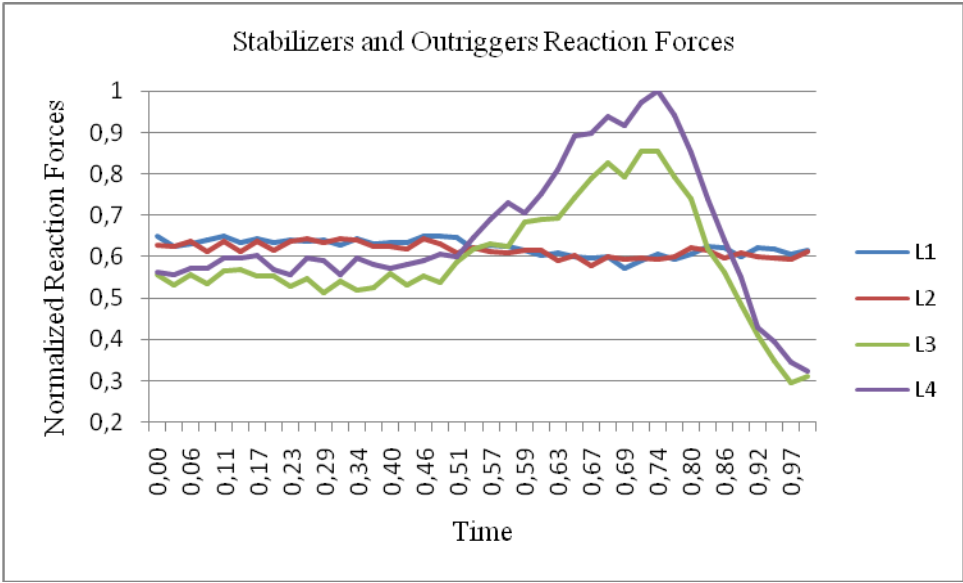


**Figure 72. Reaction forces of the stabilizers and outriggers in the Y axis**

The displacement in the Y axis (opposite direction with the gravity) of the elevation platform's tip point is given in Figure 73. The tip-off values are calculated from the tip point of the elevation platform.

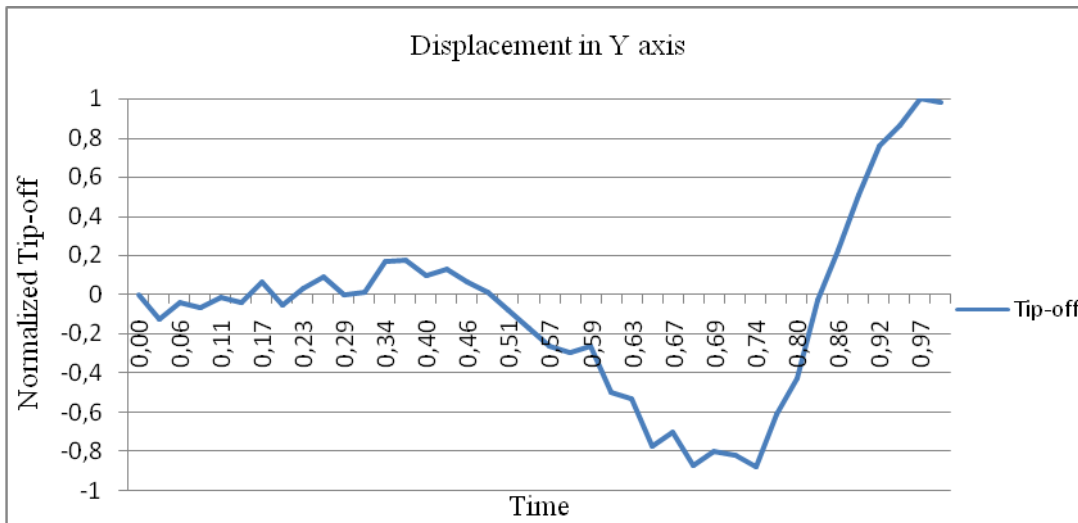


**Figure 73. Displacement in the Y axis of the tip point of the elevation platform**

## 5.2 Verification of the Finite Element Models

Finite element models are created by using some approximations. In order to figure out the success of these approximations, comparison should be performed with the actual system. Therefore, detailed finite element model and simplified model are compared with the prototype rocket launcher system by comparing the reaction forces and displacements. Same numbering method is used for the actual system.

At first, total reaction forces are compared in order to understand the transmissibility of the models. Total reaction forces are calculated by adding all stabilizers and outriggers with respect to time in order to examine the behavior of the system. Total reaction force comparison is shown in Figure 74.

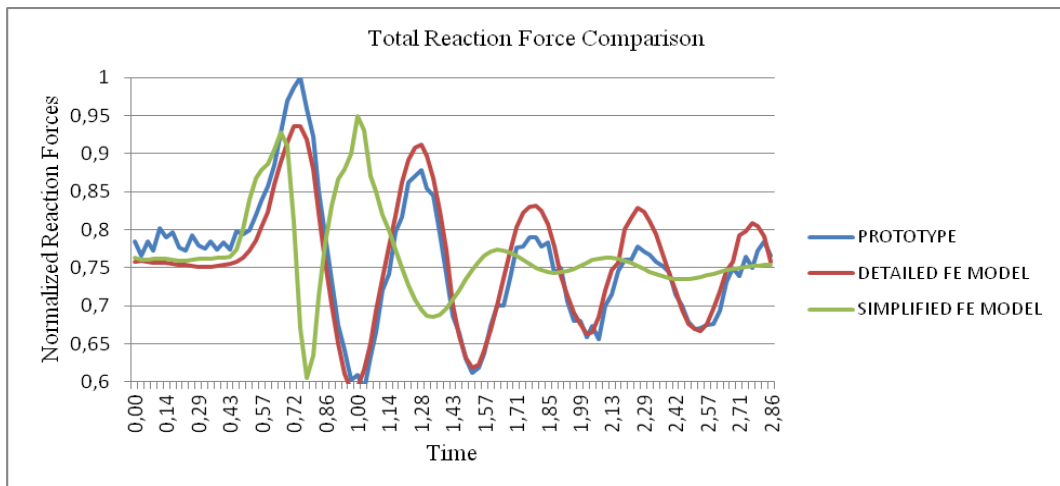


**Figure 74. Total reaction force comparison**

Total reaction forces are seems so close by magnitude. This shows that transmissibility of the finite element models is similar with the actual model. On the other hand simplified model get response more quickly. This is a sign for rigidity of the simplified model is higher.

The reaction forces for the stabilizers and the outriggers are examined individually. Reaction force of the left and front stabilizer is shown in Figure 75.

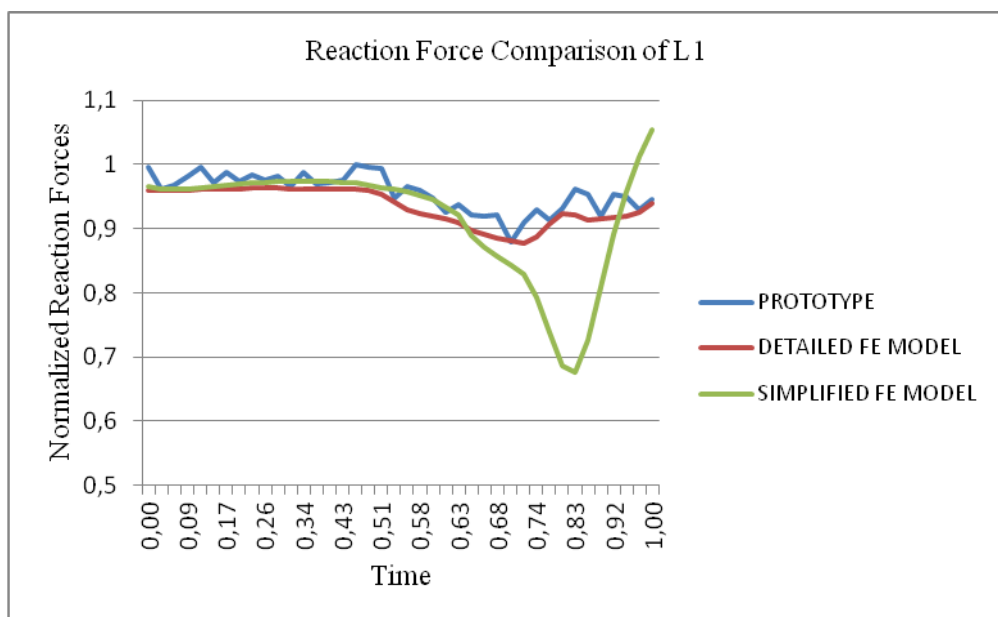


**Figure 75. Reaction force of L1**

The reaction force of the right and front stabilizer is shown in Figure 76.

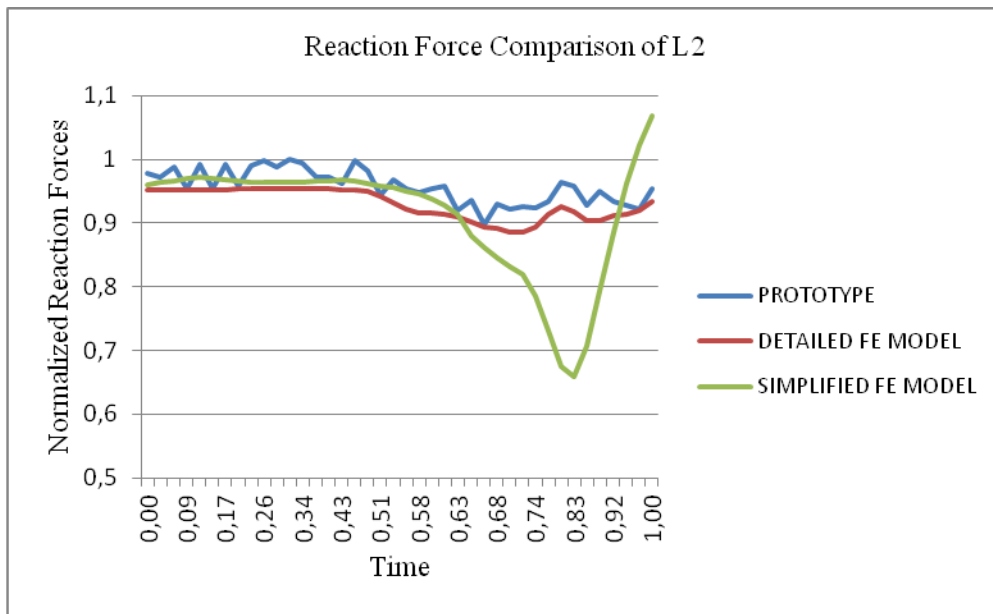


**Figure 76. Reaction force of L2**

The reaction force of the left and backward outrigger is shown in Figure 77.

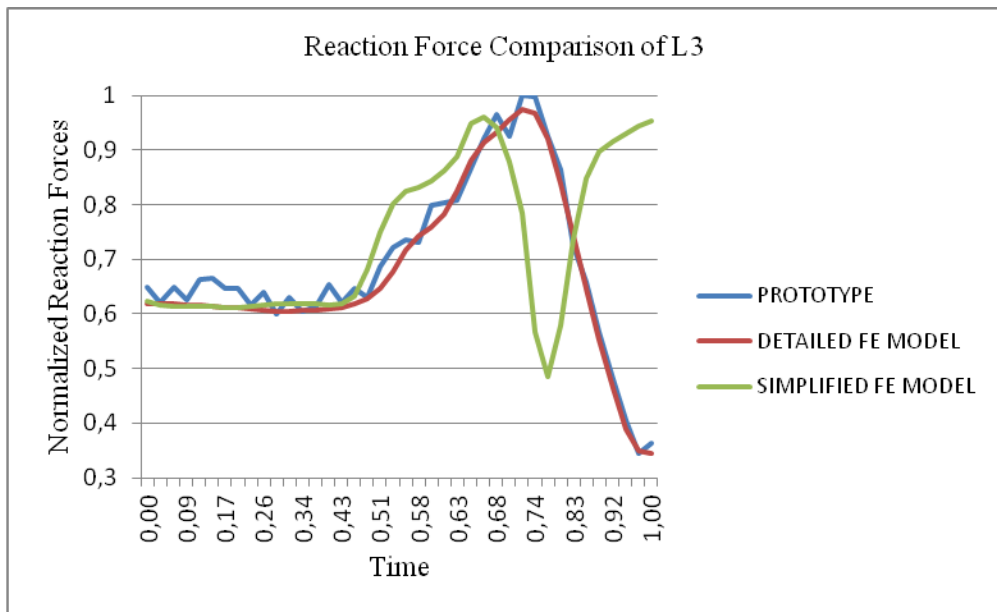


**Figure 77. Reaction force of L3**

The reaction force of the right and backward outrigger is shown in Figure 78.

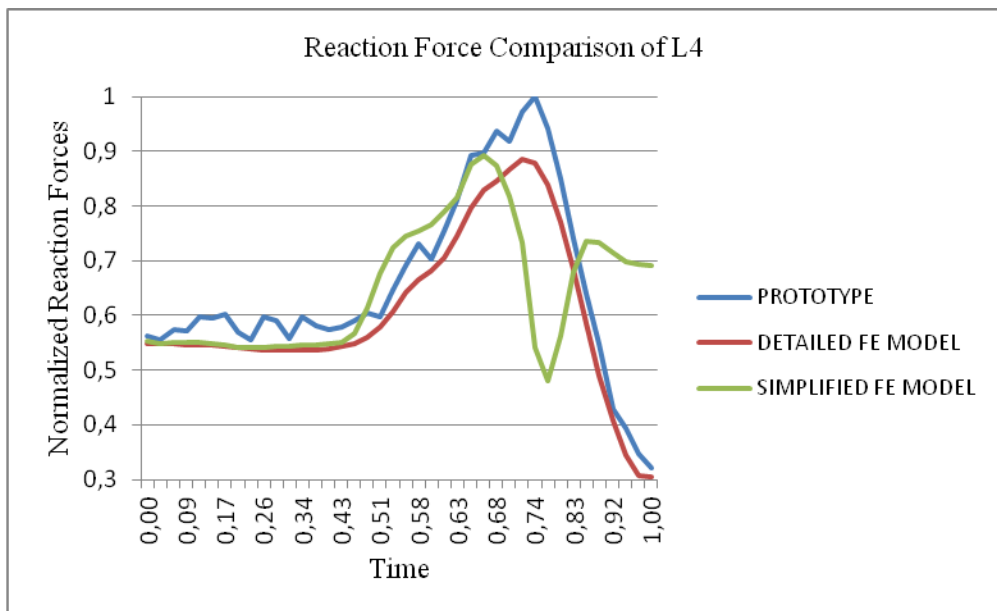


**Figure 78. Reaction force of L4**

the displacements of the cradles in the Y axes are shown in Figure 79. For actual system, displacement of the tip point of the cradle in Y axes is measured and used for tip-off calculation. For the detailed FE model, displacement of the firing tube's center in Y axes is calculated and used for tip-off calculation. For simplified FE model, displacement of the cradle's mass center in Y axes is calculated and used for tip-off calculation.

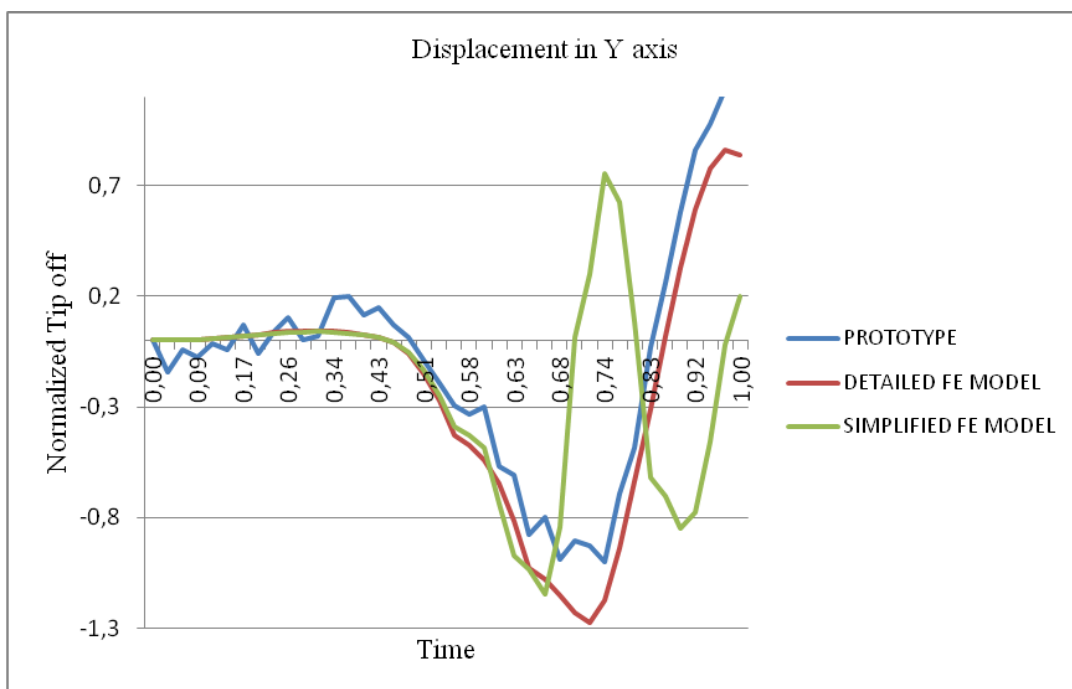


**Figure 79. Displacement in Y axis (Tip-off)**

Magnitude of the simplified FE model total, L1 and L2 reaction forces are similar with the detailed model. The difference between simplified FEM and detailed model is 10% and prototype is 15% during tip-off phase.



Magnitude of the simplified FE model total, L3 and L4 reaction forces are nearly the same with the detailed model. The difference between simplified FE model and detailed model is 2% and prototype is 10% during tip-off phase.

The difference between simplified FE model and detailed FE model in magnitude of the displacement in Y axis is 10% and prototype is 8%. Simplified FE model is among the detailed FE model and prototype during tip-off phase.

On the other hand, there is a phase difference between simplified FE model and detailed FE model due to the fact that dynamic load is applied to firing tube in the detailed FE model and fixed platform in the simplified FE model.

When the results are examined, it can be concluded that both simplified FE model and detailed FE model are verified.

## **CHAPTER 6**

### **INDIVIDUAL EFFECTS OF THE PARAMETERS**

Simplified model that includes necessary kinematic and elastic connections is created in order to decrease preparation time, effort, computation cost and get faster results. Detailed finite element model takes too much time to generate and it is hard to modify and make the analysis again and again. Therefore, parametric model has a huge advantage on detailed model on preparation time and making modifications. In this chapter, individual effects of the parameters are examined. Parameters are clamp attachment positions on the chassis, outrigger deployment, stabilizer case cross section and outrigger case cross section. These parameters are defined in the APDL code. Therefore, they can easily be changed, analysis can be performed for each case and results can be gathered.

#### **6.1 Clamp Attachment Positions**

The rocket launcher system has 3 couple of clamp attachments. First and second couples are so close to the front part of the chassis. Moreover their positions are restricted by the cross members. Therefore third couple's positions will be changed in the simplified model. In the present FE model the third clamp attachment couple is so close to the fixed platform's position. The distance between the third clamp

attachment and the fixed platform is increased. Clamp attachments are shown in Figure 80 and clamp attachment couples are shown in Figure 81.

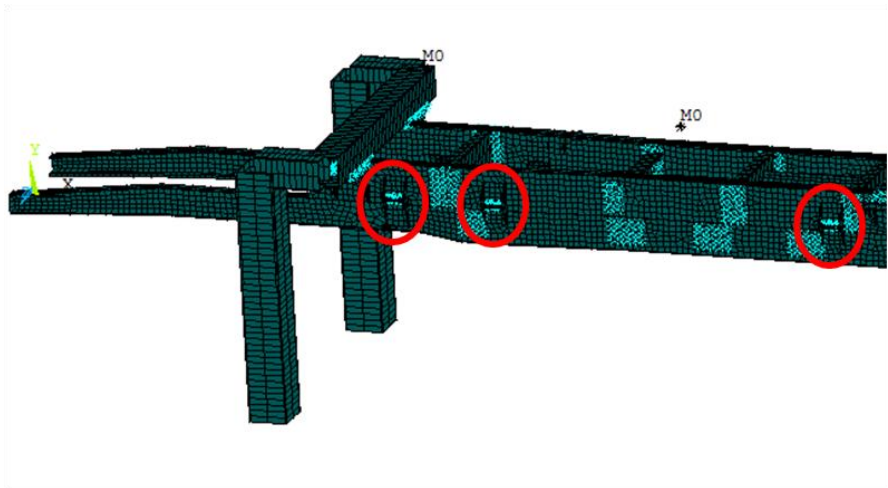


**Figure 80. Clamp attachments' positions on the chassis**

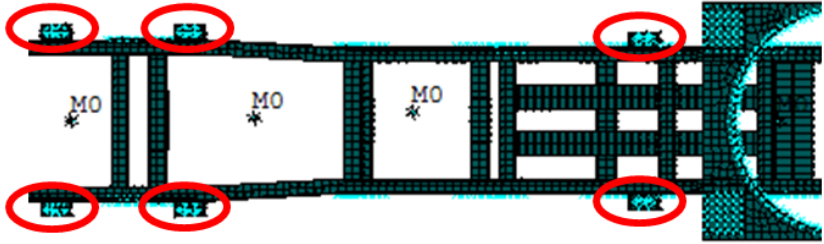


**Figure 81. Clamp attachment couples on the chassis**

The distance of the third clamp attachment couple is measured from the front part of the chassis. The distance values for the different cases are shown in Table 4.

**Table 4. The distance values of the third clamp attachment (Normalized to baseline)**

Model Name	Distance From the Tip Point
Baseline	1
CAP1	0.9
CAP2	0.8

Measuring method for the distance of the third clamp attachment is shown in Figure 82.

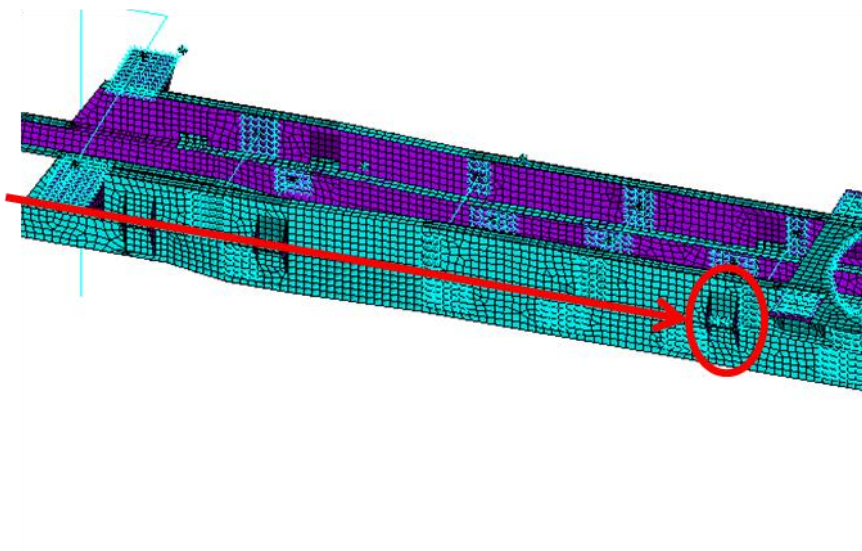


**Figure 82. Third clamp attachment's position measurement method**

Third clamp attachment position of the CAP1 model is shown in Figure 83.

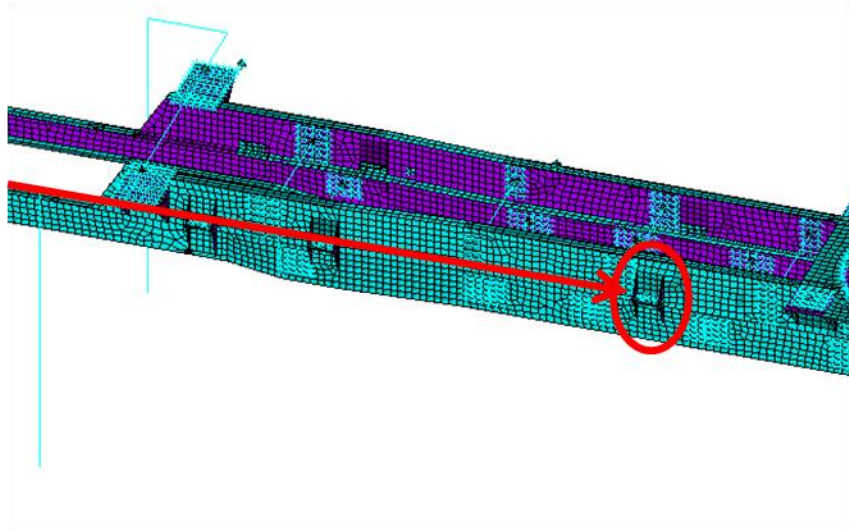


**Figure 83. Third clamp attachment's position of CAP1 model**

Third clamp attachment position of the CAP2 model is shown in Figure 84.

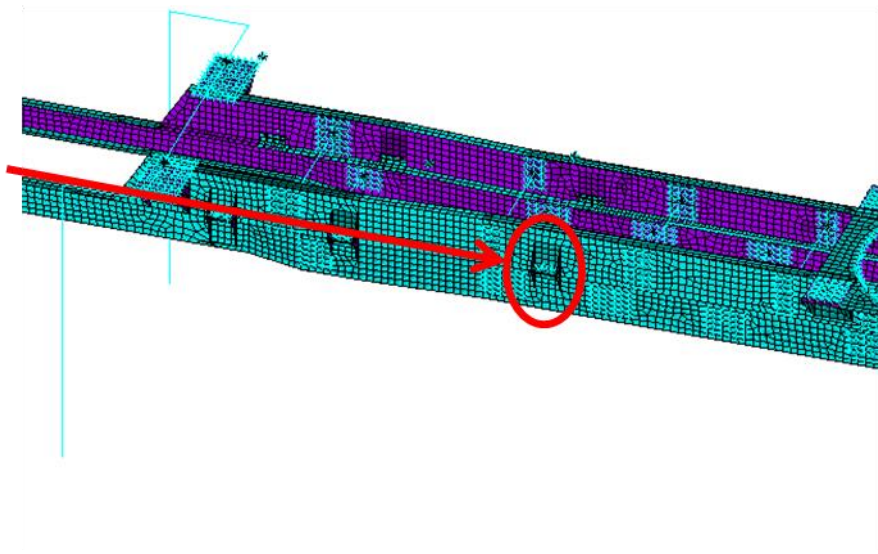


**Figure 84. Third clamp attachment's position of CAP2 model**

Reaction forces and displacement of the mass center of the cradle results are compared in order to figure out the effect of the third clamp attachment position change. At first total reaction forces of all the stabilizers and the outriggers are compared. This comparison is shown in Figure 85.

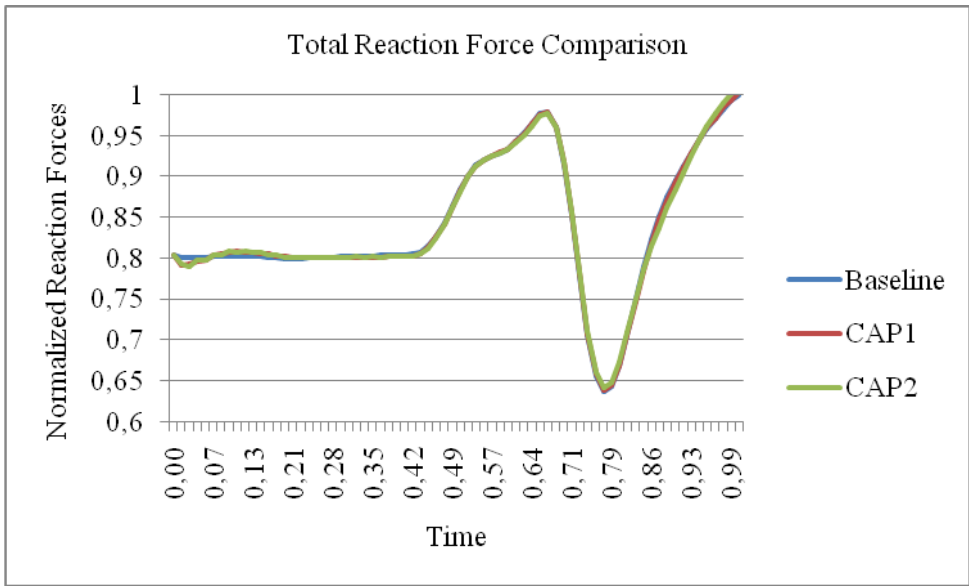


**Figure 85. Comparison of the total reaction forces**

The reaction force comparison for the left front stabilizer is shown in Figure 86.

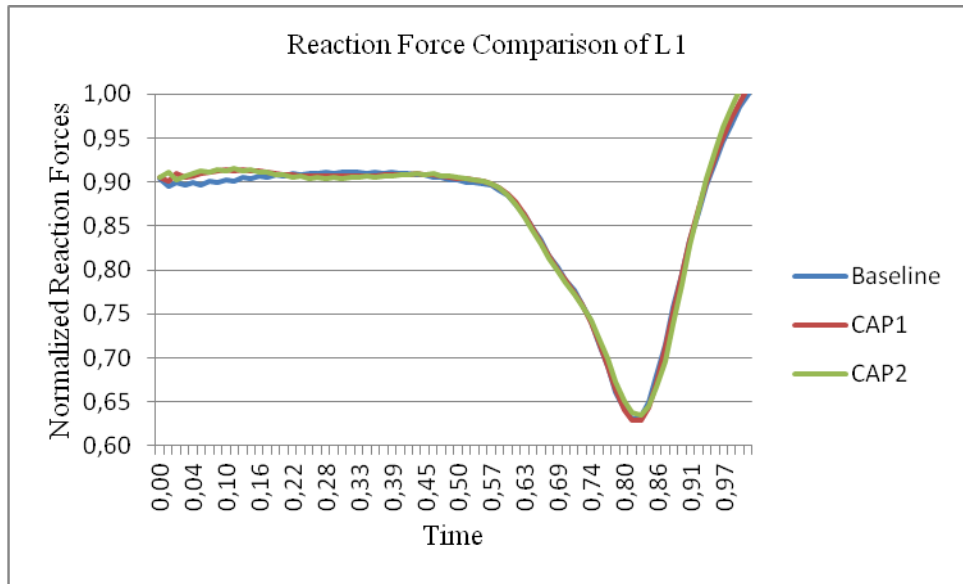


**Figure 86. Comparison of the reaction forces of L1**

Reaction force comparison for the right front stabilizer is shown in Figure 87.

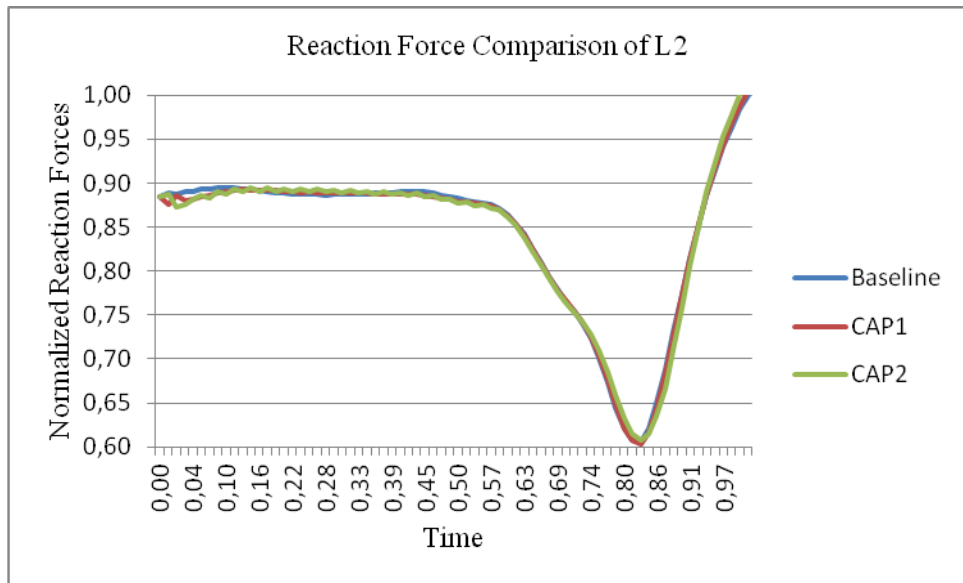


**Figure 87. Comparison of the reaction forces of L2**

Reaction force comparison for the left backward outrigger is shown in Figure 88.

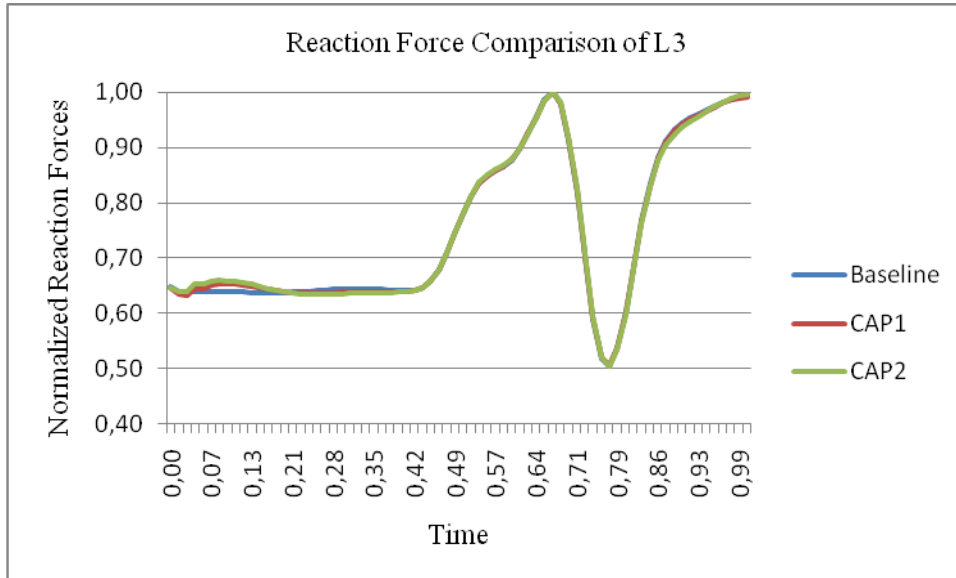


**Figure 88. Comparison of the reaction forces of L3**

Reaction force comparison for the right backward outrigger is shown in Figure 89.

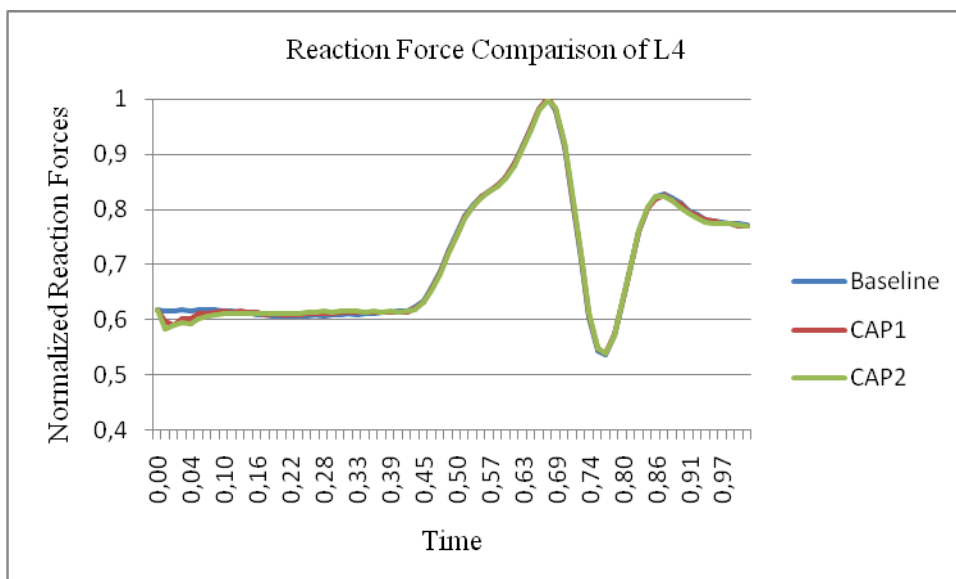


**Figure 89. Comparison of the reaction forces of L4**



Displacement of the mass center of the cradle comparison is shown in Figure 90.

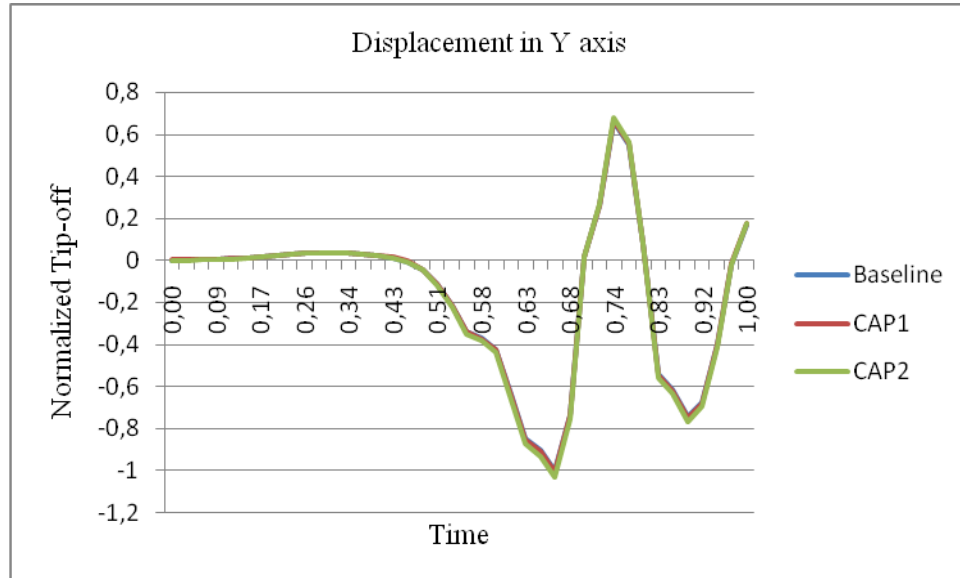


**Figure 90. Comparison of the mass center of the cradle in Y axis**

Changing the position of the third clamp attachment couple is not a significant parameter for the dynamic behavior of the rocket launcher system since both reaction forces and the tip-off values are alters beggarly. On the other hand, keeping third clamp attachment couple far from the fixed platform reduces the stiffness advantage of the chassis. Therefore, tip-off value increases 1% for CAP1 and 3% for CAP2 models due to decrease in stiffness.

## 6.2 Outrigger's Deployment

The rocket launcher system has a stabilizer couple and outrigger couple. Stabilizers cannot be deployed in the horizontal direction. On the other hand outriggers can be deployed in the horizontal direction via a hydraulic system. Outrigger's deployment

ratio has an effect on the dynamic characteristics of the rocket launcher system. Deployment in the vertical axis is remained the same when the deployment in the horizontal axis is changing. Deployment ratio in the horizontal axis is restricted by the stroke of the hydraulic system. Stabilizers and outriggers are shown in Figure 91.

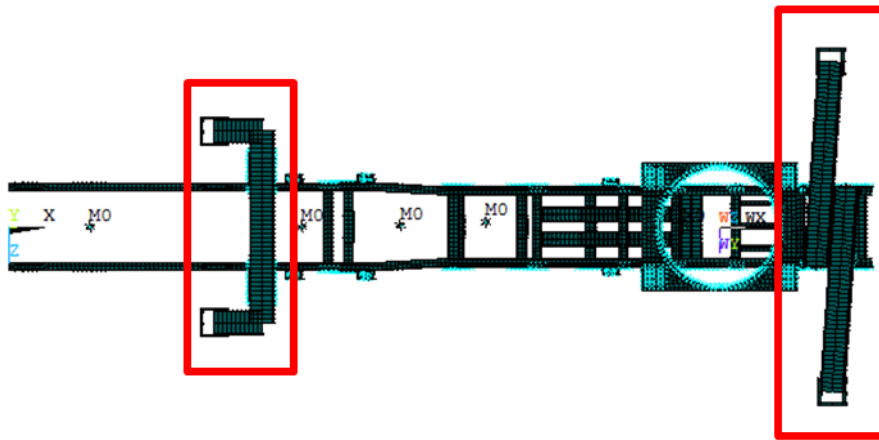


**Figure 91. Stabilizers and outriggers of the rocket launcher system**

The deployment is measured from the beginning of the outrigger. The deployment ratio values for the different cases are shown in Table 5.

**Table 5. Deployment ratio values of the outriggers (Normalized to baseline)**

Model Name	Deployment Ratio
Baseline	1
DR1	0.8
DR2	0.6

Measuring method for the distance of the third clamp attachment is shown in Figure 92.

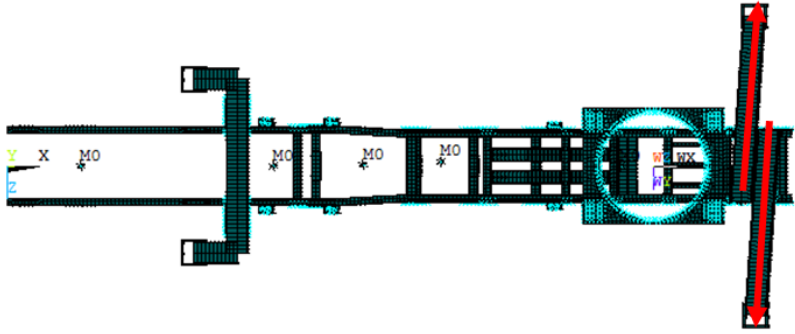


**Figure 92. Outrigger's deployment ratio measurement method**

Outrigger deployment of the DR1 model is shown in Figure 93.

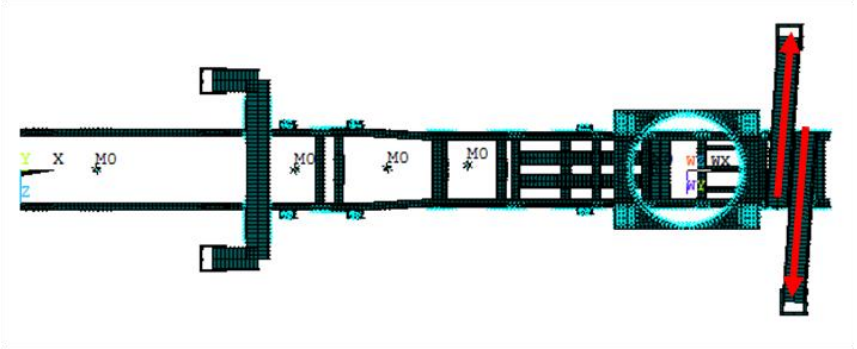


**Figure 93. Outrigger's deployment of DR1 model**

Outrigger deployment of the DR2 model is shown in Figure 94.

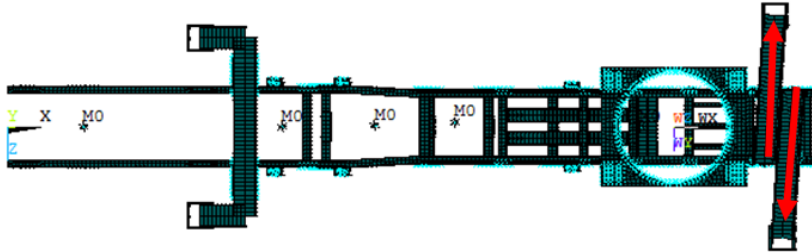


**Figure 94. Outrigger's deployment of DR2 model**

Reaction forces and displacement of the mass center of the cradle results are compared in order to figure out the effect of the deployment ratio. At first total reaction forces of all the stabilizers and the outriggers are compared. This comparison is shown in Figure 95.

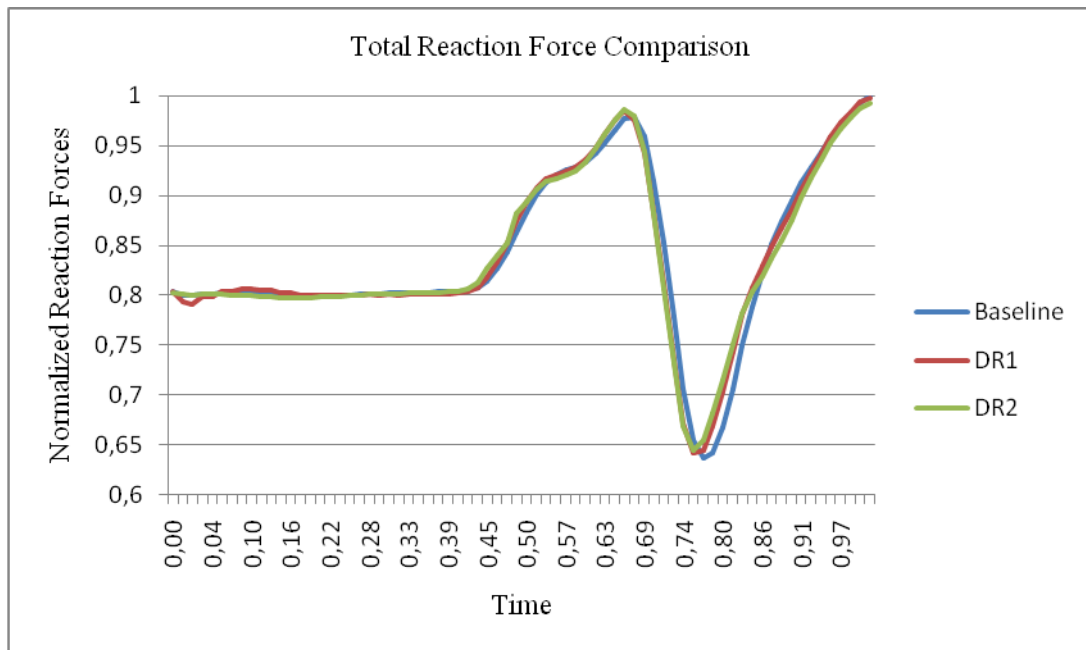


**Figure 95. Comparison of the total reaction forces**

Reaction force comparison for the left front stabilizer is shown in Figure 96.

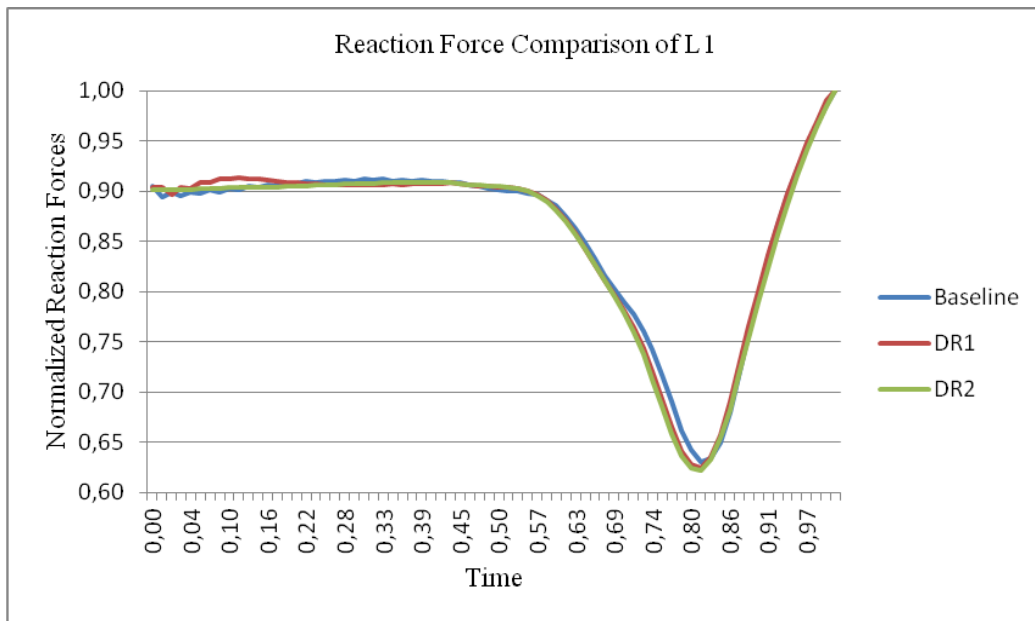


**Figure 96. Comparison of the reaction forces of L1**

Reaction force comparison for the right front stabilizer is shown in Figure 97.

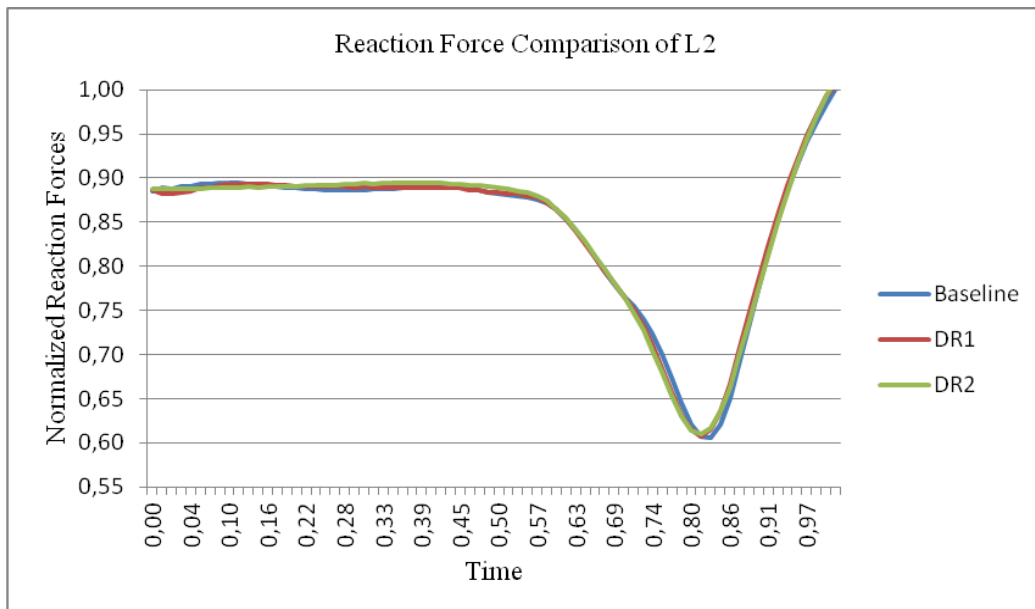


**Figure 97. Comparison of the reaction forces of L2**

Reaction force comparison for the left backward outrigger is shown in Figure 98.

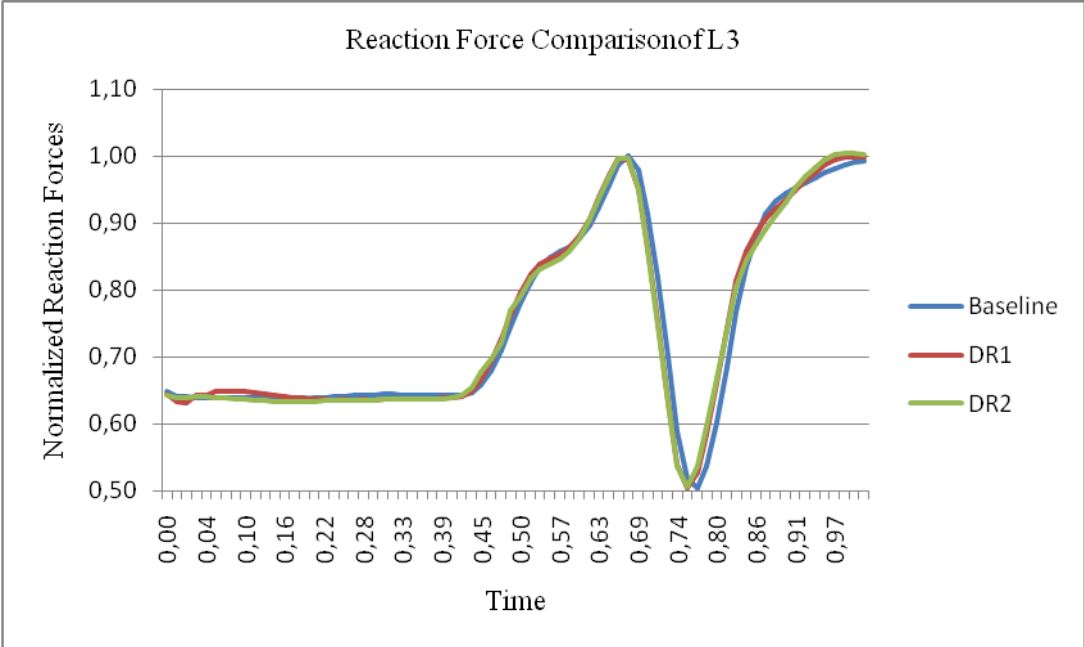
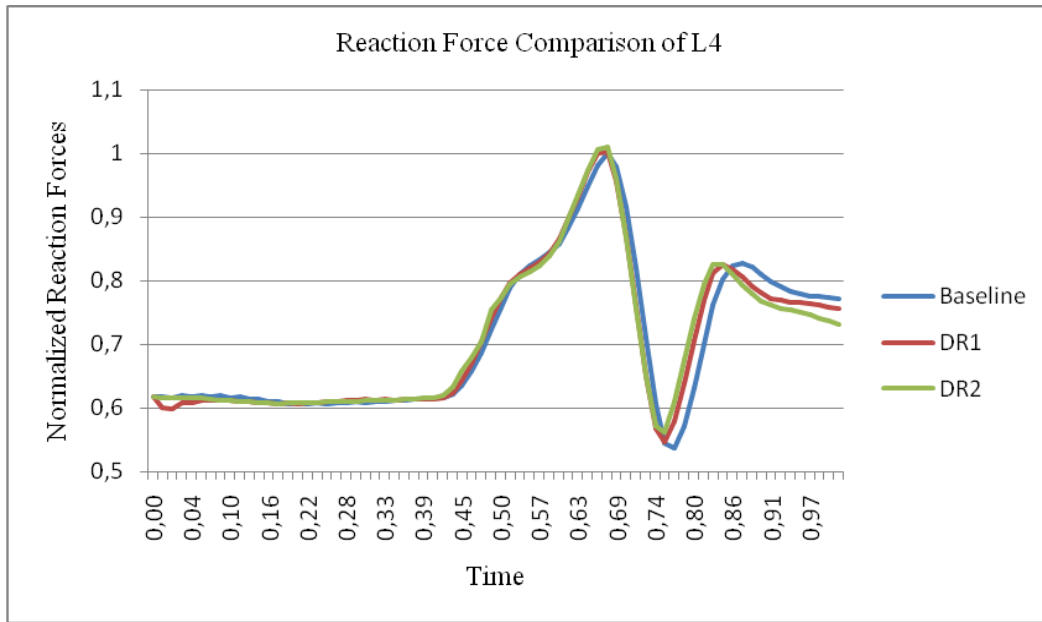


Figure 98. Comparison of the reaction forces of L3

Reaction force comparison for the right backward outrigger is shown in Figure 99.



**Figure 99. Comparison of the reaction forces of L4**

Displacement of the mass center of the cradle comparison is shown in Figure 100.

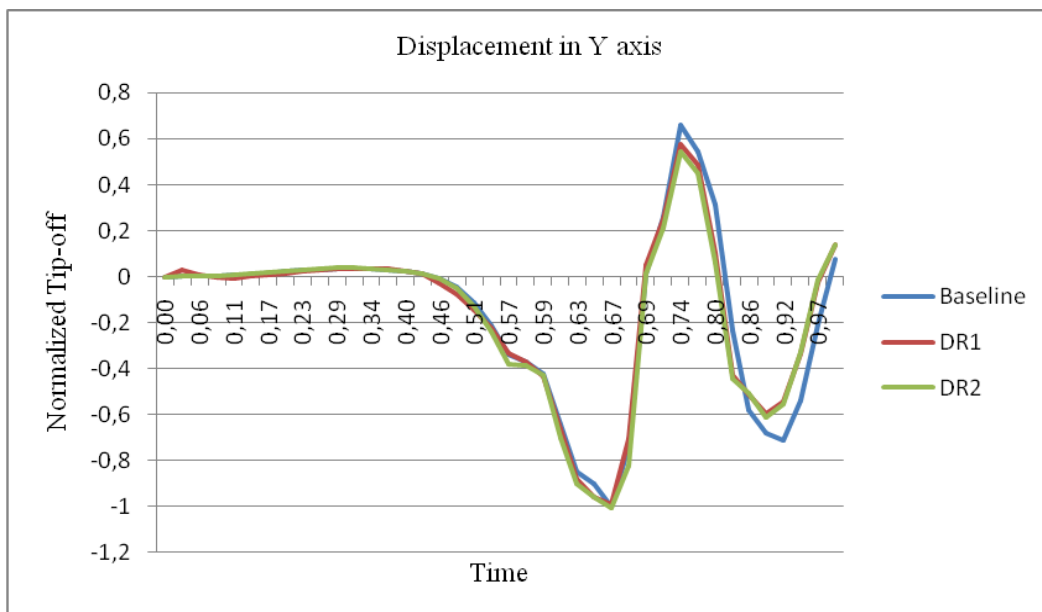


**Figure 100. Comparison of the mass center of the cradle in Y axis**



Decreasing the deployment ratio of the outriggers is significant for the dynamic behavior of the rocket launcher system since both reaction forces and the tip-off values are affected. On the other hand, system behavior is similar during tip-off phase and difference is less than 2%.

After rocket leaves the firing tube reaction forces and displacement in Y axis are changed and phase shift occurs due to rigidity increase. Displacement in Y axis is reduced 7% for DR1 and 10% for DR2. Moreover, the rocket is not affected from the rocket launcher system's behavior during the free flight phase. Therefore, deployment ratio change can be taken into account for successive firings.

### 6.3 Stabilizer's Cross Section Modification

The rocket launcher system has a stabilizer couple. Stabilizer's cross section has an effect on the dynamic behavior of the rocket launcher system since the stiffness of the system alters dependently. Stabilizer's cross section can be changed by changing the thickness of the stabilizer profiles easily due to the fact that stabilizers are modeled with beam elements. Stabilizers are shown in Figure 101.

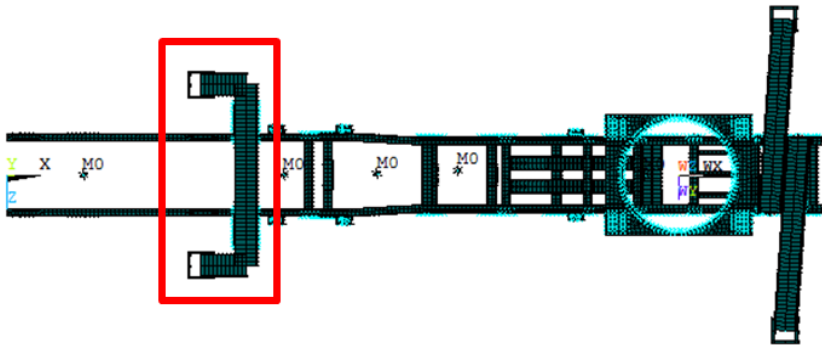


Figure 101. Stabilizers of the rocket launcher system

The thickness values of the stabilizer couple are shown in Table 6.

**Table 6. Thickness values of the stabilizers (Normalized to baseline)**

Model Name	Thickness
Actual Design	1
ST1	0.75
ST2	0.5

Changing method for the thickness of the stabilizers is shown in Figure 102.

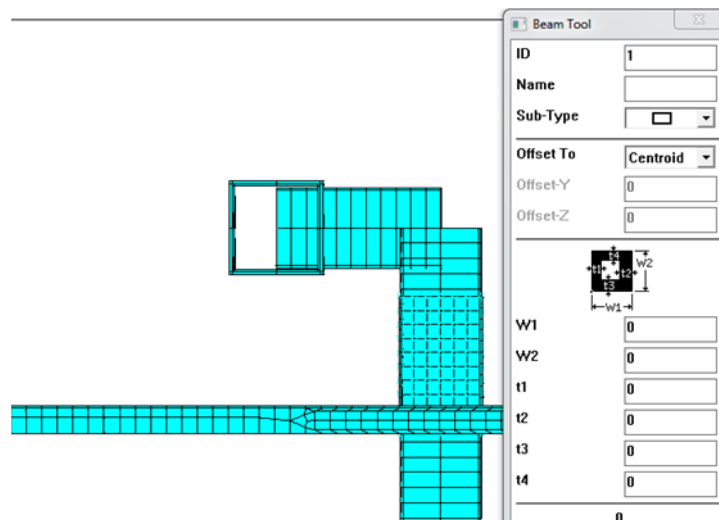


**Figure 102. Stabilizer's thickness changing method**

Displacements of stabilizers and outriggers in the transverse direction (in Z axis) and displacement of the mass center of the cradle results are compared in order to figure out the effect of the stabilizer's thickness change. Mid points of stabilizers

and outriggers where displacement values are collected shown is shown in Figure 103.

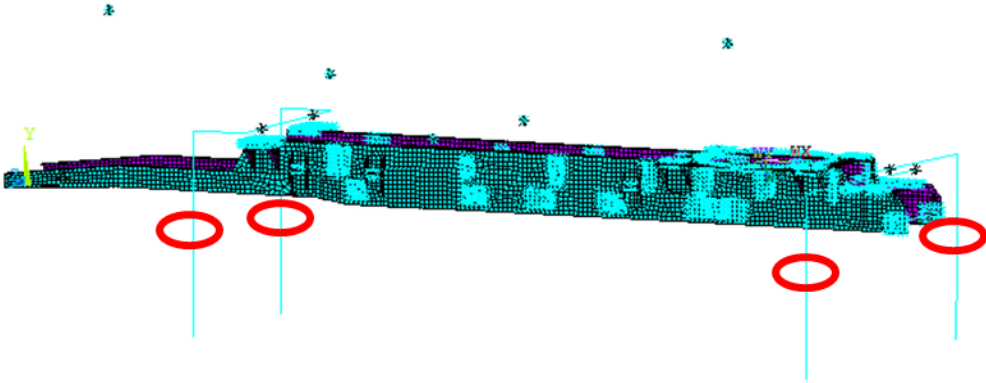


**Figure 103. Mid points of the stabilizers and outriggers**

Displacement comparison in Z axis for the left front stabilizer is shown in Figure 104.

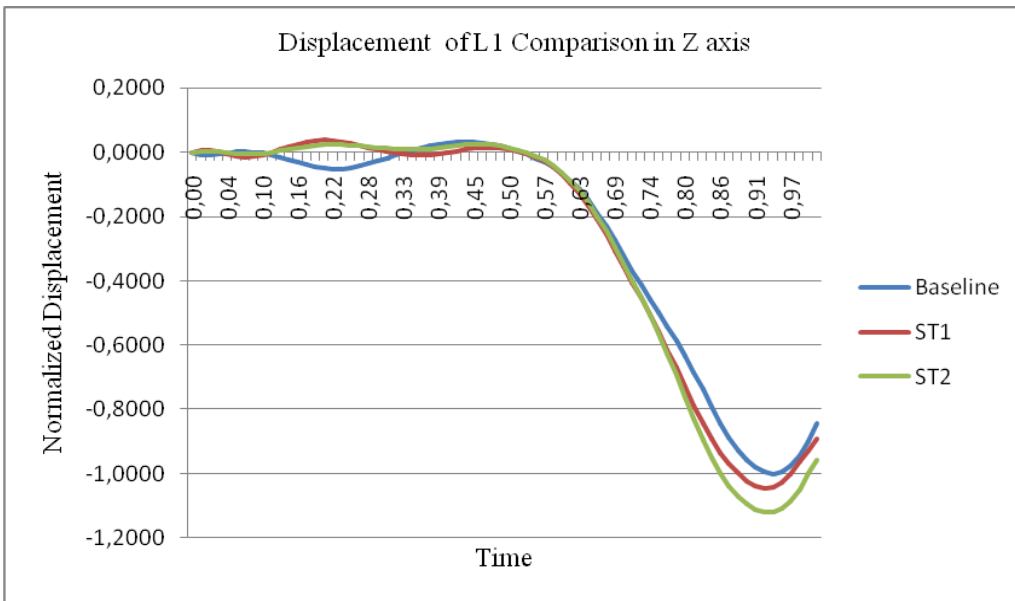


**Figure 104. Comparison of the displacement of L1 in Z axis**

Displacement comparison in Z axis for the right front stabilizer is shown in Figure 105.

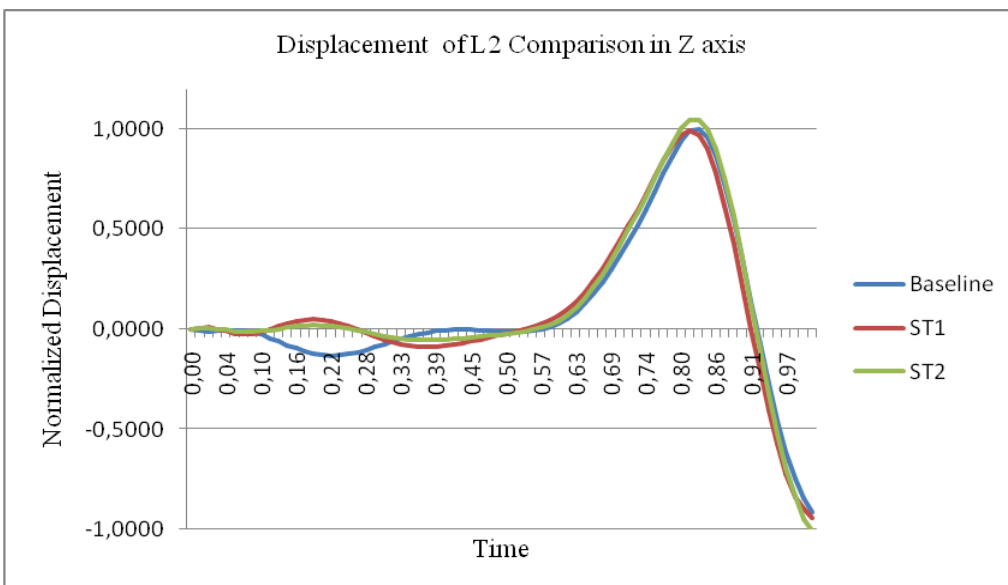


**Figure 105. Comparison of the displacement of L2 in Z axis**

Displacement comparison in Z axis for the left backward outrigger is shown in Figure 106.

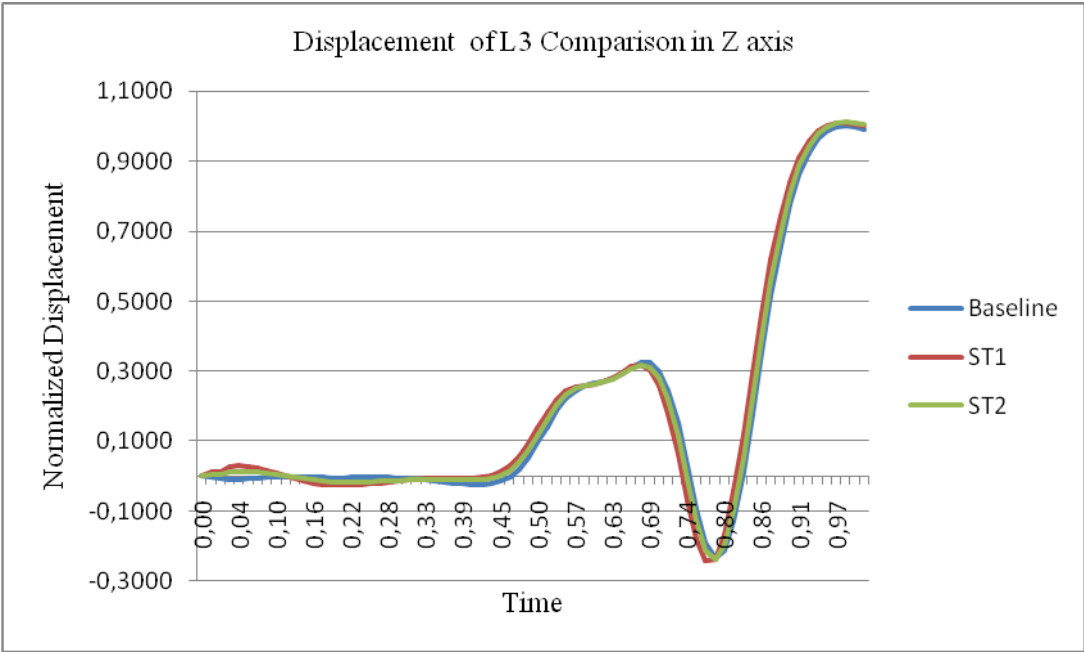


**Figure 106. Comparison of the displacement of L3 in Z axis**

Displacement comparison in Z axis for the right backward outrigger is shown in Figure 107.

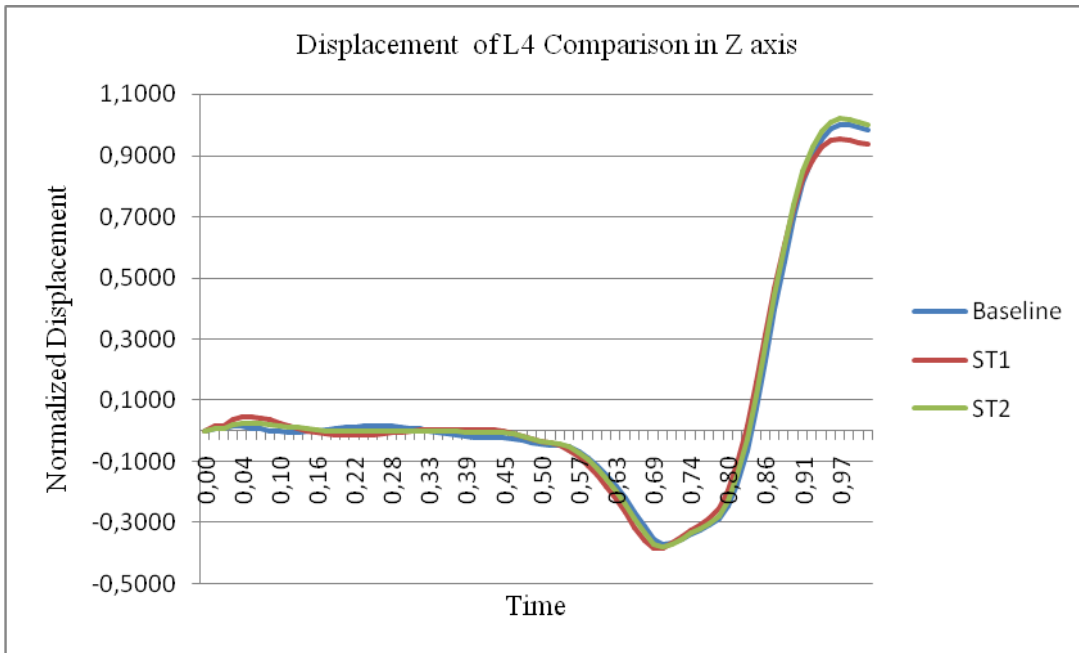


**Figure 107. Comparison of the displacement of L4 in Z axis**

Displacement of the mass center of the cradle comparison is shown in Figure 108.

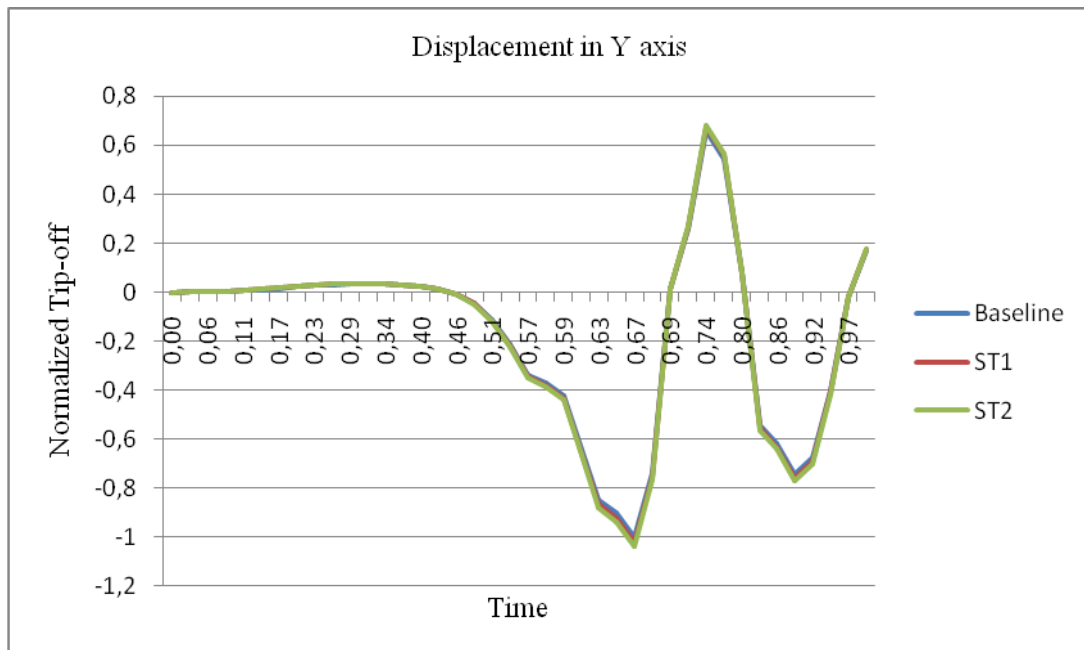


**Figure 108. Comparison of the mass center of the cradle in Y axis**

Decreasing the thickness of the stabilizer's causes changes in the behavior of the stabilizers. It can be concluded that stress values are increased as a result of thickness reduction due to the fact that displacement in the Z axis are increased up to 10%.

On the other hand, outriggers are affected less than 1%.

Moreover, tip-off values are increased 2.3% in ST1 and 3.8% in ST2 since the stiffness of the stabilizers is decreased.

Stress calculations are significant when compared to the tip-off values for stabilizers' thickness reduction.

## 6.4 Outrigger's Cross Section Modification

The rocket launcher system has an outrigger couple. Outrigger's cross section has an effect on the dynamic behavior of the rocket launcher system since the stiffness of the system alters dependently. Outrigger's cross section can be changed by changing the thickness of the outrigger profiles easily due to the fact that outriggers are modeled with beam elements. Outriggers are shown in Figure 109.

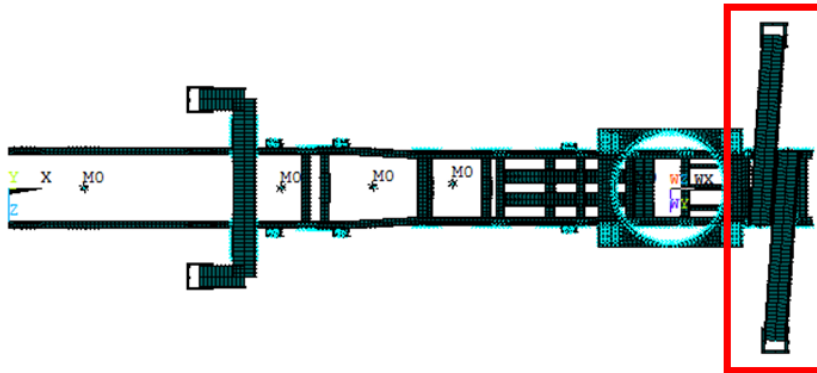


**Figure 109. Outriggers of the rocket launcher system**

The thickness values of the outrigger couple are shown in Table 7.

**Table 7. Thickness values of the outriggers (Normalized to baseline)**

Model Name	Thickness
Actual Design	1
OT1	0.75
OT2	0.5



Changing method for the thickness of the outriggers is shown in Figure 110.

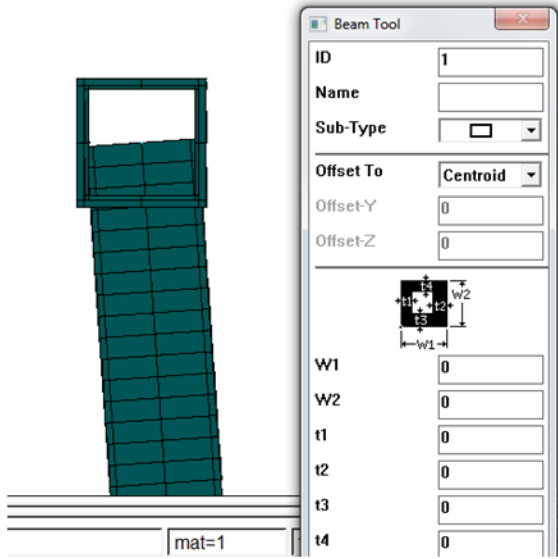


**Figure 110. Outrigger's thickness changing method**

Displacements of stabilizers and outriggers in the transverse direction (in Z axis) and displacement of the mass center of the cradle results are compared in order to figure out the effect of the stabilizer's thickness change. Mid points of stabilizers and outriggers where displacement values are collected shown is shown in Figure 111.

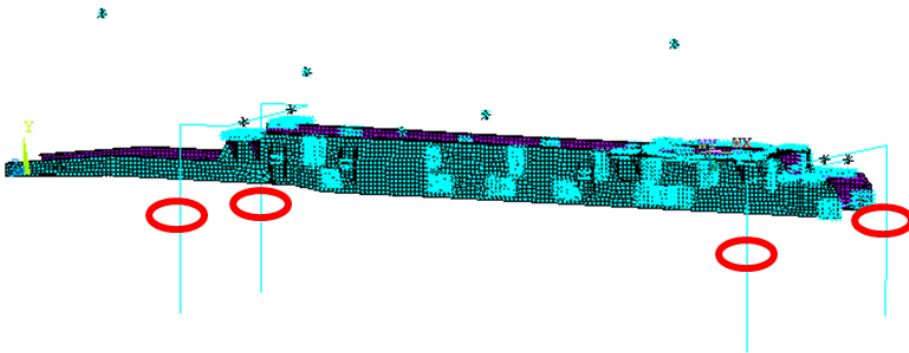


**Figure 111. Mid points of the stabilizers and outriggers**

Displacement comparison in Z axis for the left front stabilizer is shown in Figure 112.

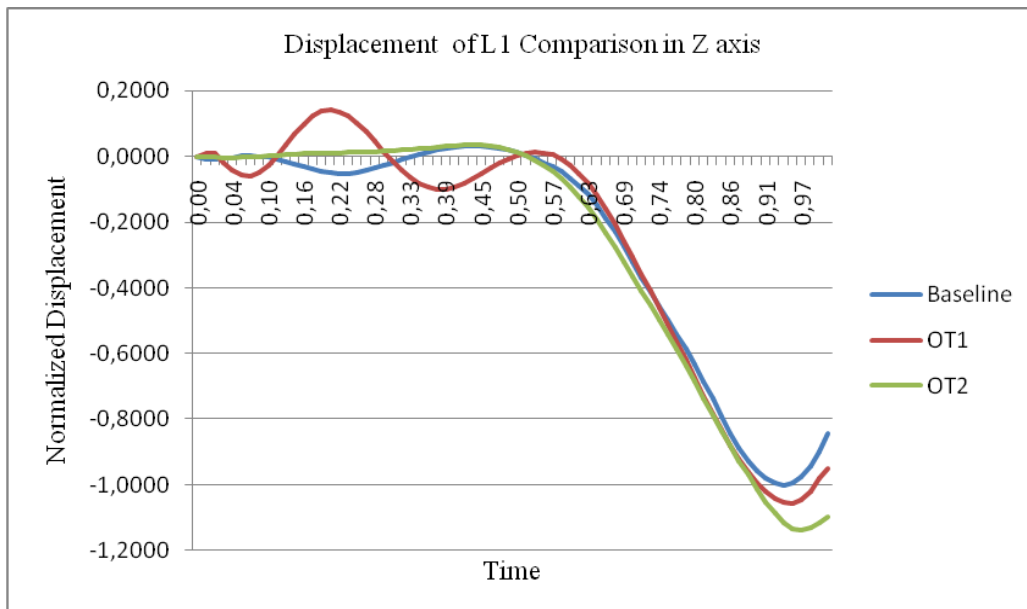


**Figure 112. Comparison of the displacement of L1 in Z axis**

Displacement comparison in Z axis for the right front stabilizer is shown in Figure 113.

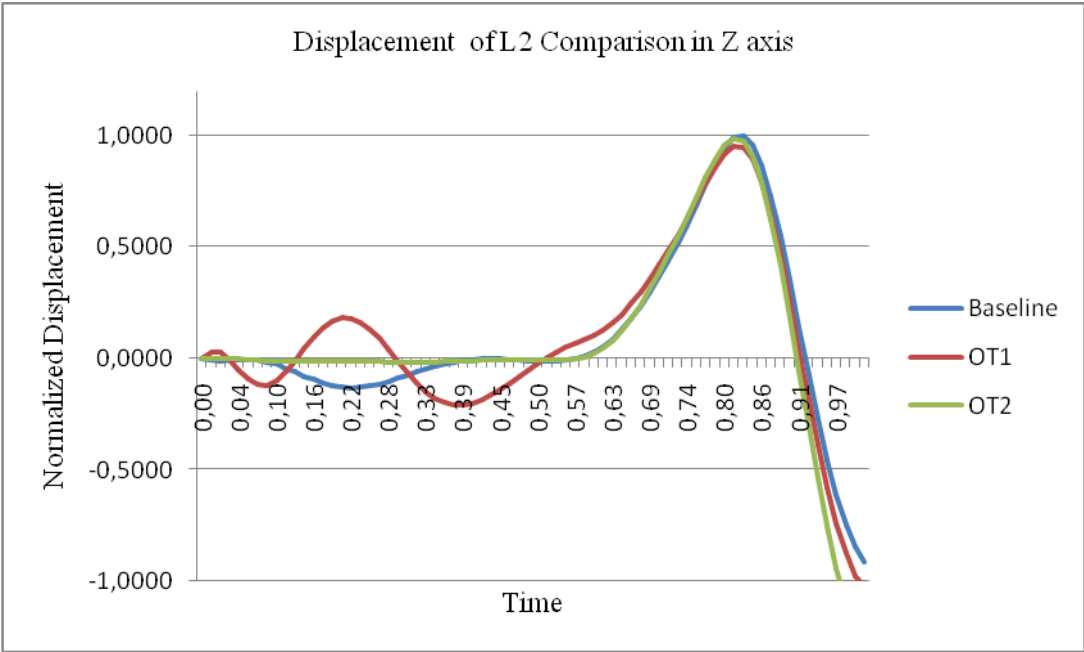


**Figure 113. Comparison of the displacement of L2 in Z axis**

Displacement comparison in Z axis for the left backward outrigger is shown in Figure 114.

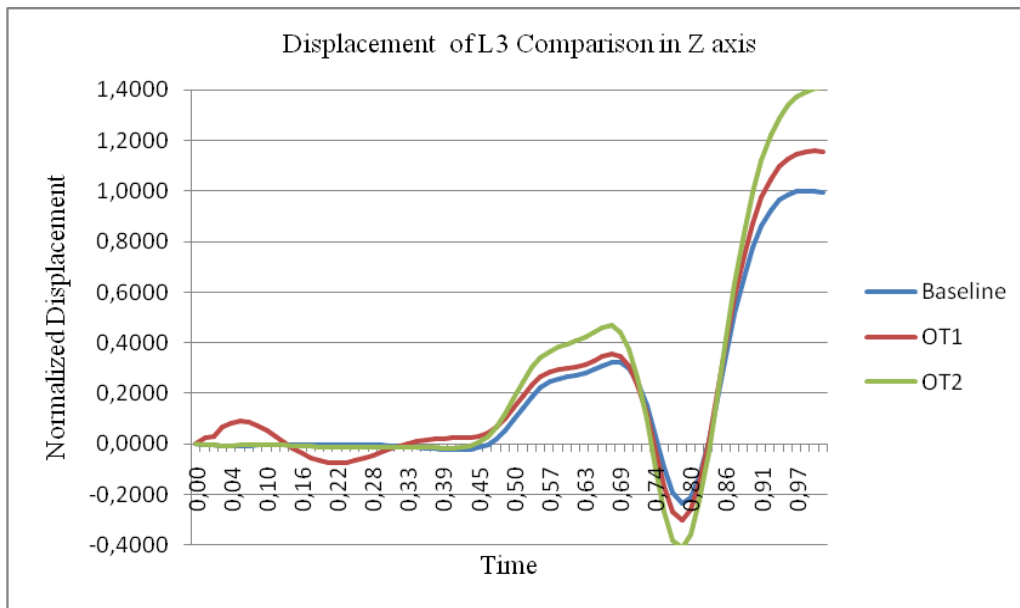


**Figure 114. Comparison of the displacement of L3 in Z axis**

Displacement comparison in Z axis for the right backward outrigger is shown in Figure 115.

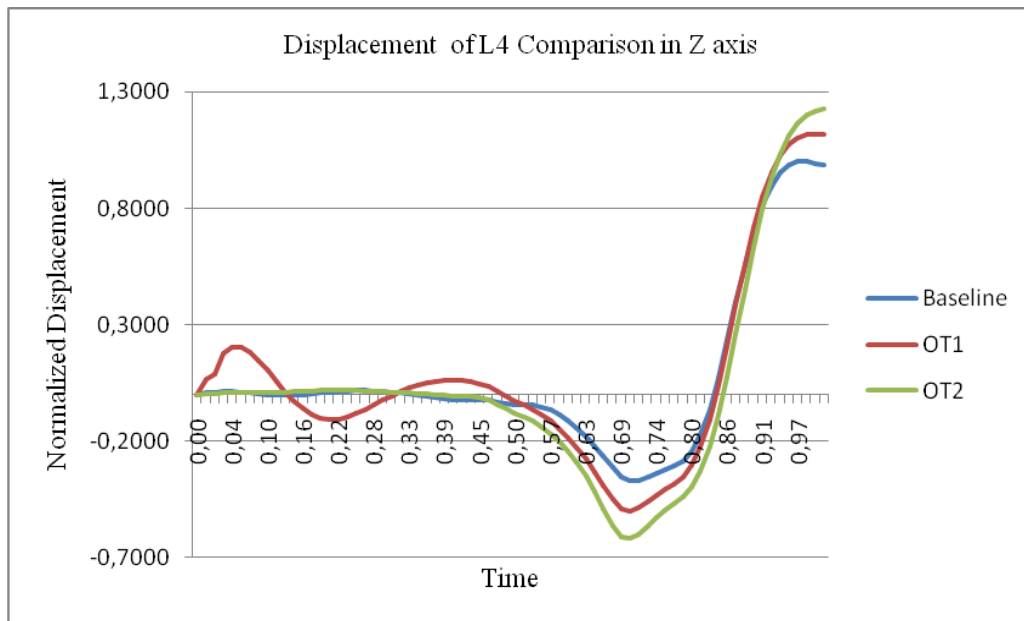


**Figure 115. Comparison of the displacement of L4 in Z axis**

Displacement of the mass center of the cradle comparison is shown in Figure 116.

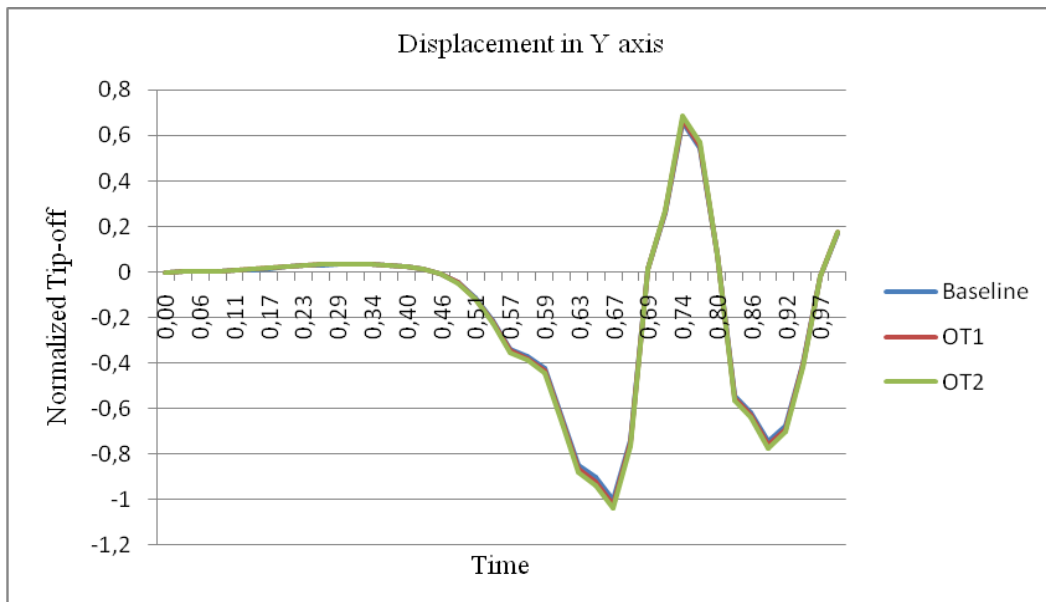


**Figure 116. Comparison of the mass center of the cradle in Y axis**

Decreasing the thickness of the outriggers cause changes in the behavior of the outriggers. It can be concluded that stress values are increased as a result of thickness reduction and firing load is applied very close to outriggers due to the fact that displacement in the Z axis are increased up to 10% for L3 and 15% for L4 in OT1 model, 20% for L3 and 30% for L4 in OT2 model.

On the other hand, stabilizers are affected less than 10% due to the fact that firing load is far from stabilizers.

Moreover, tip-off values are increased 2% in OT1 and 3.1% in OT2 since the stiffness of the stabilizers is decreased.

Stress calculations are significant when compared to the tip-off values for outriggers' thickness reduction.



## **CHAPTER 7**

### **SUMMARY AND CONCLUSIONS**

In this chapter, general summary of this thesis, some conclusion and remarks are presented.

#### **7.1 Summary**

In this thesis dynamic behavior of a rocket launcher system is investigated under dynamic plume load on dynamic analysis basis. Two distinct models of the rocket launcher system are composed. These are detailed FE model and simplified FE model. These models are verified with the experimental studies. Flowchart which can be followed as related to the requirements of the future projects is shown in Figure 117.



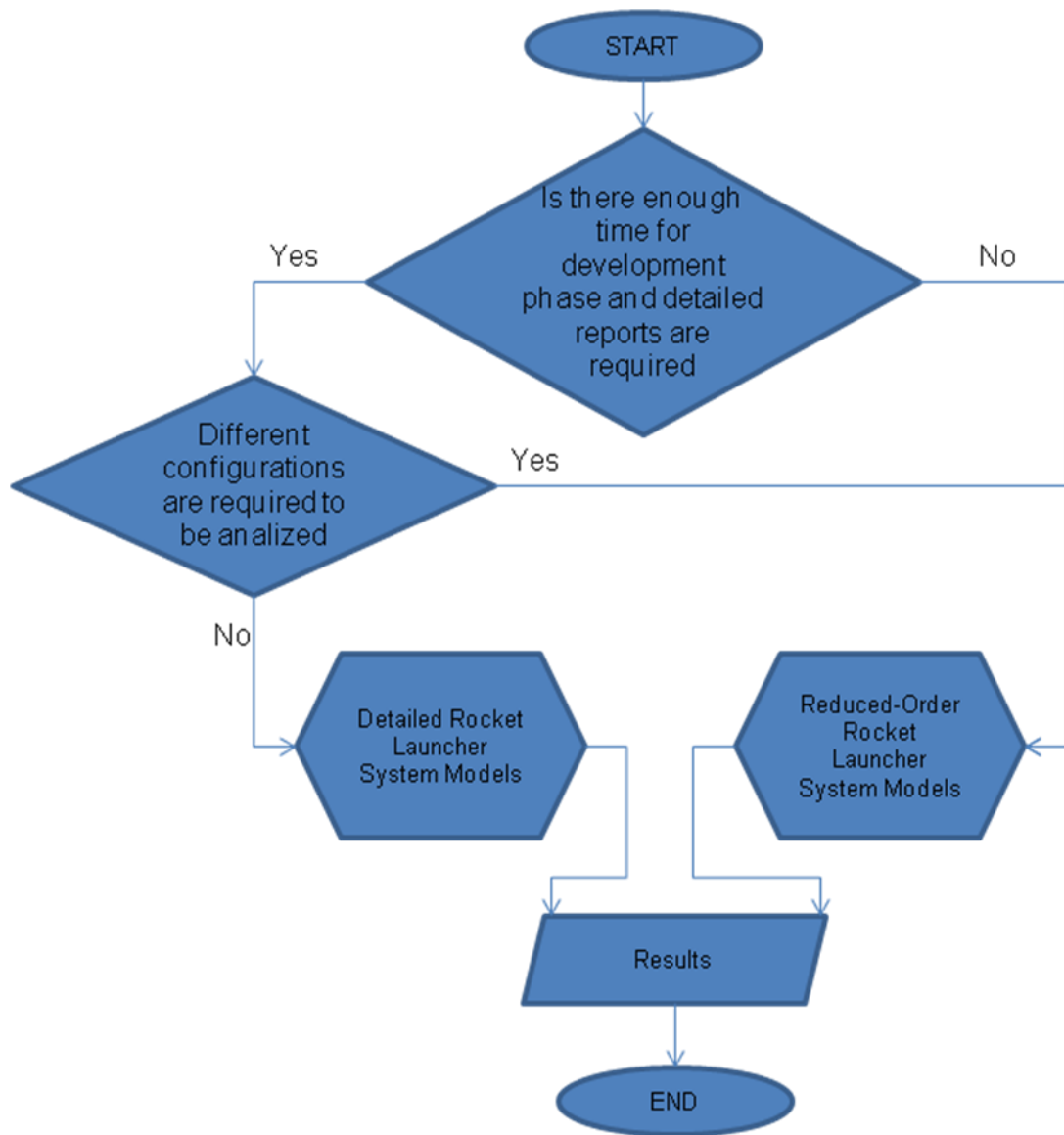


**Figure 117. Flowchart for the future projects**

Detailed FE model created in the first step. This model contains necessary kinematic and elastic connections with as much detail as possible. Only simplification is done for meshing simplifications on CAD model. Only nonstructural parts are modeled with lumped masses. These lumped masses are connected to the relevant parts with force distributed elements. Then, material properties are inserted in the FEA.

As a next step, boundary conditions applied. Modal analysis performed in order to figure out the dynamic characteristics of the rocket launcher system. Modal effective mass values are calculated in order to determine the most significant natural frequencies and mode shapes.

After that, static analysis is performed under static load. As a next step, dynamic load is applied on the FE model in the equilibrium position. Then, reaction forces and the firing tube center's displacement is calculated in the same axis with the gravity in order to figure out the tip-off value.

The simplified FE model is created as a second model in order to reduce the cost, time and effort. Chassis and auxiliary chassis are modeled with shell elements and friction is defined between them. Cross members of the chassis and auxiliary chassis are modeled with beam elements. Cross elements are connected to the relevant parts with rigid elements. Stabilizers and outriggers are modeled with beam elements. Stabilizers and outriggers are attached to the auxiliary chassis with rigid elements. Hydraulic system in the stabilizers and outriggers are modeled with truss elements. Clamp attachments between chassis and auxiliary chassis are modeled with shell elements, bolts of them are modeled with beam elements. fixed platform is modeled with shell elements. Azimuth platform, elevation platform, firing tubes and rockets are modeled with lumped masses and inertia values. Moreover, clamp attachment positions on the chassis, outrigger deployment, stabilizer case cross section and outrigger case cross sections are modeled as parametric for performing modifications just by changing a single parameter. A FORTRAN based ANYS Parametric Design Language (APDL) code is create in order to compose the parametric simplified FE model, define the boundary conditions and material properties, perform analysis and get the results. This code automates the aforementioned tasks and performs these tasks just by running the code in the finite element software.

After that, boundary conditions applied. Modal analysis performed in order to figure out the dynamic characteristics of the rocket launcher system. Most significant Natural frequencies and Mode shapes are examined and compared with

the detailed FE model. It is discovered that, Mode shapes are similar however, Natural frequencies are calculated higher since the rigid elements are used for the connections. Results are examined in order to figure out the success of this approximation.

Then, static analysis is performed under static load. Then, dynamic load is applied on the FE model in the equilibrium position. Moreover, different damping parameters are defined for the FE model and analyses are performed, results are compared in order to determine the reaction forces and displacement of the mass center of the cradle is calculated in the same axis with the gravity in order to figure out the tip-off value.

In addition to these two models, experimental studies are performed in order to compare the results and perform verifications of the aforementioned FE models. Detailed FE model and test results are so similar both magnitude and behavior. The difference is less than 10%. Moreover, simplified model's trend and the magnitude of the dynamic behavior is similar and the difference is less than 15%. However, there is a phase difference between simplified FE model and detailed FE model due to the fact that dynamic load is applied to firing tube in the detailed FE model and fixed platform in the simplified FE model.

After verification of the two FE models, individual effects of the parameters on the rocket launcher system's dynamic characteristics are examined by changing the parameters of simplified FE model. This operation is performed very fast since the rocket launcher system is created by an APDL code and every analysis is done by just changing a single parameter. Then, modifications are applied on the FE model accordingly.

Third clamp attachment couple's position change is not an important parameter for the dynamic behavior of the rocket launcher system. On the other hand, keeping third clamp attachment couple far from the fixed platform reduces the stiffness advantage of the chassis. Therefore, tip-off value increases 1% for CAP1 and 3% for CAP2 models due to decrease in stiffness.

Reducing the deployment ratio of the outriggers is significant for the dynamic behavior of the rocket launcher system since both reaction forces and the tip-off values are affected. On the other hand, system behavior is similar during tip-off phase and difference is less than 2%. During free flight phase, reaction forces and displacement in Y axis are changed and phase shift occurs due to rigidity increase. Displacement in Y axis is reduced 7% for DR1 and 10% for DR2. Therefore, deployment ratio change can be taken into account for successive firings.

Reducing the thickness of the stabilizer's causes difference in the behavior of the stabilizers. It can be resulted that stress values are increased as a result of thickness decrease due since displacements in the Z axis are increased up to 10%. However, outriggers are affected less than 1%. Furthermore, tip-off values are increased 2.3% in ST1 and 3.8% in ST2 since the stiffness of the stabilizers is decreased. Therefore, stress calculations are significant when compared to the tip-off values for stabilizers' thickness reduction.

Reducing the thickness of the outriggers cause changes in the behavior of the outriggers. It can be concluded that stress values are increased as a result of thickness reduction and firing load is applied very close to outriggers since displacement in the Z axis are increased up to 10% for L3 and 15% for L4 in OT1 model, 20% for L3 and 30% for L4 in OT2 model. However, stabilizers are affected less than 10% due to the fact that firing load is far from stabilizers. Furthermore, tip-off values are increased 2% in OT1 and 3.1% in OT2 since the stiffness of the stabilizers are decreased. Therefore, stress calculations are significant when compared to the tip-off values for outriggers' thickness reduction.

## **7.2 General Conclusions and Discussion**

Simplified FE model is an important tool in order to get results faster and figure out the individual effects of the every single modification on a rocket launcher system without creating a complex FE model and performing expensive firing tests. The

results of the simplified FE model with the detailed FE model and test results do not yield exactly the same results but general behavior and magnitudes are similar. Besides, composing a very detailed and complex FE model and performing so expensive firing tests take too much time and brings too much effort and cost. On the other hand, composing, making modifications are 10 times faster and getting the results is 100 times faster for the simplified FE model.

Detailed FE model is a way of modeling a rocket launcher system. On the other hand, composing mentioned FE model takes at least 5 months and the solution can be obtained at the end of minimum 4 days. However, composing simplified FE model takes 2 weeks if the designer has an experience on APDL and rocket launcher systems. Furthermore, results can be obtained less than 1 hour. Modifications can be done just by changing a value in the APDL code. Comparison of the preparation, solution and post-processing of these two models with respect to time is given in Figure 118.

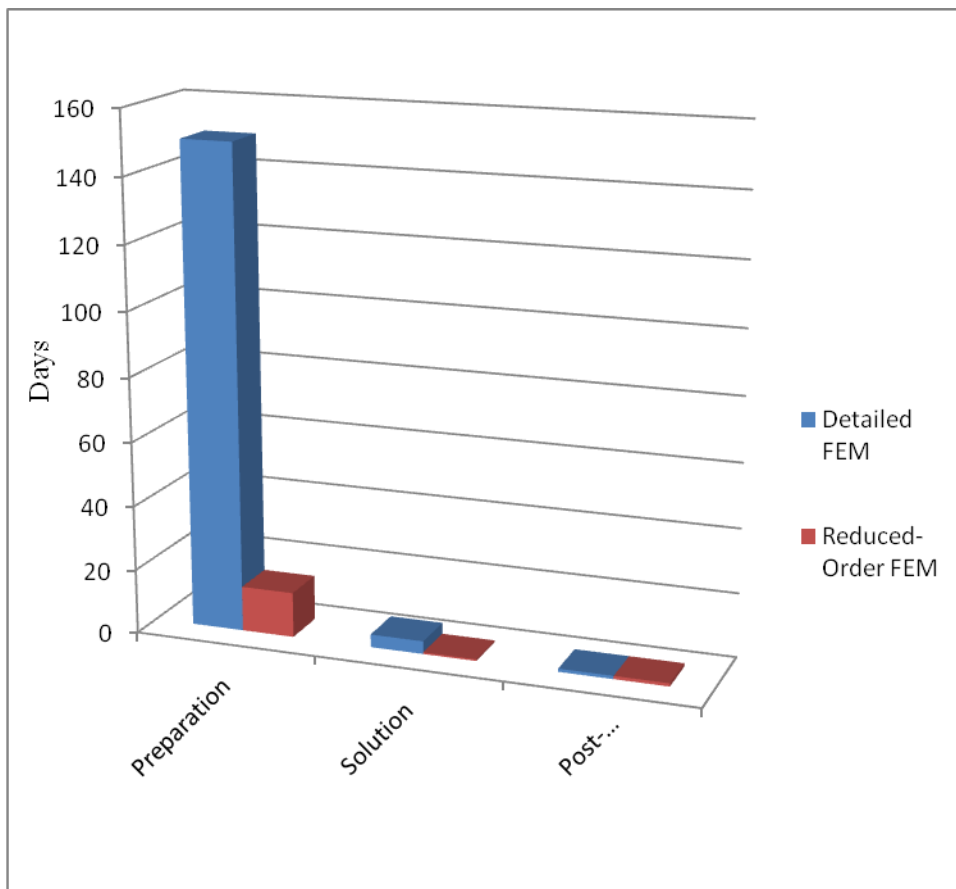


**Figure 118. Comparison of the preparation, solution and post-processing of the detailed FE model and simplified FE model with respect to time**

Phase shift occurs since the firing load is directly applied to fixed platform as a result of the lumped mass approximation of the cradle's remaining parts such as azimuth platform, elevation platform and firing tubes.

Verification of the FE models is important for the accurate evaluations of the rocket launcher system. Although preparation and verification studies are brings too many efforts, it affects further analyses based on it.

To conclude, comparison of the detailed FE model and simplified FE model is given in Table 8.

**Table 8. Comparison of detailed FE model and simplified FE model**

	Detailed FE model	Simplified FE model
Composing FEM	-	+
Solution	-	+
Modifications	-	+
Results	+	-
Total cost and effort	-	+

In conclusion, both detailed and simplified FE model's are reliable models due to the fact that it is verified with the available test results and one of them can be utilized for the dynamic analyses with respect to the circumstances of the project.





## REFERENCES

- [1] Işık Ç., “Experimental analysis and modeling of a missile launcher system”, Master’s Thesis, 2012.
- [2] Wicks, M., “Investigation Of Spinning Missile Tipoff Launch Errors Due to Dynamic Mass Imbalance”, M.S. Thesis, University of Alabama, 1994.
- [3] Cochran, E. J., “Investigation of Factors Which Contribute to Mallaunch Of Free Rockets”, Technical Report RL-CR-76-4, Auburn University, Alabama, 1975.
- [4] Dziopa Z., Krzysztofik I., Koruba Z., “An Analysis of the Dynamics of a Launcher-Missile System on a Moveable Base”, Bulletin of the Polish Academy of Sciences Technical Sciences, Vol. 58, No.4, 2010, pp. 645-650.
- [5] Lee S.K., Wilms E.V., “Analysis of Missile Launchers, Part J, Phase 1: Four Degree of Freedom Multiple Launcher”, T&AM Report 188, University of Illinois, 1961.
- [6] Zhang D., Xiao J., “A dynamic model for rocket launcher with coupled rigid and flexible motion”, Applied Mathematics and Mechanics, Vol.26(5), 2005, pp.609-617.
- [7] Selmic R., Mijailovic R. and Durkovic V., “Analysis of Parameters Affecting the Dynamic Stability of a Rocket Launcher”, Scientific-Technical Review, Vol. LIV, No.1, 2004, pp.27-33.
- [8] Cömert M.D., “Dynamics of interacting missile launcher systems having flexibility”, Ph.D. Thesis, 2000.

- [9] Raducanu D., Nedelcu I., Safta D., Şomoiaş P. and Moldoveanu C., “Particularly concerning evaluation of unguided rocket trajectories deviation under the disturbance factors action”, WCE, Vol.2, 2009.
- [10] Rixen D. J., “A dual Craig-Bampton method for dynamic substructuring”, Journal of Computational and Applied Mathematics, Vol.168, 2004, pp.383-391
- [11] Fransen S., “Methodologies for launcher-payload coupled dynamic analysis”, European Space Agency, ESA SP, Proceedings of the European Conference on Spacecraft Structures, Materials and Mechanical Testing 2005, Vol.581, 2005, pp.987-999
- [12] Zhao C., Chen S., Liu X., Zhang J. and Zeng J., “Study on modeling methods of flexible body in ADAMS”, IEIT Journal of Adaptive & Dynamic Computing, 2012(2), pp.17-22
- [13] Zhang Y., Xiao P., Palmer T. and Farahani A., “Vehicle chassis/suspension dynamics analysis-finite element model vs. rigid body model”, SAE Technical Paper 980900, 1998, doi:10.4271/980900.
- [14] Tiso P., Jansen E. and Abdalla M., “Reduction method for finite element nonlinear dynamic analysis of shells”, AIAA, Vol. 49, 2011, pp.2295-2304
- [15] Liu C. Q., “Combination of an improved FRF-based substructure synthesis and power flow method with application to vehicle axle noise analysis”, Shock and vibration, Vol.15, 2008, pp.51-60
- [16] “Western star vehicles cab and chassis modification guide” Last accessed on October 17, 2013, [http://www.westernstartrucks.com/\\_Assets/BodyBuilderBook/09General\\_Aug2012.pdf](http://www.westernstartrucks.com/_Assets/BodyBuilderBook/09General_Aug2012.pdf).
- [17] Hadipour M., Alambeigi F., Hosseini R., Masoudinejad R., “A study on the vibrational effects of adding an auxiliary chassis to a 6-ton truck”, Journal of American Science, Vol.7(6), 2011, pp.1219-1226

- [18] Roslan A. R., Mustafa Y., Mohd. N. T., “Development of a truck chassis” Last accessed on October 17, 2013, <http://eprints.utm.my/9702/1/79064.pdf>.
- [19] “Iveco body builder's guidelines and equipment mounting recommendations” Last accessed on October 17, 2013, <http://www.docstoc.com/docs/70975489/Body-Builders-Guidelines>.
- [20] “Heavy duty truck frames” Last accessed on October 17, 2013, <http://transportation.centennialcollege.ca/oduffy/Trailers/Level%201/Frames%20handout.pdf>.
- [21] “Lightweight SUV frame design development” Last accessed on October 17, 2013, [http://www.altairproductdesign.com/\(S\(eenaz4eq2au5vtqiesoke1u2\)\)/ResLibDownload.aspx?file\\_id=1285&keywords=Lightweight+SUV+Frame+Design+Development&industry=All&product\\_service=All&category=All&order\\_by=title&AspxAutoDetectCookieSupport=1&resource\\_id=2502](http://www.altairproductdesign.com/(S(eenaz4eq2au5vtqiesoke1u2))/ResLibDownload.aspx?file_id=1285&keywords=Lightweight+SUV+Frame+Design+Development&industry=All&product_service=All&category=All&order_by=title&AspxAutoDetectCookieSupport=1&resource_id=2502).
- [22] Sane S. S., Jadhav G., Anandaraj H., “Stress analysis of a light commercial vehicle chassis by FEM” Last accessed on February 10, 2013, <http://www.scribd.com/doc/86866889/08-fem-fea-stress-analysis-of-a-light-commercial-vehicle-chassis-by-fem-piaggio>.
- [23] Davidson C., “All about flex bodies in Adams webinar” April 15, 2010.
- [24] Design of Aerodynamically Stabilized Free Rockets, Military Handbook, MIL-HDBK-762, US Department of Defense, July 1990.
- [25] ANSYS Structural Analysis Guide 14.0, 2011.
- [26] Cai C., Zheng H., Khan M. S. and Hung K. C. “Modeling of material damping properties in ANSYS” CADFEM Users’ Meeting & ANSYS Conference, 2002, pp.9-11.
- [27] Ider K., ME 528 Flexible Multibody Dynamics, Middle East Technical University 2010

[28] Özgören M. K., ME 502 Advanced Dynamics, Middle East Technical University 2012

[29] “PCB Accelerometers”, Technical Data, 2011.

[30] ADAMS User’s Reference Manual, Appendix D, 2005.

[31] “Omega Strain Gage Series”, Technical Data, 2011.

[32] OMEGA Linear Potentiometers, Manual M2034-0405, 2012

[33] Private communication with Bülent ACAR